IMMOBILIZED ENZYMES IN FLOW INJECTION ANALYSIS

Methods with Hydrogen Peroxide Detection

Bo Olsson

Lund 1985

Digitized by the Internet Archive
in 2026

https://archive.org/details/IA41552414_0085

IMMOBILIZED ENZYMES IN FLOW INJECTION ANALYSIS

Methods with Hydrogen Peroxide Detection

by

Bo Olsson, fil. kand., Hld

Akademisk avhandling som med vederbörligt tillstånd av matematisk-naturvetenskapliga fakulteten vid Universitetet i Lund för avläggande av filosofie doktorsexamen kommer att offentligen försvaras å Kemicentrum, Sölvegatan 39, hörsal C, fredagen den 27 september 1985, kl 10.15.

Avhandlingen försvaras på engelska.

Organization
LUND UNIVERSITY

Department of Analytical Chemistry

Document name
DOCTORAL DISSERTATION

Date of issue
September 1985

CODEN:
LUNKDL/(NKAK-1009)/1-178(1985)

Author(s)
Bo Olsson

Sponsoring organization

Title and subtitle

Immobilized Enzymes in Flow Injection Analysis; Methods with Hydrogen Peroxide Detectio

Abstract

Analytical methods for the determination of hydrogen peroxide were developed for application in Flow Injection Analysis (FIA). Hydrogen peroxide was determined by peroxidase catalyzed reactions yielding species detected by chemiluminescence, spectrophotometry, and amperometry.

Automated FIA systems were developed for the determination of oxygen, galactose, lactose, dihydroxyaceton, sucrose, and glucose via the hydrogen peroxide produced in reactions catalyzed by immobilized glucose oxidase, galactose oxidase, invertase, mutarotase, and catalase.

Theory and applications of immobilized-enzyme reactors and enzyme-membrane electrodes in FIA are discussed. Methods for on-line sample work-up such as flow dialysis, chemical treatment, and enzymatic conversion were used for complex matrices.

Optimization of the methods for high sensitivity and high sample throughput was done with respect to flow system, immobilization procedure, reactor design, chromogenic reagent, and electrochemical mediator.

Key words

Classification system and/or index terms (if any)

Supplementary bibliographical information

Language
English

ISSN and key title

ISBN

Recipient's notes

Number of pages
178

Price

Security classification

Distribution by (name and address)

I, the undersigned, being the copyright owner of the abstract of the above-mentioned dissertation, hereby grant to all reference sources permission to publish and disseminate the abstract of the above-mentioned dissertation.

Signature Bo Olsson Date 1985-07-25

em SIS 61 41 21

IMMOBILIZED ENZYMES IN FLOW INJECTION ANALYSIS

Methods with Hydrogen Peroxide Detection

This thesis is based on the following papers, referred to in the text by their Roman numerals

I Determination of Hydrogen Peroxide in a Flow System with Microperoxidase as Catalyst for the Luminol Chemiluminescence Reaction
Bo Olsson, Anal. Chim. Acta, 136 (1982) 113

II Optimization of Peroxidase Immobilization and of the Design of Packed-Bed Enzyme Reactors for Flow Injection Analysis
Bo Olsson and Lars Ögren, Anal. Chim. Acta 145 (1983) 87

III Determination of Hydrogen Peroxide in a Flow Injection System with Immobilized Peroxidase and Chromogenic Reagents
Bo Olsson, submitted

IV Enzyme Reactors in Unsegmented Flow Injection Analysis
Gillis Johansson, Lars Ögren, and Bo Olsson, Anal. Chim. Acta 145 (1983) 71

V An Enzymatic Flow Injection Method for the Determination of Oxygen
Bo Olsson, Lars Ögren, and Gillis Johansson, Anal. Chim. Acta 145 (1983) 101

VI Galactose Determination in an Automated Flow-Injection System Containing Enzyme Reactors and an On-Line Dialyzer
Bo Olsson, Hans Lundbäck, and Gillis Johansson, Anal. Chim. Acta 167 (1985) 123

VII Amperometric Determination of Galactose, Lactose, and Dihydroxyacetone using Galactose Oxidase in a Flow System with Immobilized Enzyme Reactors and On-Line Dialysis
Hans Lundbäck and Bo Olsson, Anal. Lett. B 18(7) (1985) 871

VIII Determination of Sucrose in the Presence of Glucose in a Flow Injection System with Immobilized Multienzyme Reactors
Bo Olsson, Berit Stålbom, and Gillis Johansson, submitted

IX Theory and Application of Diffusion-Limited Amperometric Enzyme Electrode Detection in Flow Injection Analysis of Glucose
Bo Olsson, Hans Lundbäck, Gillis Johansson, Frieder Scheller, and Jürgen Nentwig, submitted

CONTENTS

	page
1. INTRODUCTION	1
2. FLOW INJECTION ANALYSIS	1
2.1 Principles	1
2.2 Dispersion	2
2.3 Injection	4
2.4 Detection	4
2.5 On-line sample work-up	5
3. IMMOBILIZED ENZYME REACTORS	6
3.1 Introduction	6
3.2 Immobilization	7
3.3 Kinetics	8
3.4 Conversion level	10
3.5 Enzyme reactors in FIA	11
3.6 Multienzyme systems	13
3.7 Applications	14
4. ENZYME MEMBRANE ELECTRODES	17
5. DETERMINATION OF HYDROGEN PEROXIDE	17
5.1 Direct amperometry	17
5.2 Indirect methods	18
ACKNOWLEDGEMENTS	20
REFERENCES	21
APPENDIX: Improvement of an Enzymatic Flow Injection Method for the Determination of Oxygen	25

1. INTRODUCTION

Enzymes are used in analytical chemistry mainly due to their ability to selectively catalyze a variety of chemical reactions, and enzymatic methods have been reported for a very large number of substances [1,2]. Most methods rely on the monitoring of a species produced or consumed in the enzyme catalyzed reaction and which can be detected more conveniently than the analyte. Common indicator species are O_2, H_2O_2, CO_2, NH_4^+, NAD(P)H, ATP, and H^+, each of which can be determined by a host of methods.

Immobilization of the enzyme onto insoluble carriers has greatly extended the potential of enzymatic analysis and recent reviews of the properties and uses of immobilized enzymes are available [3,4]. The principal advantages obtained with immobilized enzymes are the reusability and the increased stability. Since they can be used for many analyses it is also feasible to augment the analytical quality of the enzyme by e.g. rigorous purification. Moreover, a large amount of catalyst can be used for each assay which may result in very short reaction times. However, immobilization of enzymes provides more than economical usage; it allows the catalyst to become a part of the analytical instrument.

Various physical forms have been devised for the immobilized enzyme module and the method for bringing the sample into contact with the enzyme varies accordingly. The major types are enzyme electrodes and thin layers of enzyme for discrete measurements, and open tubular and packed-bed enzyme reactors for air-segmented and unsegmented continuous flow analysis, respectively. Flow methods are easily automated and Flow Injection Analysis [5] has in the last decade become the method of choice for unsegmented flow.

2. FLOW INJECTION ANALYSIS

2.1 Principles

Flow Injection Analysis (FIA) refers to methods of sample processing in which a discrete sample is carried from the place of introduction to the place of observation in a non-segmented moving fluid stream. Chemical and physical processes may be made to act on the sample components during the transport for

reasons of improved sensitivity and/or selectivity. The success of the concept lies in its versatility and in the precise control of the dynamic processes.

A FIA system may simply be used as an easily automated sampling device that carries the sample to the detection device in a highly reproducible way. This approach calls for a selective detector and is exemplified in paper IX where an enzyme membrane electrode was used for determination of glucose. However, in most FIA systems a relatively non-selective detector, e.g. a spectrophotometer, is used in combination with highly selective chemical reactions (papers I-VIII). The reaction proceeds at a finite rate and a certain time is therefore needed for the reaction to go to a desired degree of completion.

During this time, the sample zone, travelling through the flow system becomes broadened and diluted due to the dispersive forces induced by the flow. The peak broadening limits the frequency at which individual samples can be analyzed independently and increases the reagent and sample consumption for each analysis. A major design objective in FIA is therefore to minimize the axial dispersion and, of course, to find optimum reaction conditions. As pointed out by Poppe [6], the total peak broadening in FIA is the sum of the contributions from the injection process, the flow-through reactors and connectors, and the detection process. The rule of additivity of variances can be used

$$\sigma^2_{total} = \sigma^2_{injection} + \Sigma \sigma^2_{flow} + \sigma^2_{detection} \qquad (1)$$

although it should be born in mind that for skewed peaks, which are always observed in FIA, there is no simple relationship between the variance and the width of the peak at the baseline. A value of 6σ for the base-width [7] is probably a realistic estimate.

It should at this stage be mentioned that several other types of FIA techniques may have completely different design objectives [8].

2.2 Dispersion

Dispersion in flowing systems is a very complicated hydrodynamic process governed by convective and diffusive forces. Moreover, fully developed flow profiles are seldom reached under normal FIA conditions which means that the

dispersion is not constant with time and mathematical solutions are exceedingly hard to obtain. Several authors have investigated the dispersion induced by flow through passive components like straight, coiled, twisted, wavy , or knitted open narrow tubes, single bead string reactors and packed-bed reactors [9-15] and optimum conditions, under various limitations have been discussed [11,17].

A fully developed flow profile in an ideal straight open tube is parabolic, i.e. a molecule in the center of the tube moves with twice the average linear flow velocity, whereas at the tube wall it is stagnant. This gives rise to a progressive spreading of the sample zone which, however, is counteracted by radial movements induced by diffusion, and in practice, also by convective forces due to pulsating flow, surface roughness etc. [13]. The peak variance increases approximately in proportion to the square of the radius in a straight open narrow tube.

The centrifugal forces induced by the bends in deformed tubes creates secondary flows which increase the radial mixing and may have very large effects on the dispersion [14]. Disruption of the parabolic flow profile by beads serves the same purpose [16].

The dispersion in packed-bed reactors have a high significance for the performance of FIA systems with enzyme reactors. Elaborated theories have been established for the description of the dispersion process and a wealth of literature is available [17-19]. Models are commonly based either on the concept of axial dispersion or on the tank-in-series approach [20,21]. The pertinent question in FIA is how to minimize the variance per unit residence time (σ_t^2/τ) within the constraints set by practical considerations [7]. Knox [22] and Unger et al. [23] have shown that for columns packed with porous particles of different average diameter (d_p) and operated at not too low linear flow velocities (F) the dispersion can be estimated from

$$\frac{\sigma_t^2}{\tau} = A \frac{d_p^{4/3}}{D_m^{1/3} F^{2/3}} + C \frac{d_p^2}{D_m} \qquad (2)$$

where D_m is the molecular diffusion coefficient.

The first term on the right hand side of eq. 2 accounts for the contribution from the dispersion in the mobile phase and the value of the dimensionless coefficient A is below 2 for a well packed column [24]. The second term accounts for the limited rate of mass transfer in and around the porous particle and C is assumed to be around 0.03 but may be considerably larger depending on e.g. the turtuosity and porosity of the material. The well known importance of miniaturization is apparent from eq. 2.

It can be estimated from this equation that for a typical enzyme reactor, poorly packed with large particles and operated at a high linear flow rate, both terms will contribute to the variance to approximately the same extent.

2.3 The Injection

The sample volume is a very powerful variable in FIA and its effects on the response has been treated in detail [25,26]. It has been observed [27] that a sample volume equal to the volumetric standard deviation of the flow reactors gives a peak height that is about half of that obtained with a continuous supply of sample while the width of the response peak is almost unaffected by the sample bolus. Smaller injection volumes give correspondingly lower peak heights while larger volumes give broader peaks. A crude estimate of the dispersion can thus be obtained from the sample volume. Dilution of samples that are too concentrated for e.g. enzymatic analysis is easily done on-line by using an injection volume which is small compared to the dispersion. It is, on the other hand, always possible to compensate for sensitivity losses caused by insertion of dispersive elements in the flow path by adjusting the sample volume.

2.4 Detection

Selectivity is desirable also in the detection step since FIA entirely relies on this property. Other important properties are a large dynamic range, a low noise level, and a low dead volume. In FIA base line drift is of less consequence because the peak height is measured relative to the background, and noise levels are generally lower since the detector is in a fixed position [28]. As was pointed at by Knox [29], the peak broadening in the detector may limit the performance of the whole system and it may eventually constrain the miniaturization. Poppe [30] has discussed the performance of some liquid phase

flow-through detectors in this context. The contribution of the detector to the peak width is in most FIA systems unsignificant. However, for an enzyme membrane electrode detector the width of the response peak may be entirely determined by the diffusion in the membrane (paper IX).

2.5 On-line sample work-up

2.5.1 Dialysis

On-line dialysis can be used in FIA to exclude high molecular weight sample components from the analytical detection system [31-34, papers VI, VII]. The active part of a dialyzer is a semipermeable membrane through which small molecules (e.g. the analyte) may pass but which physically separates the injection line from the rest of the FIA manifold. It has been found that equal flow rate and direction in dialyzer channels of equal heights are advantageous for FIA [34]. For this configuration of a dialyzer the dialyzed fraction (D) is ideally expressed by [35]

$$-\ln(1-2D) = 2\,P\tau/h \qquad (3)$$

where τ is the mean residence time, h is the channel height and P is the apparent permeability which depends on e.g. the diffusion through the membrane and boundary layers and on the convective transport out of and into the flowing streams [36]. Under constant operational conditions, e.g. flow rate, temperature, viscosity etc. the transferred amount is proportional to the original concentration in the sample.

A dialyzer in the flow system causes additional peak broadening and the usual trade-off between sample throughput and sensitivity must be considered. The channels of the dialyzer can be packed with solid glass beads [33, papers VI, VII] to disrupt the laminar flow in analogy with the single bead string reactor [18]. The increased radial mixing reduces the axial dispersion and increase the convectional mass transport to and from the membrane. Both a higher sample throughput rate and a higher sensitivity were thus obtained with a packed dialyzer as compared to that obtained with a dialyzer with open channels [papers VI, VII].

Dialyzers may also be convenient when a very large dilution of a sample is required. A small dialyzer will not increase the dispersion significantly [paper VII].

2.5.2 Chemical treatment

The risk for analytical errors from interfering substances increases with the complexity of the sample matrice. Serum and urine contain reducing substances, such as ascorbic acid and uric acid, and these compounds, which pass a dialysis membrane, interfere in methods based on hydrogen peroxide detection [37]. By careful selection of detection method the interferences may be diminished (paper III) and by chemical treatment they may be completely eliminated. Alkali deproteinization [38] and oxidation of the reducing agent with heavy metal salts [39] are recommended methods. On-line methods for treatment in flow analysis include chemical [40,41] and electrochemical [42] oxidation. A copper(II)-amine column was used in paper VI for on-line elimination of reducing agents.

A different type of interference may be present in multienzyme systems (paper VIII). If any of the intermediates of the enzyme reactions occur naturally in the sample it will give at least the same response as the analyte. Such very specific interferences may be eliminated by destruction of the substance in an on-line prereactor containing the corresponding enzyme (paper VIII).

3. IMMOBILIZED-ENZYME REACTORS

3.1 Introduction

The immobilized enzyme can be contained in a flow-through reactor so that the analytically useful reaction may be performed in a continuous stream of flowing solution. One merit of the configuration is that further chemical processing can be made downstream, making it compatible with almost all detection systems. Flow analysis may in addition provide high sample frequency, good reproducibility and ease of automation. The merits of various enzyme reactor configurations have been discussed [3,4,43, paper IV]. This section will be concerned with packed-bed reactors only.

Catalytic reactors have been used and studied for a long time in the field of chemical engineering. The basic relationships between physical and chemical parameters are similar in the miniature reactors used for analytical purposes and the large-scale reactors used in industrial processing, and the chemical engineering literature provides many useful correlations [44-48]. However, while production economy is vital in the engineering field, analytical reactors should be optimized for high, preferably quantitative conversion of substrate to product with a minimum of dispersion.

A main objective in reactor optimization for analytical purposes is thus to achieve a high specific activity of the immobilized enzyme preparation which may allow short reaction times. Equally important are the physical parameters of the reactor and the enzyme support because they will determine the effectiveness of the enzyme, the dispersion, and the operational characteristics of the reactor.

3.2 Immobilization of enzymes

A packed-bed reactor will develope dead-volumes unless it is filled with an unshrinkable, pressure-resistant support material. Controlled pore glass seems to be one of the most suitable supports commonly used, although it is commercially available only in the form of relatively large chips of irregular size and shape. High performance chromatography packing materials may well prove to be advantageous due to their superior flow characteristics.

To obtain a high loading of enzyme, particles of high porosity with the smallest possible pore size for free entrance of the enzyme should be selected [49, paper II].

Covalent linkage is almost exclusively used for immobilization of enzymes to porous glass and a large number of different methods have been developed [50-53], most of which are based on organosilane chemistry [54]. No single method is generally superior to the other. Both specific factors, such as the type of functional groups involved in the reaction, and more general properties like hydrophobic and ionic interactions influence the immobilization yield. The purity of the enzyme solution, especially with regard to low molecular weight competitors often present in commercial enzyme preparations, seems to be of

paramount importance in many cases [papers VII, VIII]. Optimization of the immobilization procedure is generally a worthwhile effort.

3.3 Kinetics

The Michaelis-Menten rate equation

$$\frac{dS}{dT} = \frac{V_{max}\, S}{K_M + S} \qquad (4)$$

describes the rate of an enzyme reaction as a function of the instantaneous substrate concentration (S). The characteristic constant K_M represents the substrate concentration at which the rate is half of the maximum (V_{max}). The original derivation [55] was made for a simple one-substrate reaction but rate equations of many, much more complicated kinetic schemes may under certain conditions be well approximated by the Michaelis-Menten equation [56].

Integration of the rate equation yields an expression which relates the fraction of reacted substrate ($X = (S_o - S)/S_o$) with the time elapsed, t.

$$-\ln(1-X) = V_{max} \cdot t/K_M - S_o X/K_M \qquad (5)$$

This equation can be used to described the conversion in a packed-bed reactor provided the residence time distribution is narrow, i.e. when the dispersion is low. The mean residence time (τ) is taken as the reaction time, t. Immobilization of an enzyme may, due to mass-transfer limitation (see below) [57] and microenvironmental effects [57-59] alter its kinetic properties, which is acknowledged by treating them as apparent properties. Eq. 5 predicts that the fractional conversion of substrate in a reactor varies with initial substrate concentration. However, when $S_o << K_M^{app}$ the last term in eq. 5 can be neglected, which gives the pseudo-first order approximation

$$-\ln(1-X) = K_{ps}^{app} \cdot \tau \qquad (6)$$

where $K_{ps}^{app} = V_{max}/K_M^{app}$ is the pseudo-first order rate coefficient for the enzyme reaction in the reactor. A linear calibration curve can thus be obtained for $S_o << K_M^{app}$ because the conversion will be independent of the substrate concentration. The linear range can, of course, be extended to cover substrate concentrations above K_M^{app} if the reaction is allowed to go to

near completion. This will, however, take increasingly longer times as S_o/K_M^{app} becomes larger [60]. The kinetic properties of an enzyme reactor can be determined by measurements of the fractional conversion at various substrate concentrations and residence times [61, paper II]. Eq. 5, or in the first-order region eq. 6, can then be used to predict the residence time required to obtain the desired degree of conversion [papers III, V-VIII].

3.3.1 External mass transfer limitation

The substrate concentration at the external surface of a particle containing a catalyst will always be lower than the bulk concentration. The degree of depletion depends on the activity of the catalyst as well as on the efficiency of the mass transport from the bulk of the solution to the interphase. The overall effect is a decreased efficiency of the catalyst which for a pseudo-first order reaction can be described by eq. 7 [62, paper II].

$$(K_{ps}^{app})^{-1} = d_p^{3/2}/BF^{1/2} + (K_{ps})^{-1} \qquad (7)$$

Here, K_{ps} is the rate coefficient at infinitely fast external mass transfer and B is a collection of constants (see paper II). The external resistance to mass transfer can be diminished by increasing the linear flow rate (F) and more effectively by decreasing the particle size (d_p). An extensive review of transport properties in packed-bed reactors is available [63].

It can be estimated from eq. 7 that, for e.g. a 2.5 mm i.d. reactor filled with particles with a size of 100 μm and operated at 1 ml min^{-1}, external mass transfer resistance reduces the rate coefficient of the reactor by 10% already at the fairly low activity of $K_{ps}app = 0.4\ s^{-1}$, while for particles of 50 μm an external effectiveness of >90% is obtained up to $K_{ps}^{app} = 1.3\ s^{-1}$.

3.3.2 Internal mass transfer limitation

The catalytic sites are generally (but not always [64,65]) distributed throughout the interior of the porous particle where convective mass transport is inoperative. Because of the limited rate of diffusion, there will be a gradual depletion of substrate inwards towards the center of the particle, as the substrate is continually converted to product. The extent to which the reaction

rate is lowered depends on the ratio of the diffusion and reaction coefficients and on the diffusion distance. For a (pseudo)-first order reaction [66]

$$K_{ps} = \frac{K}{\Phi}\left(\frac{1}{\tanh 3\Phi} - \frac{1}{3\Phi}\right) \qquad (8)$$

where K is the inherent rate coefficient, and Φ is the Thiele modulus (often referred to as the enzyme loading factor)

$$\Phi = \frac{d_p}{6}\sqrt{\frac{K}{D_{eff}}} \qquad (9)$$

D_{eff} is the effective diffusivity in the porous support.

As an example, for a 100 μm particle with an inherent rate coefficient of 1 s^{-1} the effectiveness is less than 60% with almost all substrates (see e.g. fig. 3 in paper IV).

3.3.3 Effects of mass-transfer limitations

Substrate depletion decreases the apparent enzyme activity, except at high enough bulk concentration where V_{max} is approached. In the presence of mass-transfer resistances the enzyme activity still follows limiting first and zero order dependence on bulk concentration but the Michaelis-Menten rate law may not be exactly valid [57]. Yet the characteristic half-maximum-activity substrate concentration K_M^{app} is convenient for description and analysis of the system. Mass-transfer resistances always serves to increase K_M^{app} and the linear range of substrate conversion may thus be extended well above that obtained in a homogeneous solution [paper II]. Mass-transfer limitations are nearly always present in analytical reactors as can be inferred from the examples given above. Detailed analysis of the effects of simultaneous internal and external resistances can be found in the literature [44,67-69] as well as general discussions on the subject [3,48,57,70].

3.4 Conversion level

A flow-system with an enzyme reactor operating with less than quantitative conversion is in essence a one-point kinetic method according to the definition of Purdue [71]. The quality of the analytical result is therefore crucially dependent on the constancy of the rate coefficient of the analytical reaction.

Any factor in the sample which affects the activity of the reactor will produce an erroneous result. Likewise, inactivation of the catalyst with use and with time will directly be reflected in a decrease of the response factor. Moreover, the calibration curves will start to deviate from linearity already for substrate concentrations singificantly lower than K_M^{app}. A mass-transfer limited reactor is more immune towards activity changes.

With a sufficienty large enzyme reactor the extent of the analytical reaction can be made to approach completion (i.e. equilibrium). As discussed in paper IV the end-point type of analysis overcomes the problems caused by the potential presence of rate effectors in the sample, provides a better long-time stability and extends the linearity of the calibration curves. The price to be paid for these valuable analytical qualities is a slower sample throughput rate. It is simple to calculate from eq. 6 that a 10-fold increase in reactor length is required to raise the conversion from 50% to 99.9%. However, as shown in section 2.3 the dispersion will only increase about 3 times and, as is shown in papers II-V, VII and VIII it is feasible to obtain methods with high conversion factors (>99%) and high throughput rates (45-600 samples h^{-1}) for many substances.

There is a loss of selectivity in going from low to high conversion. This may be an advantage for e.g. group selective detection with post-column reactors for HPLC [72] but in most cases it is probably a drawback. Finally, the product of the enzyme reaction may not be sufficiently stable in the reactor to allow complete conversion as can be exemplified by the effects of catalase impurities in hydrogen peroxide producing reactors (papers VI and VII).

3.5 Enzyme reactors in FIA

So far, most of the theory of enzyme reactors have been developed with the assumption of a steady-state feed of substrate to the reactor while in fact the substrate has been injected as a pulse in most of the analytical applications. A closer inspection of the validity of the predictions when the steady-state assumption is violated is therefore required.

The first important issue is related to the kinetics of mass-transfer i.e. how fast the steady-state concentration profile is approached in and around a single catalyst pellet. Neglecting mass-transfer limitations in the mobile

phase, Kühnau and Lasch [73] derived an analytical solution to the evolution of presteady-state concentration profiles in spherical enzyme supports. It can be seen from their results that for particles smaller than 100 μm the "time constant" is always less than 1 s. For a high reaction rate coefficent and for smaller particles it is much less. Since the concentration gradients obtained with present-day FIA systems are nearly always less sharp it can be concluded that the reactors, in this respect, are operated under pseudo-steady-state conditions. The next question relates to the effect of dispersion in the reactor. Most dispersion experiments and theories pertain to non-reacting solutes but several studies on dispersion coupled with reaction has been published [74-78]. The results suggest and it has been concluded elsewhere [79] that, to a first approximation, the reaction and dispersion can be treated as independent processes for (pseudo-)first order reactions. A theoretical method for predicting the elution profile of a pulse response in an immobilized-enzyme reactor has been proposed [81]. It has been shown that a moderate spread in residence time, caused by dispersion, has little effect on the conversion [80]. However, even in low dispersive reactors dispersion may be important. If the sample pulse is very short the concentration of substrate will decrease as a consequence of both reaction and dilution. This may have significance if a method is accomodated for analysis of highly concentrated samples by using very small injection volumes. Nevertheless, experimental values and design equations obtained for steady-state conditions can probably in most cases be used for development of flow injection methods. It was in fact demonstrated in paper VII that the conversion of various substrate in a reactor was the same for a steady-state feed of substrate and for sample injection.

The required residence time (τ) in the reactor is determined by the degree of conversion aspired and by the rate coefficient given by the reactor under the conditions of use (section 3.3). The variance per unit residence time (σ_t^2/τ) was related to these conditions in section 2.2 and an approximate design equation for the first order regime can thus be obtained by combining eq. 2 and eqs. 6-9.

$$\frac{\sigma_t^2}{\tau} = \left[\frac{d_p^{3/2}}{BF^{1/2}} + \frac{\Phi}{K}\left(\frac{1}{\tanh 3\Phi} - \frac{1}{3\Phi}\right)^{-1}\right]\left[-\ln(1-X)\right]\left[A\,\frac{d_p^{4/3}}{D_m^{1/3}F^{2/3}} + C\,\frac{d_p^2}{D_m}\right] \qquad (10)$$

i ii iii

where i gives the effective activity of the catalyst, $1/K_{ps}^{app}$

ii depends on the desired degree of conversion, X

iii accounts for the dispersion per unit residence time, σ_t^2/τ

} gives τ

The most powerful variables are the inherent activity, K, the desired conversion, X, and the particle diameter, d_p. The residence time is easily translated to a reactor length through the linear flow-rate and the diameter is then obtained from the desired volumetric flow-rate.

The peak height depends on the dilution of the sample in the flow system and on the degree of conversion (X). In FIA the dilution can be controlled by the injection volume and it was noted in section 2.4 that the dilution could be restricted to a factor of 2 (neglecting added streams) so that a product concentration of X/2 at the peak maximum can be obtained without peak broadening effects.

Several real-world complexities will limit the freedom of parameter selection. Some factors like allowable back pressure can be taken into account mathematically (Darcy's equation, paper II) whereas other cannot be explicitely formulated e.g. the increased risk of clogging when the particle size is diminished. Thorough discussions on optimization of packed-bed reactors for chromatography [29,82] and for homogeneous reactions [7,83] can be found in recent papers.

3.6 Multienzyme systems

If none of the products of an enzyme reaction are directly detectable auxiliary enzymes may be used in sequence to produce a measurable species.

The consecutive reactions

$$S \xrightarrow[E_1]{K_1} I \xrightarrow[E_2]{K_2} P \qquad (11)$$

can be carried out either in two separate consecutive reactors containing E_1 and E_2, respectively, or in one reactor containing both catalysts. For consecutive reactors the kinetics of each reaction can be represented by eq. 6.

For the mixed enzyme system it can easily be shown from the expression for the time dependence of I (eq. 3, paper VI) that the product concentration will be

$$\frac{P}{S_o} = 1 - \frac{K_2}{K_2-K_1}\exp(-K_1t) + \frac{K_1}{K_2-K_1}\exp(-K_2t) \qquad (12)$$

The result as compared with a one-step reaction is a delay in the maximum production rate of P. It can be derived from eqs. 6 and 12 that it is more efficient to carry out the reactions in separate reactors, which is also the natural choice when the optimum reaction or immobilization conditions differ (paper V-VII).

If the first reaction is reversible it is obvious that both enzymes should be present simultaneously to drive the reactions to completion (paper VIII) and optimum catalyst composition profiles have been calculated [84] and tested experimentally [85].

Mass-transfer resistances may have a profound effect on the productivity of consecutive enzyme reactions [86-89]. It has been shown that the lag-phase observed with free enzymes (described by eq. 12) is shortened or disappears if the enzymes are coimmobilized because of an accumulation of the intermediate in the diffusion layer [88]. For a three-enzyme system rate enhancement of up to 400% has been demonstrated [89].

3.7 Applications of immobilized-enzyme reactors in FIA

One of the first useful analytical applications of immobilized enzyme preparations utilized an immobilized enzyme reactor in a flow system [90]. Pulsed sample injection techniques for enzyme reactors started to be developed at about the same time as Ruzicka [91] introduced this technique for homogeneous reactions, and sample throughput rates of 30 samples h^{-1} and above was reported for systems with electrochemical [92-94]. spectrophotometric [95], chemiluminescent [96], and thermal [97-99] methods of detection. Carr and Bowers [3] and Guilbault [4] have recently reviewed the analytical applications of enzyme reactors and Table I is a compilation of flow injection methods with an emphasis on papers that have appeared in the time period not covered by these authors.

TABLE I. FIA methods using immobilized-enzyme reactors.

analyte	enzyme(s)	indicator spec., det. method	inj. vol (µl)	range	throughput h^{-1}	Ref.
alanine	alanine DH	NADH, amp	50	0.1-1 mM	15	100
ascorbic acid	ascorbic-acid O	ascorbic acid, diff. amp	500	0.1-400 µM	12	101
cholesterol	cholesterol-esterase/ cholesterol O	H_2O_2,amp	10	<1-4 g L^{-1}	12	102
cephalosporines	cephalosporinase	diff.UV	100	10-800 mg L^{-1}	30	103
dihydroxyacetone	galactose O	H_2O_2,amp	1.5	0.01-0.5 M	70	P VII
ethanol	alcohol DH	NADH,amp	100	0.1-5 mM	30	104
"	alcohol DH	NADH,amp	50	1-1000 mM	15	100
"	alcohol DH	NADH,UV				95
formate	formate DH	NADH,amp	50	1-100 mM	15	100
galactose	galactose O	O_2, amp	100	0.03-0.6 mM	30	94
"	galactose O	(H_2O_2) dye,VIS	160	0.01-14 mM	45	P VI
"	galactose O	H_2O_2,amp	10	0.002-60 mM	45	P VII
glucose	hexokinase	T	120	0.5-25 mM	40	99
"	glucose DH	NADH, amp	50	0.1-10 mM	15	100
"	glucose DH	NADH, amp	50	0.25-1000 µM	70	105
"	glucose O	O_2, amp	9			92
"	glucose O/HRP	(H_2O_2)I, UV		3-100 nmoles	40	95
"	glucose O/HRP	(H_2O_2) dye,VIS	25	0.16-16 mM	45	34
"	glucose O/HRP	(H_2O_2)Fe(CN),amp	2	0.05-10 g L^{-1}	100	106
"	glucose O	H_2O_2,amp	2	<0.25-4 g L^{-1}	60	107
"	glucose O	H_2O_2,amp	20	0.001-1 mM	150	141
"	glucose O	H_2O_2,amp	5	0.01-8 g L^{-1}	100	108
"	glucose O	H_2O_2,CL		0.01-100 µM	24	96
"	glucose O	H_2O_2,amp	1.5	0.01-100 mM	300	P IX
glutamate	glutamate DH	NADH,amp	50	0.1-10 mM	15	100
hydrogen peroxide	HRP	dye,VIS	20	0.1-500 µM	210	P III

isocitrate	isocitrate DH	NADH,amp	50	0.1-1 mM	15	100
lactate	lactate DH	NADH,amp	100	1-80 μM	30	109
"	lactate DH	NADH,amp	50	0.1-150 mM	15	100
lactose	galactose O	O_2 ,amp	40	10-150 mM	30	94
"	galactose O	H_2O_2,amp	20	0.05-300 mM	45	P VII
leucine	leucine DH	NADH,amp	50	0.1-1 mM	15	100
malate	malate DH	NADH,amp	50	1-500 mM	15	100
oxalate	oxalate decarboxylase	$(CO_2)CH_4$,FID	1000	1-75 μM	15	110
oxygen	glucose O/HRP	(H_2O_2) dye,VIS	50	5-300 μM	60	P V
penicillin	penicillinase	T	100	0.5-10 g L^{-1}	45	111
phosphatidylcholine	phospholipase /cholin O	H_2O_2,amp	20	<0.5-3 g L^{-1}	15	112
sucrose	invertase/mut/GOD	H_2O_2 amp		1-5 mM		113
"	invertase/mut 6OD/catalase	(H_2O_2) dye,VIS	80	0.1-500 μM	80	P VIII
testosterone	steroid DH	NADH,UV		0.1-3 nmoles		95
triglycerides	triacylglycerol-lipase	T	500	0.05-5 mM	12	114
urea	urease	NH_3,ISE	100	0.1-100 mM	>30	34
"	urease	T	120	2-25 mM	40	98
"	urease	NH_3,ISE	20		45	93
uric acid	uricase/catalase	O_2 ,amp	80	0.01-1 g L^{-1}	100	115

O = oxidase, DH = dehydrogenase, mut = mutarotase, HRP = peroxidase, T = thermal

The papers on which this thesis is based demonstrates, in my opinion, the modular character of FIA. The flow system concept lends itself to a sectioning of the task into analytical unit operations, e.g. dialysis, sample pretreatment chemical reactions and final detection. Flow-through enzyme reactors are ideally suited for providing the analytical flow system with a high selectivity and other components may be incorporated into the manifold depending on the type of sample. Rather complex processing schemes may thus be devised which combines high sensitivity and selectivity with high sample throughput rates.

4. ENZYME-MEMBRANE ELECTRODES

An enzyme membrane electrode consists of a thin layer of enzyme in close proximity to an electrochemical sensor. The basic principle of its operation is to place a substrate of the enzyme in contact with the membrane to allow it to diffuse inwards towards the transducer surface. During the diffusive transport it is converted to a product which may be sensed. Both amperometric and potentiometric transducers are common and the theory and practice of different enzyme electrode designs are well covered in recent reviews [3,4]. The common practice for measurements with an enzyme electrode has been to dip the electrode into a well stirred mixture of sample and buffer and to take a reading when a stable signal is reached. Alternatively, the time derivative of the signal has been used for presteady-state measurements. A washing step completes the measurement cycle. As detailed in paper IX there are many advantages in performing these steps in a continuous fashion by implementing the electrode in a FIA system. The only apparent disadvantage with the use of a FIA system for bringing the sample to the electrode is that the probe characteristics of the electrode are lost.

5. DETERMINATION OF HYDROGEN PEROXIDE IN FLOW SYSTEMS

Hydrogen peroxide is involved in many enzymatic reactions. At least forty oxidases are known to generate hydrogen peroxide [116,117] and by linking reactions which produce substrates for the oxidases (paper VIII) the utility of hydrogen peroxide as an indicator species becomes even broader. Hydrogen peroxide is also becoming increasingly important for a variety of industrial applications and a large body of literature exists on its measurement, see ref. [118].

5.1 Direct amperometry

Hydrogen peroxide can be oxidized directly at an electrode which provides a simple, reagentless method for its determination. However, at most electrode materials, e.g. noble metals and various types of carbon, the reaction is highly irreversible [119] and a large overpotential is therefore required. The current depends on the activity state of the electrode and frequent pretreatments are often necessary [120]. It has nevertheless been shown that reproducible results can be obtained also with quite complex sample matrices by

direct oxidation, especially at (enzyme-)membrane covered electrodes [107,121-124], see also Table I. This mode of hydrogen peroxide detection was used in paper IX with an enzyme membrane electrode in a FIA manifold.

A new very promising electrode material consists of a thin layer of vacuum deposited Pd/Au on carbon [125]. The electrode surface is very reproducible and hydrogen peroxide is oxidized at a favourable potential.

5.2 Indirect methods

Most of these methods rely on a selective oxidation of a mediator by the hydrogen peroxide in the presence of a catalyst to produce a new indicator species which is conveniently detectable by e.g. spectroscopic or electrochemical methods. The catalyst of choice is often peroxidase because it provides a high catalytic rate, is rather selective for hydrogen peroxide and can be used with a variety of both inorganic and organic mediators. This enzyme was used for an assay of peroxide already in 1845 [126]. The immobilization of peroxidase to porous glass for use in analytical flow-through reactors was investigated in papers II and III. Very active preparations can be obtained so that the time required for quantitative reaction of the hydrogen peroxide becomes in the order of seconds.

5.2.1 Electrochemical detection

The mediator can be selected to give with its oxidized form a reversible redox couple which can be monitored either potentiometrically or amperometrically. Amperometric methods have proven to be very suitable for application in flow systems [127-129, see also Table I] and in paper VII ferrocyanide was used as mediator for amperometric detection of hydrogen peroxide. Ferricyanide was produced by catalytic oxidation of the ferrocyanide in a reactor containing the immobilized peroxidase preparation described in paper II. A weakly reducing electrode potential gave a low background current and a very favourable detection limit ($4 \cdot 10^{-8}$ M H_2O_2).

5.2.2 Spectrophotometric detection

Very many reagents have been investigated for hydrogen peroxide determinations and most modern methods use peroxidase as catalyst for the colour forming reaction. Many of these are based either on direct oxidation of a leucodye to the corresponding dye or on coupling of the oxidized mediator with a second compound to produce a coloured conjugate. Although the selection of a reagent must be based on the requirements of the specific application, some general qualities, including stable reagents and high molar absorptivity at a suitable wavelength, can be specified [130]. It has been observed that leucodye reagents, acting as reversible redox indicators, show a larger susceptability towards interferences from reducing agents than do the coupled dye reagents [37, paper III].

For immobilized enzymes another important aspect is the interaction between the support and the reagent. Most coloured products adsorb to the hydrophobic surface of the porous glass used to obtain very active immobilized peroxidase preparations [paper II]. Different combinations of immobilization procedure and reagent composition were investigated in paper III and some very sensitive (det. limit $0.4\text{-}8 \cdot 10^{-7}$ M H_2O_2) FIA methods were developed which do not suffer from the impairing effects of adsorption noted in paper V. A reagent originally developed by Barham and Trinder [131] was used in combination with peroxidase immobilized to a hydrophilic carrier in paper VI and VIII for hydrogen peroxide based determinations of galactose and sucrose respectively. The method for oxygen determination developed in paper V was improved by applying this hydrogen peroxide detection system, see the Appendix.

5.2.3 Fluorometric detection

These methods use mediators that on oxidation produce a fluorophore and they generally provide very low detection limits (10^{-7}–10^{-8} M H_2O_2) [132-134]. Quenchers, other fluorophores, and reductants may, however, seriously affect the response.

5.2.4 Chemiluminescence

Extremely sensitive measurements of hydrogen peroxide, with limits of detection in the nanomolar range, can be obtained with chemiluminescent reagents [paper I]. The light-emitting reaction of hydrogen peroxide with luminol, which has been the most used reagent, is catalyzed by transition metal complexes and heme containing compounds and takes place in alkaline solutions [135]. The light intensity is influenced by many parameters and the method suffers from strong interferences from both oxidizing and reducing compounds [136]. Nevertheless, several enzymatic FIA methods with chemiluminescent detection for determination of glucose in clinical samples have been reported [96,137,138].

The chemiluminescence reagents based on diaryloxalates [139,140] can be used at near neutral pH and the interferences seem to be less severe [141]. However, a partly organic solvent is required for solubility reasons and the limit of detection becomes comparable to that obtained with electrochemical and spectrophotometric detection.

ACKNOWLEDGEMENTS

I express my gratitude to professor Gillis Johansson who initiated this work, for his interest and continuous support. I also want to thank all my friends and colleagues at the department for creating a warm and stimulating atmosphere. I am especially grateful for the pleasant cooperation with Dr Hans Lundbäck and special thanks are also given to Dr Frieder Scheller and his research group in Berlin. Dr Eduardo Martins is acknowledged for revising the English text and thanks are due to Annica Bergkvist for skilfull typing of the manuscript.
Elsevier Scientific Publishing Company and Marcel Dekker Inc. are acknowledged for permissions to reproduce the papers originally appearing in Analytica Chimica Acta and Analytical Letters, respectively.

REFERENCES

1. H.U. Bergmeyer (ed.), "Methods of Enzymatic Analysis", Springer Verlag, Berlin, 1974.
2. G.G. Guilbault, "Handbook of Enzymatic Methods of Analysis", Marcel Dekker, New York, 1976.
3. P.W. Carr and L.D. Bowers, "Immobilized Enzymes in Analytical and Clinical Chemistry", John Wiley & Sons, New York, 1980.
4. G.G. Guilbault, "Analytical Uses of Immobilized Enzymes", Marcel Dekker, New York, 1984.
5. J. Ruzicka and E.H. Hansen, "Flow Injection Analysis", John Wiley & Sons, New York, 1981.
6. H. Poppe, Anal. Chim. Acta, 114(1980)59.
7. J.M. Reijn, H. Poppe, and W.E. Van der Linden, Anal. Chim. Acta, 145(1983)59.
8. J. Ruzicka, Anal. Chim. Acta, 145(1983)1.
9. J.F.K. Huber, K.M. Jonker and H. Poppe, Anal. Chem. 52(1980)2.
10. R. Tijssen, Anal. Chim. Acta, 114(1980)71.
11. J.H.M. van der Berg, R.S. Deelder and G.M. Egebrink, Anal. Chim. Acta, 114(1980)91.
12. T.J. Vanderslice, K.K. Stewart, A.G. Rosenfeld and D.J. Higgs, Talanta 28(1981)11.
13. K. Hofmann and I. Halasz, J. Chrom., 173(1979)211.
14. K. Hofmann and I. Halasz, J. Chrom., 199(1980)3.
15. E.O. Katz and R.P.W. Scott, J. Chrom., 268(1983)169.
16. J.M. Reijn, W.E. Van der Linden, and H. Poppe, Anal. Chim. Acta, 126(1981)1.
17. J.C. Giddings, "Dynamics of Chromatography", Marcel Dekker, New York, 1965.
18. C.L. de Ligny and W.E. Hammers, J. Chrom., 141(1977)91.
19. A.S. Said, "Theory and Mathematics of Chromatography", Hüthig, Heidelberg, 1981.
20. O. Levenspiel, K.B. Bischoff, Adv. Chem. Eng. 4(1963)95.
21. G.K. Froment, K.B. Bischoff, "Chemical reactor analysis and design", J. Wiley, New York, 1979.
22. J.H. Knox, J. Chrom. Sci., 15(1977)352.
23. K. Unger, W. Messer, and K.F. Krebs, J. Chrom., 149(1978)1.
24. G. Guiochon, J. Chrom., 185(1979)3.
25. R.S. Schifreen, D.A. Hanna, L.D. Bowers and P.W. Carr, Anal. Chem., 49(1977)1932.
26. J.M. Reijn, W.E. Van der Linden, H. Poppe, Anal. Chim. Acta, 114(1980)105.
27. Ref. [5], p. 49.
28. Ref. [5], p. 29.
29. J.H. Knox, M.T. Gilbert, J. Chrom. 186(1979)405.
30. H. Poppe, Anal. Chim. Acta, 145(1983)17.
31. E.H. Hansen, J. Ruzicka, and B. Rietz, Anal. Chim. Acta, 89(1977)241.
32. J. Ruzicka and E.H. Hansen, Anal. Chim. Acta, 87(1976)353.
33. W.E. Van der Linden, Anal. Chim. Acta, 151(1983)359.
34. L. Gorton and L. Ögren, Anal. Chim. Acta, 130(1981)45.
35. E. Mårtins, Ph.D. Thesis, University of Lund, p. 17.
36. B. Bernhardsson, E. Martins and G. Johansson, Anal. Chim. Acta, 167(1985)111.
37. D.L. Witte, L.F. Brown and R.D. Feld, Clin. Chem., 24(1978)1778.

38. R.J. Henry, D.C. Cannon, and J.W. Winkelman, Clinical Chemistry, Principles and Techniques, 2nd ed., Harper & Row, Hagerstown, MD, 1974, p. 398.
39. R.H. White-Stevens, Clin. Chem., 28(1982)578.
40. T. Yao, Anal. Chim. Acta, 153(1983)175.
41. M. Masoom and A. Townshend, Anal. Chim. Acta, 166(1984)111.
42. T. Yao and Y. Kabayashi, Bunseki Kagaku, 32(1983)253.
43. H.A. Mottola, Anal. Chim. Acta, 145(1983)27.
44. C.N. Satterfield, Mass Transfer in Heterogeneous Catalysis, MIT Press, Cambridge, M.A., 1970.
45. O. Levenspiel, Chemical Reaction Engineering, 2nd ed., Wiley, New York, 1972.
46. C.Y. Wen and L.T. Fan, Models for Flow Systems and Chemical Reactors, Marcel Dekker, New York, 1975.
47. W.R. Vieth, K. Venkatasubramanian, A. Constantinides, and B. Davidson in L. Wingard (Ed.), Applied Biochemistry and Bioengineering, Vol. 1, Academic Press, New York, 1976.
48. W.H. Pitcher Jr., Adv. Biochem. Eng., 10(1978)1.
49. D.L. Eaton, in R.B. Dunlop (Ed.), Immobilized Enzymes and Affinity Chromatography, Plenum Press, New York, 1974, p. 246.
50. O.R. Zaborsky, Immobilized Enzymes, CRC Press, Cleveland, OH, 1973.
51. H.H. WEetall and S. Suzuki (Eds.), Immobilized Enzyme Technology, Plenum Press, New York, 1975.
52. K. Mosbach (ed.), Methods in Enzymology, Vol. 44, Academic Press, New York, 1976.
53. K. Nilsson, Ph.D. Thesis, University of Lund.
54. D.E. Leyden and W.T. Collins (Eds.), Silylated Surfaces, Gordon and Breach, New York, 1980.
55. L. Michaelis and M.L. Menten, Biochem. Z., 49(1913)333.
56. Ref. [3], chapter 2.
57. L. Goldstein, in ref. [76], p. 397.
58. C.M. Wharton, E.M. Crook, and K. Brocklehurst, Eur. J. Biochem., 6(1968)572.
59. A.C. Johansson and K. Mosbach Biochim. Biophys. Acta, 370(1974)348.
60. Ref. [3], p. 71.
61. M.D. Lilly, W.E. Hornby, and E.M. Crook, Biochem. J., 100(1966)718.
62. B.J. Rovito and J.R. Kittrell, Biotech. Bioeng., 15(1973)143.
63. B.D. Kulkarni and L.K. Doraiswamy, Catal. Rev. Sci. Eng., 22(1980)431.
64. J. Lasch, Proc. FEBS Meet., 52(1978)495 (publ. 1979).
65. C. Horvath and J.-M. Engasser, Ind. Eng. Chem. Fundam., 12(1973)229.
66. Ref. [44], p. 129.
67. D.J. Fink, T. Na, and J.S. Schultz, Biotech. Bioeng., 15(1973)879.
68. M.J. Frouws, K. Vellenga and H.G.J. de Wilt, Biotech. Bioeng., 18(1976)53.
69. W.N. Marrazzo, R.L. Merson, and B.J. McCoy, Biotech. Bioeng., 17(1975)1515.
70. M. Moo-Young, H.W. Blanch, Adv. Biochem. Eng., 19(1981)1.
71. H.L. Pardue, Clin. Chem., 23(1977)2189.
72. L. Ögren, I. Csiky, L. Risinger, L.G. Nilsson, and G. Johansson, Anal. Chim. Acta, 117(1980)71.
73. R. Kühnau and J. Lasch, J. Theor. Biol., 84(1980)217.
74. G.E. Klinzing, Chem. Eng. Sci., 32(1977)1536.
75. R. Shyam, B. Davidson, and W.R. Vieth, Chem. Eng. Sci., 30(1975)669.
76. J.M. Reijn, H. Poppe, and W.E. Van der Linden, Anal. Chem., 56(1984)943.
77. C.C. Painton and H.A. Mottola, Anal. Chem., 53(1981)1713.
78. C.C. Painton and H.A. Mottola, Anal. Chim. Acta, 158(1984)67.

79. Ref. [3], p. 389.
80. T. Kobayashi and M. Moo-Young, Biotech. Bioeng., 13(1971)893.
81. S. Adachi, K. Hashimoto, R. Matsuno, K. Nakanishi, and T. Kamikubo, Biotech. Bioeng., 22(1980)779.
82. G. Guiochon, Anal. Chem., 53(1981)1318.
83. Y.T. Shiah and P.W. Carr, Anal. Chim. Acta, 167(1985)137.
84. W.J. Thomas and R.M. Wood, Chem. Eng. Sci., 22(1967)1607.
85. H.N. Chang and P.J. Reilly, Biotech. Bioeng., 20(1978)243.
86. R. Goldman, E. Katchalski, J. Theor. Biol., 32(1971)243.
87. S.A. Barker and P.J. Somers, Adv. Biochem. Eng., 10(1978)27.
88. R. Krishna and P.A. Ramachandran, J. Appl. Chem. Biotechnol., 25(1975)623.
89. P.A. Srere, B. Mattiasson, and K. Mosbach, Proc. Nat. Acad. Sci. USA, 70(1973)2534.
90. G.P. Hicks and S.J. Updike, Anal. Chem., 36(1966)726.
91. J. Ruzicka and E.H. Hansen, Anal. Chim. Acta, 78(1975)145.
92. H.J. Kunz and M. Stasny, Clin. Chem., 20(1974)1018.
93. B. Watson and M.H. Keyes, Anal. Lett., 9(1976)713.
94. S.K. Dahodvala, M.K. Weibel, and A.E. Humphrey, Biotech. Bioeng., 18(1976)1679.
95. P. Cremonesi and R. Bovara, Biotechnol. Bioeng., 18(1976)1487.
96. D.T. Bostick and D.M. Hercules, Anal. Chem. 47(1975)447.
97. L.M. Canning and P.W. Carr, Anal. Lett., 8(1975)354.
98. L.D. Bowers, L.M. Canning, C.N. Sayers, and P.W. Carr, Clin. CHem., 22(1976)1314.
99. L.D. Bowers and P.W. Carr, Clin. Chem., 22(1976)1427.
100. A. Schelter-Graf, H.-L. Schmidt and H. Huck, Anal. Chim. Acta., 299(1984)299.
101. C.W. Bradberry and R.N. Adams, Anal. Chem., 55(1983)2439.
102. I. Karube, K. Hara, H. Matsuoka, and S. Suzuki, Anal. Chim. Acta, 139(1982)127.
103. G. Decristoforo and F. Knauseder, Anal. Chim. Acta, 163(1984)73.
104. T. Yao, Y. Kabayashi, and S. Musha, Anal. Chim. Acta, 139(1982)363.
105. R. Appelqvist, G. Marko-Varga, L. Gorton, A. Torstensson, and G. Johansson, Anal. Chim. Acta, 169(1985)237.
106. T. Yao, M. Sato, Y. Kobayashi, and T. Wasa, Anal. Chim. Acta, 165(1984)291.
107. B. Watson, D.N. Stifel and F.E. Semersky, Anal. Chim. Acta, 106(1979)233.
108. T. Yao, Anal. Chim. Acta, 153(1983)175.
109. T. Yao, Y. Kobayashi, and S. Musha, Anal. Chim. Acta, 138(1982)81.
110. A.O. Lindberg, Anal. Chim. Acta, 152(1983)113.
111. G. Decristoforo and B. Danielsson, Anal. Chem. 56(1984)263.
112. I. Karube, K. Hara, I. Satoh, and S. Suzuki, Anal. Chim. Acta, 106(1979)243.
113. M. Masoom and A. Townshend, Anal. Proceed., 22(1985)6.
114. I. Satoh, B. Danielsson, and K. Mosbach, Anal. Chim. Acta, 131(1981)255.
115. A. Iob and H.A. Mottola, Anal. Chem., 52(1980)2332.
116. L.C. Clark Jr., in Methods in Enzymology, Vol. 56, Academic Press, New York, 1979, p. 448.
117. T.E. Barman, Enzyme Handbook, Vol. 1, Springer Verlag, New York, 1969.
118. H. Lundbäck, Ph.D. Thesis, University of Lund, 1984.
119. A. Hickling and W.H. Wilson, J. Electrochem. Soc., 98(1951)425.
120. L.C. Clark, Biotechnol. Bioeng. Symp., 3(1972)377.
121. P.R. Coulet and L.J. Blum, Anal. Lett., 16(1983)541.
122. L.C. Clark and G. Sachs, Ann. N.Y. Acad. Sci., 148(1968)133.

123. L.C. Clark, C. Duggan, T. Grooms, L. Hart, and M. Moore, Clin. Chem., 27(1981)1982.
124. D. Pfeiffer, F. Scheller, M. Jänchen, K. Bertermann, and H. Weise, Anal. Lett., 13 B(1980)1179.
125. L. Gorton, in press.
126. G. Osann, Poggendorf's Ann. 67(1845)372.
127. W.J. Blaedel and C.L. Olson, Anal. Chem., 34(1964)343.
128. C. Toshio, Y. Shigeru, and H. Shingo, Bunseki Kagaku, 32(1983)6.
129. E.L. Gulberg, A.S. Attiyat, and G.D. Christian, J. Autom. Chem., 2(1980)189.
130. T.T. Ngo and H.M. Lenhoff, Anal. Biochem., 105(1980)389.
131. D. Barham and P. Trinder, Analyst, 97(1972)142.
132. Ref [2], p. 149.
133. K. Zaitsu and Y. Onkura, Anal. Biochem., 109(1980)109.
134. H.Hwang and P.K. Dasgupta, Anal. Chim. Acta, 170(1985)347.
135. W.R. Seitz, in M.A. de Luca (Ed.), Methods in Enzymology, Vol. 57, Academic Press, New York, 1978, p. 445.
136. N.L. Malavolti, D: Pilosof, and T.A. Nieman, Anal. Chim. Acta, 170(1985)199.
137. C. Ridder, E.H. Hansen, and J. Ruzicka, Anal. Lett., 15(1982)1751.
138. P.J. Worsfold, J. Farrelly, and M.S. Matharu, Anal. Chim. Acta, 164(1984)103.
139. D.C. Williams and W.R. Seitz, Anal. Chem., 48(1976)1478.
140. P. van Zoonen, D.A. Kamminga, C. Gooijer, N.H. Velthorst, and R.W. Frei, Anal. Chim. Acta, 167(1985)249.
141. D. Klockow and P. Jacob in W. Jaeschke and V. Mohner (Eds.), Chemistry of Multiphase Atmospheric Systems, Springer-Verlag, Berlin, 1984.

Appendix

IMPROVEMENT OF AN ENZYMATIC FLOW INJECTION METHOD FOR THE DETERMINATION OF OXYGEN[a)]

Bo Olsson

An enzymatic flow injection method for the determination of dissolved oxygen was described previously [1]. Oxygen in the sample is quantitatively reduced to hydrogen peroxide in a packed-bed reactor containing immobilized glucose oxidase with β-D-glucose as the hydrogen donor. A chromogenic reaction in a reactor containing immobilized peroxidase is used for spectrophotometric detection of the hydrogen peroxide. The performance of the previous method was limited by adsorption of the coloured product to the enzyme support. The present method uses an improved combination of colour reagent and immobilized peroxidase preparation [2]. The method was used to monitor oxygen in a reaction medium for microbial production at dihydroxyaceton from glycerol [3].

Experimental

A reactor (84 µl) containing diazoimmobilized glucose oxidase [1] and a reactor (55 µl) containing tresyl immobilized peroxidase [2] were prepared as described previously and inserted into a flow injection system (Fig. 1). The reagent was a solution of 3 mM D-glucose, 1 mM 4-aminophenazone, 10 mM 2,4-dichlorophenol-6-sulphonate, and 1 mM 2,4-dichlorophenol in a 0.1 M citrate buffer, pH 6.0. The reaction medium consisted for 0.5 M glycerol and 5 mM calcium chloride in 50 mM succinate buffer, pH 5.0. Th carrier was destilled water or fresh reaction medium, depending on the sample. The reagent, carrier, and a box confining the system was flushed with nitrogen as described before [1]. The flow rate was 0.5 ml min^{-1} in each channel and the injection volume was 20 µl.

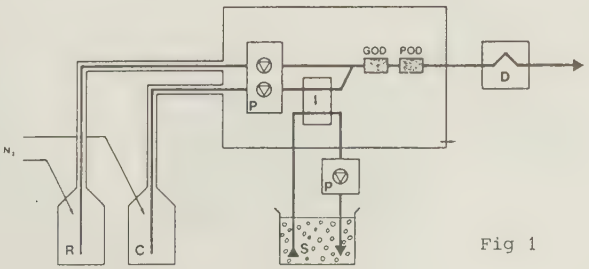

Fig 1

Results and Discussion

Fig. 2 shows the peak absorbance as a function of oxygen tension for destilled water samples. The limit of detection was 0.5 μM O_2 (po_2 = 0.0004 atm) and the response was linear up to 1 mM O_2 (po_2 = 0.8 atm). The relative standard deviation was 0.2% (n=10) for air saturated samples and 0.5% (n=13) for samples with ten times lower concentration. The sample throughput was 120 samples h^{-1} with baseline separation.

In Fig. 3 the oxygen concentration in the reaction medium was followed with time. The six first peaks at the right hand side of the figure were obtained with air saturated water and illustrate the higher solubility of oxygen in the absence of dissolved matter. A Clark oxygen electrode was used for simultaneous measurement of the oxygen tension (feint line). Beads of alginate-immobilized Gluconobacter oxydans was added to the air saturated medium and the oxygen level was followed by both methods.

References

1. Paper V
2. Paper III
3. H. Lundbäck, G. Johansson, and O. Holst, Anal. Chim. Acta, 155(1983)47.

a) presented at the International Symposium on Analytical Methods and Problems in Biotechnology, ANABIOTEC '84, Noordwijkerhout, The Netherlands, 1984.

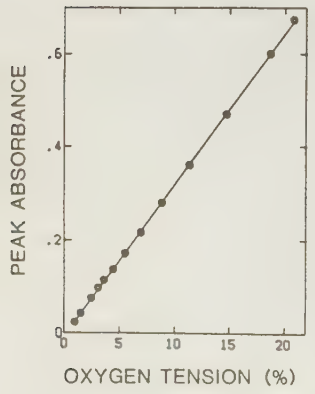

Fig 2

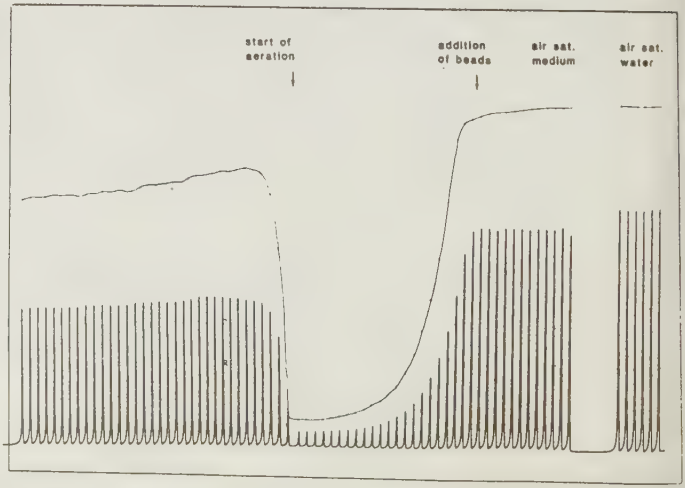

Fig 3

I

Analytica Chimica Acta, 136 (1982) 113—119
Elsevier Scientific Publishing Company, Amsterdam — Printed in The Netherlands

DETERMINATION OF HYDROGEN PEROXIDE IN A FLOW SYSTEM WITH MICROPEROXIDASE AS CATALYST FOR THE LUMINOL CHEMILUMINESCENCE REACTION

BO OLSSON

Analytical Chemistry, University of Lund, P.O. Box 740, S-220 07 Lund (Sweden)

(Received 14th September 1981)

SUMMARY

Hydrogen peroxide is determined by a chemiluminescence method with a reagent containing 100 μM luminol and 3 μM microperoxidase at pH 10 (carbonate buffer). Microperoxidase is superior to hematin as a catalyst. The method uses an automated flow injection system with a throughput of 2 samples per minute. The log—log calibration plot is linear (slope 1.3) from the detection limit, 3×10^{-9} M up to 10^{-5} M H_2O_2. The background emission is low. Impurities in the carrier stream and from some plastics may cause elevated background unless precautions are taken.

Determination of hydrogen peroxide by chemiluminescence offers numerous advantages [1, 2] compared to other methods. In spite of this, the methods have been relatively little studied. Diacylhydrazides such as luminol (5-amino-2,3-dihydro-1,4-phthalazinedione) or diaryloxalates such as TCPO (bis(2,4,6-trichlorophenyl)oxalate) have been the preferred reagents. The luminol reaction proceeds in aqueous alkaline solutions and the oxalate reaction shows luminescence in neutral, partly organic solvents. The diaryloxalate reaction is sensitized with a fluorophore, and the diacylhydrazide reactions are catalyzed by transition metal ions or heme-containing compounds. The type of catalyst has a profound effect on the behavior of the system.

The commonest catalyst for hydrogen peroxide determination with luminol has been hexacyanoferrate(III). The sensitivity is very high but the background is large. The background must be controlled in order to get a low detection limit. This can be achieved with a pulseless pump and a flow system [3]. Copper(II) has also been used as catalyst. Kok et al. [4] have recently shown that the response is linear and that the background and detection limit are low.

Schroeder and Yeager [5] found that hydrogen peroxide with hematin or microperoxidase provided the most sensitive reagents for the determination of luminol. Likewise, luminol and hydrogen peroxide have been used for the determination of heme compounds, with hematin giving the highest response [6]. The present study reports results obtained with hematin or microperoxidase as catalyst for the chemiluminescence determination of hydrogen peroxide with luminol.

0003-2670/82/0000-0000/$02.75 © 1982 Elsevier Scientific Publishing Company

EXPERIMENTAL

Apparatus

A flow injection system was assembled as shown in Fig. 1. The pump, a Gilson Minipuls 2, provided flow rates of 1 ml min^{-1} for the reagent and carrier lines and 2 ml min^{-1} for the sample line. Viton tubing (1.0 mm i.d.) was used because ordinary vinyl and silicone tubing enhanced the background emission. The injection device was a Cheminert sample injection valve SVA 8031 equipped with two pneumatic actuators, automated by a pneumatic regulator-timer with a load-injection cycle of 15 + 15 s. The sample volume was 200 μl, and the loop was filled by suction.

The light detector was an LKB-Wallac Luminometer 1250 modified to accept a flow-through cell. The injection port of the instrument was replaced by a metal feed-through pipe, bent in order to reduce the amount of light transmitted into the cell through the connecting tubing. The cell was a W-shaped glass-tube (1.0 mm i.d.) mounted close to the photomultiplier tube, with a mirror behind. The cell volume was 80 μl. The manifold consisted of PTFE tubing (0.5 mm i.d.) with a mixing T-joint made as described by Frei et al. [7]. The output signal was displayed on a recorder.

Chemicals

Luminol (Sigma A-8511) was converted to the monosodium salt with sodium hydroxide and purified by double recrystallization from basic aqueous solution [8]. Hematin (Sigma H-3505) and microperoxidase, MP-11 (Sigma M-6756) were used as received. The various reagent mixtures were prepared from 1 mM stock solutions of luminol, hematin and microperoxidase made up in the particular buffer used. Stock 0.01 M hydrogen peroxide solutions were prepared from perhydrol (30%; Merck 7209) each day. The concentration was determined by titration with permanganate. Immediately before use, the stock solution was diluted in polypropylene test tubes with a Hamilton Digital Dilutor. Water purified by a Millipore-Q system caused a high background. Ordinary distilled water from the central distillation system varied in quality but delivered acceptable water most of the time. It was collected and stored in a polyethylene container.

All other chemicals were of analytical grade.

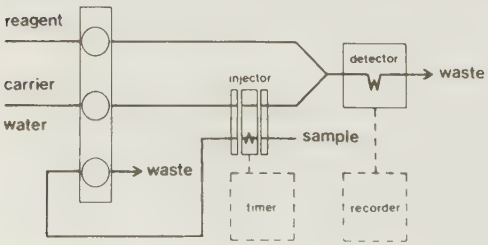

Fig. 1. The flow injection system. For details, see text.

Procedures

A static system was used for investigations of the effect of different buffer species on the peak light intensity and the chemiluminescence—time response. Test tubes with 1 ml of reagent (30 μM luminol and 10 μM catalyst in 0.1 M buffer, pH 12.4) were inserted into the luminometer in the normal way and 1 ml of 1×10^{-6} M hydrogen peroxide was injected.

In all other experiments the flow injection system was utilized. The pH profiles were obtained with 30 μM luminol and 10 μM hematin in 0.1 M phosphate buffer or with 30 μM luminol and 10 μM microperoxidase in 0.1 M carbonate buffer. The dependence on reagent concentrations was established via a three-dimensional luminol/catalyst—peak intensity plot using 0.1 M phosphate buffer, pH 12.4, for the hematin system and 0.1 M carbonate buffer, pH 10.0, for the microperoxidase system.

RESULTS

The relation between the light intensity and the concentration of the various reactants was found to be very complicated. The background emission also depended on the reagent composition. The reagent concentrations required to optimize the signal-to-noise ratio were different from those needed to optimize the emission intensity itself. Consequently, the optimum conditions reported by Schroeder and Yeager [5] for luminol determination with 0.09 M hydrogen peroxide will be completely different from the optimum conditions for the determination of traces of hydrogen peroxide.

Microperoxidase

When the microperoxidase-containing reagent solution was mixed with hydrogen peroxide in a static system, the emission increased rapidly, achieving 90% of the maximum intensity in a few seconds. The maximum was reached after about 25 s and the time between the half-height points was ca. 40 s. The intensity—time response varied with the reagent composition and the hydrogen peroxide concentration as well as with the manner of mixing. The buffer constituents (sodium carbonate, borate, phosphate or barbitone) had little influence on the peak height or the intensity—time response. The peak intensity in the carbonate buffer was the highest and carbonate buffer was therefore used in all subsequent experiments.

The flow injection system described in Fig. 1 gives a mean reaction time of 8 s. A longer delay did not significantly enhance the response. The timing involves a compromise between reaction rate and dispersion. A short reaction time gives a low dispersion and also a high sample throughput. For a 200-μl sample, the peak occurs 15 s after injection, with a peak height equal to the steady-state level. The set-up allows for a through-put of 120 samples per hour. The optimization described below was examined with the flow injection technique.

As can be seen in Fig. 2A, there is a steep rise in the peak intensity with increasing pH up to pH 10, where it levels off. It starts to rise again at pH 11.5

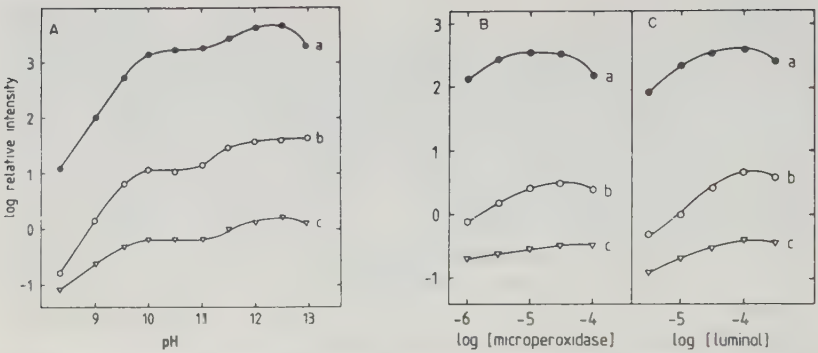

Fig. 2. Emission as a function of pH and reagent concentrations. Curves: (a) 1×10^{-6} M H_2O_2; (b) background emission; (c) peak-to-peak noise. A, pH variable, with 10 μM microperoxidase and 30 μM luminol reagent; B, microperoxidase variable (1—100 μM) with 30 μM luminol in 0.1 M carbonate buffer, pH 10.0; C, luminol variable (3—300 μM) with 10 μM microperoxidase in 0.1 M carbonate buffer, pH 10.0.

and reaches a maximum at pH 12.5. The peak-to-peak noise also increases with pH in a similar pattern. At the lowest pH, the main portion of the noise originates from the instrument. Consequently a larger cell volume would improve the detection limit at this pH, but only at the expense of a lower sample throughput. The background emission, which is caused by impurities in the carrier stream, increases with increasing pH, and becomes the dominating source of noise. This background is automatically subtracted. The signal-to-noise ratio increases up to pH 10 and becomes almost constant at higher pH values. As a low pH is desired in many applications, such as the enzyme-coupled analysis of clinical samples, a reaction pH of 10.0 was chosen. However, a pH as low as 8.3 can be used if a poorer detection limit is acceptable.

The variation of peak height with changes in the microperoxidase and luminol concentration is shown in Fig. 2B and C. Additional measurements (not shown) were made so that the three-dimensional parameter field was covered. The detection limits with different reagent concentrations are affected by the signal-to-noise ratio and the slope of the calibration curve, and are shown in Table 1; the values are $\geqslant 3$ nM hydrogen peroxide. The peak intensity varies by an order of magnitude with changes in reagent concentration, so that optimization is important. Maximum emission, obtained from 30 μm microperoxidase and 100 μM luminol, coincides with the conditions giving the best detection limit (Table 1). The maxima in Fig. 2, however, are rather flat, and, as microperoxidase is expensive, reagent consumption can be minimized. Thus, for practical purposes, the best reagent composition is 3 μM microperoxidase and 100 μM luminol, which gives about 60% of the maximum intensity and only a slightly inferior detection limit. An additional advantage is that, under these conditions, moderate changes in reagent composition have little or no effect on the sensitivity. A two-fold increase or

TABLE 1

Detection limits (nM H_2O_2) at pH 10.0

Luminol (μM)	Microperoxidase (μM)				
	1	3	10	30	100
3	12	—	10	—	—
10	—	7	6	8	—
30	7	5	5	5	6
100	—	4	4	3	—
300	13	—	7	—	—

decrease in reagent concentration changes the slope by less than 1%. The selected composition will work over the whole pH range covered in Fig. 2A, but whether this composition is the best at pH values other than 10.0 has not been investigated.

Figure 3 shows some log—log calibration graphs. Curve a for pH 10.0 has two linear segments; the slope of the lower part (1.3) is constant over almost four orders of magnitude of peroxide concentration. For curve b, pH 9.0, the intersection between the lines occurs at a lower peroxide concentration, and for curve c, pH 8.3, the intersection is presumably below the detection limit. The slope of the lower segment (which is missing in curve c) was found to be the same (±10%) between pH 9 and 12.

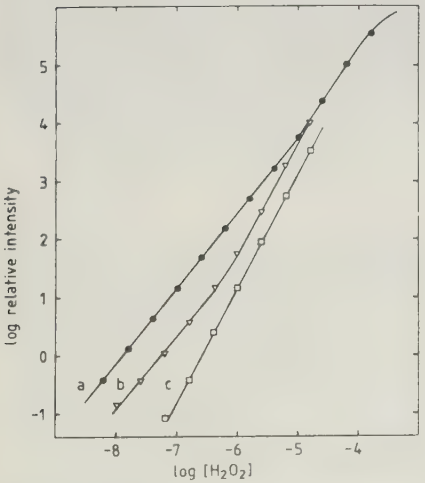

Fig. 3. Emission as a function of hydrogen peroxide concentration; 3 μM microperoxidase, 100 μM luminol in 0.1 M carbonate buffer. (a) pH 10.0; (b) pH 9.0; (c) pH 8.3.

The mixed reagent, 3 μM microperoxidase with 100 μM luminol in 0.1 M sodium carbonate buffer, pH 10.0, could be used for several weeks. The intensity of the emission decreased to about 50% after one week and to 25% after one month when the reagent was stored at room temperature. The response of the system differed from one batch of reagent to another. The relative standard deviation was 0.3% for 7 replicate measurements on a 1×10^{-6} M hydrogen peroxide solution. The detection limit typically was $2–4 \times 10^{-9}$ M peroxide (signal-to-noise ratio = 2).

Hematin

The hematin-containing reagent was investigated as outlined above for the microperoxidase system. The intensity—time response was similar to that of the microperoxidase reagent. The effect of buffer constituents was more important; phosphate was better than carbonate, with the other buffers giving even lower responses. The intensity increased steeply with pH up to pH 12, above which it became constant. The two-parameter reagent composition response was studied at pH 12.4. The maximum intensity, the best signal-to-noise ratio and the best detection limit were found at significantly different concentrations, in contrast to the microperoxidase system. A reagent composition of 3 μM hematin and 30 μM luminol in 0.1 M phosphate buffer gave a good detection limit (1×10^{-8} M H_2O_2) and an adequate signal-to-noise ratio. The batch-to-batch reproducibility for different preparations of the reagents was poor, however, and the slope of the log—log calibration graph (1.4) changed to 1.1 below 10^{-6} or 10^{-7} M peroxide with some batches, whereas with others it remained constant down to the detection limit.

The light intensity at the above optimum reagent concentration was an order of magnitude lower with hematin than with microperoxidase. A number of other disadvantages were obvious compared with the latter system. The detection limit and reproducibility were poorer, the shape of the calibration curve varied with reagent preparation and a higher pH was required.

DISCUSSION

The microperoxidase-containing reagent described above offers several advantages over previously used reagents. The flow injection system also contributes to the overall performance of the method. As with the copper(II) catalyst, the background emission is very low compared to that with the much used hexacyanoferrate(III). A peristaltic pump can therefore be used in contrast to the pulseless pump required with the latter. A very good detection limit can be obtained at a reaction pH of 10. Microperoxidase can, in contrast to the other catalysts mentioned, be used in weakly alkaline solutions. At a reaction pH of 8.3, the detection limit is 20-fold poorer than the best value.

At pH 10, reductants like uric acid interfere by reaction with hydrogen peroxide so that an erroneous result will be obtained unless the concentration

of the reductant is at least an order of magnitude lower than that of the peroxide. It is likely that this effect is less severe at a reaction pH of 8.3. Slightly acidic reagents using peroxyoxalate chemiluminescence have been developed to overcome this problem [9, 10]. However, the requirement of an organic co-solvent introduces new problems. Some solvents like dioxan were found, in this laboratory, to give a very troublesome background emission because of peroxide formation, whereas other solvents gave a poor detection limit. Mixing problems can also arise. A new method with *t*-butanol has been reported to give a detection limit of 2×10^{-6} M at a reaction pH of 8 [11].

The repeatability of the present system is very good, probably because of the automatic injection system, the low background and the absence of mixing problems. The day-to-day reproducibility is less good, owing to reagent ageing and batch-to-batch variations, the causes of which are unknown. It is therefore essential to prepare a new calibration curve each day, and when the reagent or water has been changed. The response of the system is proportional to $[H_2O_2]^n$ where $n > 1$ (≈ 1.3). This reflects an uncertainty of the mechanism and stoichiometry which is not present with some of the other methods. The validity of analytical results, therefore, must be checked more carefully than with other chemiluminescence methods as a changed stoichiometry could be an added cause of interference.

As the detection limit was improved, a number of new problems became apparent. The purity of the water and contamination from pump tubing, sample vials and other components was the most troublesome. The type of contaminants are unknown but peroxides or other oxidants may leak from compounded plastics. Pure polymers like teflon, viton and polyethylene caused no problems. A redistillation of the water in a quartz-still did not reduce the background, nor did bubbling nitrogen through the water.

The author thanks Professor Gillis Johansson and Dr. Lars Ögren for valuable discussions concerning this work.

REFERENCES

1 W. R. Seitz, in M. A. de Luca (Ed.), Methods in Enzymology, Vol. 57, Academic Press, New York, 1978, p. 445.
2 T. P. Whitehead, L. J. Kricka, T. J. N. Carter and G. H. G. Thorpe, Clin. Chem., 25 (1979) 1531.
3 D. T. Bostick and D. M. Hercules, Anal. Chem., 47 (1975) 447.
4 G. L. Kok, T. P. Holler, M. B. Lopez, H. A. Nachtrieb and M. Yuan, Environ. Sci. Technol., 12 (1978) 1072.
5 H. R. Schroeder and F. M. Yeager, Anal. Chem., 50 (1978) 1114.
6 H. A. Neufeld, C. J. Conklin and R. D. Towner, Anal. Biochem., 12 (1965) 303.
7 R. W. Frei, L. Michel and W. Santi, J. Chromatogr., 142 (1977) 261.
8 E. H. Huntress, L. N. Stanley and A. S. Parker, J. Am. Chem. Soc., 56 (1934) 241.
9 V. I. Rigin, Zh. Anal. Khim., 33 (1978) 1623.
10 D. C. Williams III, G. F. Huff and W. R. Seitz, Anal. Chem., 48 (1976) 1003.
11 G. Scott, W. R. Seitz and J. Ambrose, Anal. Chim. Acta, 115 (1980) 221.

II

Analytica Chimica Acta, 145 (1983) 87—99
Elsevier Scientific Publishing Company, Amsterdam — Printed in The Netherlands

OPTIMIZATION OF PEROXIDASE IMMOBILIZATION AND OF THE DESIGN OF PACKED-BED ENZYME REACTORS FOR FLOW INJECTION ANALYSIS

BO OLSSON* and LARS ÖGREN[a]

Department of Analytical Chemistry, University of Lund, P.O. Box 740, S-220 07 Lund (Sweden)

(Received 1st August, 1982)

SUMMARY

Packed-bed reactors containing horse radish peroxidase were optimized for use in flow injection systems. The most active and stable immobilizations were produced by azo linkage to porous glass. The influence of pore and particle diameter as well as pH of immobilization, number of coupling sites, and enzyme purity were studied. The reactor behaviour could be accurately described by a theory derived on the assumptions of first-order kinetics. The effects of internal and external mass transfer resistances were studied and the rate constants were evaluated. Design criteria for analytical reactors are discussed. A small particle diameter is shown to be of utmost importance in order to achieve low dispersion with fixed levels of back-pressure and conversion.

Although there are many theoretical treatments that can be applied to enzyme reactors in analytical flow systems, there are few relevant experimental data for the actual design. High conversion efficiency and low dispersion are of paramount importance analytically, in contrast to bioengineering where cost and productivity must be given the greatest weight. The design criteria thus differ considerably and it might be of interest to study in some detail how the variables should be selected for an analytical system. Packed-bed enzyme reactors have already been used in flow injection analysis [1, 2] and the success of the approach makes it interesting to work through an optimization in order to assess the importance of the physical parameters.

It is advantageous to convert essentially all the substrate to products [3, 4]. This can of course be accomplished by packing a sufficiently large reactor with the enzyme at hand. When low dispersion is essential for sensitivity and sample throughput, the dispersion can of course be decreased by using a smaller reactor and sacrificing some efficiency. The present study was undertaken to learn to what extent the dispersion (in practice, the mean residence time) can be decreased while 99.9% conversion is maintained. The strategy was to optimize the activity of the immobilized enzyme as well as the bed geometry.

---

[a]Present address: AB Draco, P.O. Box 1707, S-221 01 Lund (Sweden)

0003-2670/83/0000-0000/$03.00 © 1983 Elsevier Scientific Publishing Company

Peroxidase reactors are used in a method for determination of dissolved oxygen in a flow injection system [5] and for determination of β-D-glucose [1]. In both methods, hydrogen peroxide is produced on-line in another reactor containing immobilized glucose oxidase. The overall reaction between hydrogen peroxide, peroxidase and chromogens can be represented by

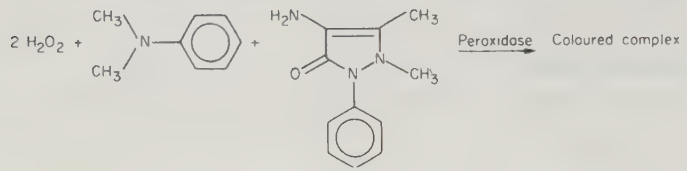

(1)

The peroxidase is first oxidized by hydrogen peroxide in a well-defined step [6]. The back-reduction takes place through an oxidative coupling of 4-aminophenazone and *N*,*N*-dimethylaniline. The reaction is only partly known [7, 8].

THEORY

Evaluation of the apparent rate constant of the immobilized enzyme

The overall kinetics of an enzyme immobilized within a porous support can be described by its apparent kinetic behaviour, which thus incorporates the resistance to mass transfer. Many enzymes with a complicated reaction scheme can be well approximated by Michaelis—Menten kinetics, which in turn can be replaced by a pseudo first-order expression, provided that the substrate concentration, S, is much smaller than the apparent Michaelis constant; thus for $S \ll K_M^{(app)}$,

$$-\mathrm{d}S/\mathrm{d}t = V_{max}^{(app)} S/(K_M^{(app)} + S) \rightarrow V_{max}^{(app)} S/K_M^{(app)} = K_{ps}^{(app)} S \qquad (2)$$

$K_{ps}^{(app)}$ is the apparent rate constant (s^{-1}) of the pseudo first-order reaction. The integral expression is obtained in the usual way

$$-\ln (S_t/S_0) = K_{ps}^{(app)} t \qquad (3)$$

where S_0 and S_t are the substrate concentrations at time 0 and t, respectively. For a reactor, the concentration at the inlet corresponds to S_0 and at the outlet to S_t, and, for steady-state measurements, the time coordinate corresponds to τ, the mean residence time (s). It is convenient to replace S_t/S_0 by $(1 - X)$ where X is the fractional conversion in the reactor

$$K_{ps}^{(app)} = -[\ln (1-X)]/\tau \qquad (4)$$

The mean residence time equals (reactor volume) × (total void fraction)/(volumetric flow rate). The fractional conversion, X, approaches unity as the reaction approaches completion. Reactors with fractional conversions in the range $X \approx 0.3$—0.7, give the most accurate values of $K_{ps}^{(app)}$.

It will be shown later that the first-order approximation is fully permissible for the peroxidase reactors.

Evaluation of the rate constant at zero external mass transfer resistance

The substrate concentration, S, at the (external) surface of a particle containing a catalyst will always be lower than the bulk concentration, S^*. The amount of depletion depends on the efficiency of the catalyst as well as on the thickness of the diffusion layer around the particles. It can be neglected for very slow reactions and very high linear flow velocities.

At steady state, the rate of transport to the particle surface will equal the rate of the reaction. For a (pseudo) first-order reaction

$$h\,(S^* - S) = K_{ps}\,S \tag{5}$$

where h is the transport coefficient (s^{-1}) and K_{ps} the rate constant (s^{-1}) at zero external mass transfer resistance. The rate can also be expressed by the apparent rate constant and the bulk concentration

$$K_{ps}^{(app)}\,S^* = K_{ps}\,S \tag{6}$$

Combination of Eqns. (5) and (6) and rearrangement gives

$$(K_{ps}^{(app)})^{-1} = h^{-1} + (K_{ps})^{-1} \tag{7}$$

Many expressions for h have been discussed by Karabelos et al. [9]. A correlation proposed by McCune and Wilhelm [10] and experimentally validated for porous glass by Rovito and Kittrell [11], can be rewritten in the form

$$h = 1.625\,a_m\,F\,(Sc)^{-2/3}\,(Re)^{-1/2} \tag{8}$$

where F is the linear flow velocity (m s^{-1}) and Sc and Re are the Schmidt and Reynold numbers. The constant is dimensionless. The external surface area per unit volume, a_m (m^{-1}), can be related to the particle size, d_p. For spherical geometry,

$$a_m = 6(1 - \epsilon_E)/d_p \tag{9}$$

where ϵ_E is the external void fraction. Substitution of Eqn. (9) into Eqn. (8) and insertion of expressions for Sc and Re gives

$$h = F^{1/2} d_p^{-3/2}\,B \tag{10}$$

$$\text{with } B = 9.75\,(1 - \epsilon_E)\,D_m^{2/3}\,\nu^{-1/6} \tag{11}$$

where D_m is the molecular diffusion coefficient ($m^2\ s^{-1}$) and ν the kinematic viscosity ($m^2\ s^{-1}$). Substitution of Eqn. (10) into Eqn. (7) gives

$$(K_{ps}^{(app)})^{-1} = d_p^{3/2}\,B^{-1}\,F^{-1/2} + (K_{ps})^{-1} \tag{12}$$

The final equation shows that K_{ps} can be evaluated from a series of $K_{ps}^{(app)}$ determined at various flow rates. Conversely, when K_{ps} is known, the effect of linear flow velocity on $K_{ps}^{(app)}$ can be predicted. $K_{ps}^{(app)}$ will increase as F increases, and at the limit, when the external mass transfer becomes infinitely fast, it will equal K_{ps}.

Evaluation of the inherent rate constant

Because of the limited rate of diffusion, there will be a gradual decrease of substrate concentration inwards towards the center of the particle, as the substrate is continually converted to products. The extent to which the reaction rate is lowered is expressed by the effectiveness factor, η_i, which for a (pseudo) first-order reaction is equal to the ratio of the rate constants

$$\eta_i = \text{external attainable rate/inherent rate} = K_{ps}/K \quad (13)$$

where K is the inherent rate constant (s^{-1}), free of all mass transfer resistance.

A full expression for η_i involves the appropriate differential equations for the rates. The solution [12] is

$$\eta_i = (1/\phi_s)\,[(1/\tanh 3\phi_s) - (1/3\,\phi_s)] \quad (14)$$

where the Thiele modulus for spherical geometry, ϕ_s, is

$$\phi_s = (d_p/6)\,(K/D_{eff})^{1/2} \quad (15)$$

with D_{eff} as the effective substrate diffusivity in the pores ($m^2\ s^{-1}$). K can be calculated from a series of K_{ps} values measured at various particle diameters.

A closer study of Eqns. (13—15) shows that for large values of ϕ_s (e.g., large d_p) the K_{ps} will be inversely proportional to d_p. For small ϕ_s (e.g., small d_p) K_{ps} will in the limit become independent of d_p. The internal mass transfer resistance is then negligible and a further reduction of d_p will not increase η_i, which already is close to unity.

EXPERIMENTAL

Immobilization of peroxidase

Horse radish peroxidase, EC 1.11.1.7. (Sigma, Type I, P-8125 and Type VI, P-8375) was immobilized on alkylamino- as well as arylamino-derivatized controlled-pore glass (CPG-10, Electro-Nucleonics, Fairfield, NJ, U.S.A.) by methods described by Weetall [13]. Different pore and particle sizes were used as well as different conditions for coupling (pH, enzyme purity, concentration of coupling sites).

Glutaraldehyde coupling to alkylamino glass. Acid-washed (boiling 5% nitric acid, 1 h) controlled-pore glass was treated (3 h, 75°C) with an aqueous 10% solution of 3-aminopropyltriethoxysilane (Merck, 821618) at pH 3.45. The preparation was dried overnight at 95°C to allow storage. A portion (0.5 ml) of glutaraldehyde solution (BDH Chemicals) 2.5% in 0.1 M phosphate buffer pH 7.0, was added to 50 mg of alkylamino glass. The reaction proceeded for 1 h at room temperature, initially at reduced pressure. Peroxidase (Type VI, 5.00 mg) in 0.25 ml of 0.1 M phosphate buffer pH 7.0, was added to the moist glass and the reaction was allowed to proceed overnight at 4°C. Each of the above steps was followed by extensive washing on a G3 glass filter.

Azo coupling to arylamino glass. The glass was aminated as described

above. A commercial organically aminated alkylamino glass was also used (Pierce, aminopropyl-CPG, 50-nm pore diameter, 80—120 mesh). The alkylamino glass was acylated by refluxing in a solution of 3% *p*-nitrobenzoyl chloride (analytical-reagent grade) in chloroform, also containing 5% triethylamine (Fluka, p.a.), for 4 h. The nitro group was reduced by boiling the glass in an aqueous 5% solution of sodium dithionite for 1 h. The arylamino glass was dried overnight at 95°C to allow storage. Diazotization was done at 0°C by mixing 50 mg of arylamino glass with 1 ml of 2 M HCl and adding 20 mg of solid sodium nitrite. The reaction was allowed to proceed for 30 min, initially at reduced pressure. Peroxidase (Type VI or Type I, 5.0 mg) in 0.25 ml of 0.1 M phosphate buffer pH 8.5 (alternatively pH 7.0 and 6.0) was added to the cold glass and the reaction was allowed to continue overnight at 4°C. Each of the above steps was followed by extensive washing on a G3 glass filter.

Characterization. The coupling yield was determined from the difference in optical absorbance before and after immobilization. The coupling yield of peroxidase was measured at 403 nm (ϵ = 91 cm^2 μmol^{-1} [14]) and of protein at 280 nm. Excess of reagent and the first washings were combined for the determinations of the yield.

Reagent

A phosphate buffer, 0.1 M, pH 6.0 was made 0.75 mM with respect to 4-aminophenazone (BDH Chemicals) and 2.5 mM with respect to *N,N*-dimethylaniline (99.5%; Riedel-de Haën). The substrate, hydrogen peroxide (Merck, Perhydrol), was also added to the solution (0.05 mM, except when otherwise stated).

Procedures

The combined reagent and substrate was pumped through the reactors with a peristaltic pump (Gilson, Minipuls 2) and the absorbance was measured at 555 nm with a flow-through spectrophotometer (Spectra Physics, model 770). The fractional conversion was taken as the absorbance ratio of the reactor under test compared to a 100-μl reactor known to give 100% conversion (no change in absorbance on a second pass). The reactors were mounted in the loop of a slide injector so that the reagent blank could be checked frequently. All measurements were made at 25.0°C.

The time stability was assessed by pumping combined reagent and substrate through 5-μl reactors continuously (3.0 ml h^{-1}) for 11 days. The fractional conversion was determined once every 24 h at a flow rate of 2 ml min^{-1}. The reactors were then stored for 22 days at 4°C and after that the fractional conversion was measured again.

The volumes of the reactors were 5 μl (1.25 mm i.d., length 4.1 mm), 20 μl (2.5 mm i.d., length 4.1 mm) and 84 μl (2.7 mm i.d., length 14.7 mm). The total and external void fractions were 0.82 and 0.48, respectively, as calculated from the densities of porous glass and silica, the specific

pore volume, and the packing density. The packing density was determined on a larger batch as 0.34 g ml^{-1}. The void fractions depend on packing and may differ from one reactor to another. The mean particle diameters were taken from the manufacturers data (see Table 3).

RESULTS AND DISCUSSION

Immobilization of peroxidase

Peroxidase has been immobilized on a variety of organic and inorganic materials. Coupling to porous glass has been accomplished with, e.g., glutaraldehyde [15], isothiocyanate [16], fluorodinitrobenzene [17], acrylic copolymers [18], and diazonium linkages [19]. Thibault et al. [15] reported on the optimization of glutaraldehyde coupling of peroxidase to porous glass. The activity and stability were found to be inferior to azo coupling.

The time stability of azo-bound peroxidase was measured on 5-μl reactors (Fig. 1). Corresponding measurements on glutaraldehyde-bound peroxidase are shown for comparison. It can be seen that the azo coupling gave a higher loading, was more active and had a better long-term stability. Preparations stored for six months in a refrigerator did not lose much activity.

All batches stabilized in the same way (Fig. 1) and measures of conversions cited in the following paragraphs relate to the stable values. Porous glass can be silylated in an aqueous or organic solvent. The latter method will introduce a larger amount of amino functional groups. Weetall [13] states that

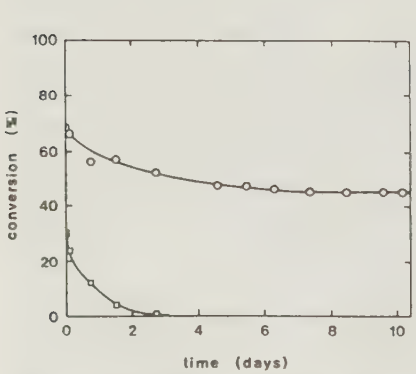

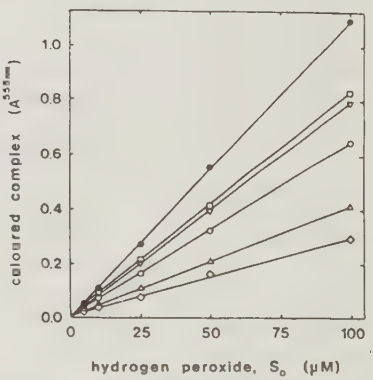

Fig. 1. Time stability of peroxidase (POD), immobilized to CPG (50 nm, 80—120 mesh): (○) azo-bound, 29 mg POD g^{-1} glass; (□) glutaraldehyde-bound, 3 mg POD g^{-1} glass.

Fig. 2. Product formation as a function of substrate concentration. (•) Complete conversion (100-μl reactor). Open symbols correspond to the 5-μl reactor with flow rates of: (□) 0.55, (▽) 1.0, (○) 2.0, (△) 4.4 and (◇) 7.5 ml min^{-1}.

the methods are of almost equal use but that the former results in a slightly more stable product. The present results (Table 1) conform essentially to earlier knowledge and aqueous silylation was used in the rest of the study. The pH during the immobilization was varied (Table 2) and it was found that more peroxidase was bound as the pH was increased. The activity is also superior for the batch made at pH 8.5.

Table 3 shows the effect of varying the pore size and the particle size of the glass, as well as the enzyme purity. It is well documented that the loading of enzyme increases with the surface area until the pores become too small for free entrance of the enzyme [20]. The coverage decreases slightly with

TABLE 1

Azo coupling of Type VI peroxidase to CPG (50 nm, 80—120 mesh). Effect of silylation technique

Silylation technique	Aqueous	Organic
POD yield (mg g^{-1})	29	26
Conversion (%)	45	50
$K_{ps}^{(app)}$ (s^{-1})	4.9	5.6

TABLE 2

Azo coupling of Type VI peroxidase to CPG (33 nm, 120—200 mesh). Effect of immobilization pH

pH of immobilization	6.0	7.0	8.5
POD yield (mg g^{-1})	22	35	58
Conversion (%)	70	71	76
$K_{ps}^{(app)}$ (s^{-1})	9.8	10.1	11.6

TABLE 3

Effect of enzyme purity, pore diameter, and particle size on the azo coupling of peroxidase to CPG

Enzyme purity	26% (Type I)			80% (Type VI)			80% (Type VI)
Mesh numbers	120—200			120—200			80—120
Mean part. diam. (μm)	←——— 100 ———→			←——— 100 ———→			150
Pore diam. (nm)	25	33	72.9	25	33	72.9	72.9
Area (m^2 g^{-1})	105	80	34	105	80	34	34
POD yield (%)	53	37	19	81	71	35	33
POD yield (mg g^{-1})	14	10	5	67	58	29	27
Protein yield (mg g^{-1})	70	71	66	68	62	35	30
Purity (% POD)	20	14	8	99	94	83	89
Coverage (mg POD m^{-2})	0.13	0.12	0.15	0.64	0.73	0.86	0.78
Conversion (%)	38	34	—	81	76	70	43
$K_{ps}^{(app)}$ (s^{-1})	3.9	3.4	—	13.5	11.6	9.8	4.6

increased area because of steric effects or a depletion of reagent. Thibault et al. [15] found the highest loading at a pore diameter of 15—25 nm.

The purity of the immobilized product was excellent with Type VI peroxidase but with Type I it was lower than that of the starting material. The preferential binding of impurities was even more marked for glutaraldehyde immobilization. Only 33% of the bound protein consisted of peroxidase, although Type VI enzyme was used. The purity of the preparation increased as the pore diameter decreased (Table 3), which indicates that some impurities are excluded from the pores. The results show that the enzyme purity has a profound influence on the peroxidase yield and activity.

Peroxidase has a molecular weight of 40 000 D which for a globular protein corresponds to an effective diameter of 8 nm, according to the Electro-Nucleonics data sheet. A full monolayer should then equal 1.2 mg protein m^{-2}. The initial coverage of peroxidase alone was found to be 0.8—0.9 mg m^{-2} at most (Table 3). As other proteins are also present, there should be very few empty sites on the surface. The activity, however, decreases with time and after one week only 5—10% active peroxidase remains. This can be estimated from the stability curves if the effects of mass transfer resistances are taken into account. $K_{ps}^{(app)}$ is a more direct measure of reactor activity than the conversion, because it is a linear rather than a logarithmic function. It is also independent of the reactor length in contrast to the conversion. The highest $K_{ps}^{(app)}$ is obtained (Table 3) with the purest enzyme, and the largest surface area. The smaller particles result in a slightly increased loading but in more than a doubled rate constant. To conclude, a reactor for an analytical system should be made through azo immobilization at pH 8.5 using Type VI peroxidase and a glass with 25-nm pore diameter with a small particle size. Such a reactor would give too high an activity for a study of bed geometry and the 72.9-nm glass was therefore used in the following study.

Tests of the validity of the mass transfer equations

Reaction order. The amount of product formed in a 5-μl peroxidase reactor was measured at various flow rates and substrate concentrations (Fig. 2). The linearity of the plots proves that the reaction follows first-order kinetics for substrate concentrations up to at least 0.1 mM. A mixed reaction order would have resulted in a downward curve of the plots, especially at high flow rates. The absorbance obtained with a 100-μl reactor known to give complete conversion is plotted in Fig. 2 for comparison.

The Michaelis constant for the soluble enzyme was determined spectrophotometrically as 12 μM. Enzyme reactors may thus show a pseudo first-order behavior at substrate concentrations which are large compared to the K_M of the soluble enzyme. Any of the lines in Fig. 2 could be a calibration graph for an analytical system and the linearity would then be a desirable property.

External mass transfer. Four different reactors varying in volume, diameter and particle size were studied. $K_{ps}^{(app)}$ was determined (from Eqn. 4) at

various linear flow velocities. The inverse $K_{ps}^{(app)}$ is plotted versus the (particle diameter)$^{3/2}$ × (linear flow velocity)$^{-1/2}$ in Fig. 3. Most of the points fall on two straight lines, one for each particle size. The slight difference in slope is most likely due to errors in d_p and ϵ_E. According to Eqn. (12) the slope should be B^{-1} and the intercept K_{ps}^{-1}. The linearity and the almost equal slopes validate Eqn. (12), at least for moderate flow velocities ($1 < Re < 20$).

A further test can be made by comparing the inverse slope, B, with a value calculated from physical constants according to Eqn. (11). With $\nu = 1 \times 10^{-6}$ m^2 s^{-1}, $D_m = 1.5 \times 10^{-9}$ m^2 s^{-1}, and $\epsilon_E = 0.48$, the constant B becomes 6.6×10^{-5}, compared to the experimental values which were 6.3 and 7.5×10^{-5}. The agreement is surprisingly good when all the uncertainties are taken into consideration.

The K_{ps} values found were 11.9 and 16.4 s^{-1} for the particle diameters 150 and 100 μm, respectively. The corresponding values of $K_{ps}^{(app)}$ for a 5-μl reactor at 1.0 ml min^{-1} were 3.3 and 6.1 s^{-1}. The external mass transfer resistance thus reduces the effectiveness of the reactor two to three times under these conditions.

The conversion efficiencies of some reactors are plotted versus the volumetric flow rate in Fig. 4. The solid lines are drawn from Eqn. (12) with the values of K_{ps} and B as found earlier. The theory describes the data well, except that the conversion at very low flow rates may be lower than predicted. This may be due to a peculiarity of the peroxidase reaction, to some neglected effect in the theory, or to systematic errors in the experiments.

Once the validity of Eqn. (12) has been proved and the K_{ps} and B values are known, the theory can be used to illustrate the effect of changing the

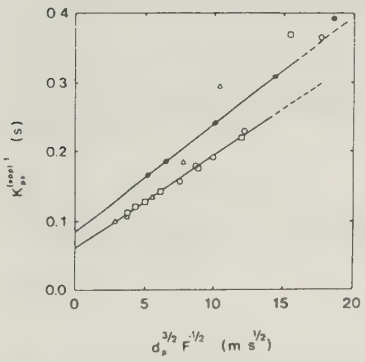

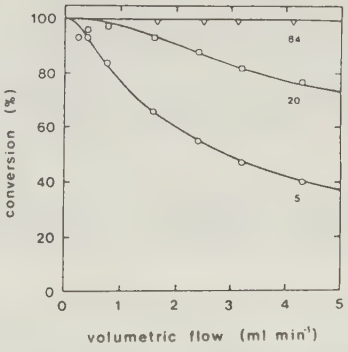

Fig. 3. Effect of linear flow velocity on the apparent rate constant: (•) 5-μl reactor, d_p = 150 μm, S_0 = 20 μM; (△) 5-μl reactor, d_p = 100 μm, S_0 = 25 μM; (□) 5-μl reactor, d_p = 100 μm, S_0 = 100 μM; (○) 20-μl reactor, d_p = 100 μm, S_0 = 100 μM.

Fig. 4. Percent conversion as a function of volumetric flow rate for reactor volumes of: (○) 5 μl, (□) 20 μl, (▽) 84 μl. The solid lines are calculated from Eqns. (4) and (12).

parameters in other ways. The fractional conversion was calculated as a function of the volumetric flow rate for some reactors all having the same volume but different diameters (Fig. 5). For a constant volumetric flow rate, the linear flow velocity will increase as the reactor diameter decreases. More substrate will then be transported into the particle and this will result in a higher conversion as shown in Fig. 5.

Internal mass transfer. The inherent rate constant, K, was calculated from Eqns. (13—15) using the K_{ps} values found (Table 4). The K values obtained with the two particle diameters agree within 15%. The Thiele modulus and the effectiveness factor are also given in the table. The small η_i values indicate that only a small fraction of the catalytic capacity of the enzyme is utilized. A total effectiveness factor including also the external mass transfer resistance would be even smaller.

The particle diameter is the most powerful variable for low effectiveness factors and there is an inverse relation between d_p and K_{ps}. The effect on

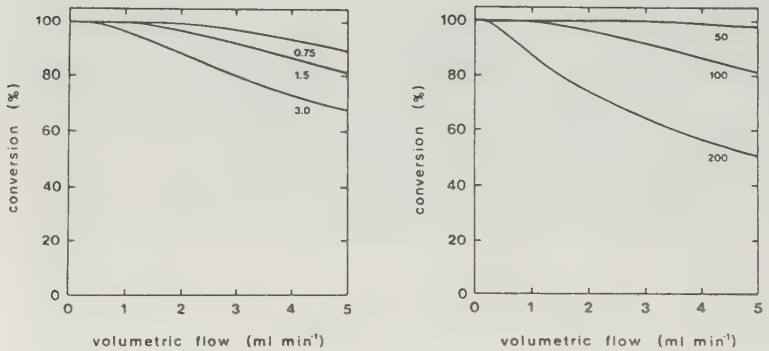

Fig. 5. Effect of reactor diameter on conversion calculated from Eqns. (4) and (12) with $K_{ps}^{(app)} = 16.4\ s^{-1}$, $d_p = 100\ \mu m$, $B = 7.5 \times 10^{-5}\ m\ s^{-1/2}$ for a reactor volume of 20 μl and reactor diameters of 0.75, 1.5 and 3.0 mm.

Fig. 6. Effect of particle diameter on conversion calculated from Eqns. (4) and (12—15) with $K = 136\ s^{-1}$, $B = 7.5 \times 10^{-5}\ m\ s^{-1/2}$, $D_{eff} = 6 \times 10^{-10}\ m^2\ s^{-1}$ for a reactor volume of 20 μl and a reactor diameter of 1.5 mm. Particle diameters: 50, 100 and 200 μm.

TABLE 4

Inherent rate constant of peroxidase immobilized on CPG (72.9 nm pore diameter). D_{eff} estimated as $6 \times 10^{-10}\ m^2\ s^{-1}$

d_p (μm)	K_{ps} (s^{-1})	K (s^{-1})	ϕ_s	η_i
100	16.4	136	8	0.12
150	11.9	156	13	0.08

conversion of changes in the particle diameters is illustrated in Fig. 6, where both internal and external mass transfer has been taken into account. The curves were calculated for reactors having the same physical form. The inherent rate constant, K, is free of all mass transfer limitations. It depends on the reagent and on the properties of the actual batch of immobilized enzyme. It is therefore a conditional rather than an intrinsic constant.

Optimization

One optimization objective for enzyme reactors in flow injection analysis, is to reach a certain level of conversion with a minimum of dispersion. The first step is to optimize the immobilization procedure in order to reach a high inherent activity. The utilization of the inherent activity should then be optimized in order to achieve a low residence time. The latter is related to low dispersion provided that some constraints on the dimensions are observed.

The residence time can be expressed in terms of the inherent rate constant, the degree of conversion, and some physical parameters, through Eqns. (4) and (12—14):

$$\tau = \left\{ [d_p^{3/2}/BF^{1/2}] + \left[\phi_s/K\left(\frac{1}{\tanh 3\phi_s} + \frac{1}{3\phi_s}\right)\right]\right\} [-\ln(1-X)] \qquad (16)$$

It can be seen that for a decreasing particle diameter (ϕ_s equals d_p multiplied by a constant (Eqn. 15)) and an increasing linear flow velocity, the residence time tends to a constant minimal value

$$\tau_{min} = K^{-1}\ [-\ln(1-X)] \qquad (17)$$

i.e., minimal dispersion is obtained when all resistance to mass transfer is absent.

Increased flow velocity and decreased particle size will both contribute to a larger pressure drop, ΔP (Nm^{-2}), over the reactor. An expression for ΔP is obtained by putting the relevant quantities into Darcy's equation, which then becomes

$$\Delta P = \tau\ F^2\ d_p^{-2}\ (\varphi\ \nu^*) \qquad (18)$$

(The product of the column resistance factor, φ, and the dynamic viscosity, ν^*, is approximately 1 N s m^{-2} [21] for irregular particle shapes and dilute aqueous solutions.)

With a limit set on the pressure drop, the relative importance of d_p and F on the residence time has to be assessed. It can be seen that in Eqn. (16) decreased particle size is of greater consequence than increased linear flow velocity, and that there will be no undue weighting for either of the parameters in Eqn. (18). It can therefore be concluded that in order to minimize the residence time, and hence the dispersion, the linear flow velocity should be sacrificed in favour of a reduced particle diameter.

The procedure to be followed in optimizing the bed geometry starts by

selecting the smallest practical particle size. The degree of conversion is then fixed. The next step involves a simultaneous computation of the residence time and the maximum linear flow velocity which fit the selected maximum value of ΔP. With the linear flow velocity fixed, the reactor diameter is adjusted to fit the desired volumetric flow rate. The reactor volume can then be determined from (residence time) × (volumetric flow)/(total void fraction).

To facilitate visualization of the relationships, two plots illustrating the dependence of reactor volume and back-pressure on the reactor diameter, are shown in Fig. 7. The plots are calculated for a particle diameter of 100 μm, with the assumptions that the conversion is 99.9%, the volumetric flow rate 1.0 ml min^{-1}, and the constants B and K as found experimentally. The dotted arrows illustrate how the selection of parameters proceeds; if the back-pressure of the reactor is chosen as 0.7 atm., the reactor diameter then should be 1 mm, which gives a required reactor volume of 20 μl. The steep rise in back-pressure below a certain reactor diameter is noteworthy.

The optimal residence time for three inherent rate constants, 10, 100 and 1000 s^{-1}, are plotted versus the particle diameter in Fig. 8. The curves are all calculated for a back-pressure of 1 atm at a fractional conversion of 99.9%. At the limit, when the particle diameter becomes very small, the

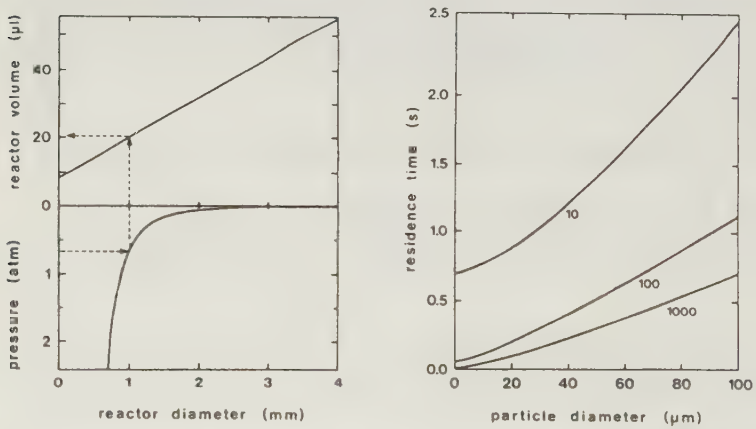

Fig. 7. Optimization of a peroxidase reactor. The dotted arrows show how the selection of parameters proceeds. Calculated from Eqns. (16) and (18) with K = 136 s^{-1}, d_p = 100 μm, $B = 7.5 \times 10^{-5}$ m $s^{-1/2}$. $D_{eff} = 6 \times 10^{-10}$ m^2 s^{-1}. $\varphi = 1 \times 10^3$, and $\nu^* = 1 \times 10^{-3}$ N $s\ m^{-2}$ for a conversion of 99.9% and a flow rate of 1 ml min^{-1}.

Fig. 8. The residence time required for 99.9% conversion at a back-pressure of 1 atm as a function of the particle diameter. Calculated from Eqns. (16) and (18) with $B = 7.5 \times 10^{-5}$ $ms^{-1/2}$, $D_{eff} = 6 \times 10^{-10}$ m^2 s^{-1}. $\varphi = 1 \times 10^3$ and $\nu^* = 1 \times 10^{-3}$ Ns m^{-2} for the inherent rate constants: 10, 100 and 1000 s^{-1}.

apparent rate constant approaches the inherent rate constant. It can also be seen that for an active enzyme preparation ($K > 100\ s^{-1}$), the smallest possible particle diameter should be selected. For a less active preparation ($K < 10\ s^{-1}$), there is little to be gained from particle sizes smaller than 20–30 μm.

The authors are indebted to Professor Gillis Johansson for his stimulating interest and valuable discussions concerning this work.

REFERENCES

1 L. Gorton and L. Ögren, Anal. Chim. Acta, 130 (1981) 45.
2 A. Iob and H. A. Mottola, Anal. Chem., 52 (1980) 2332.
3 G. Johansson, Appl. Biochem. Biotech., 7 (1982) 99.
4 G. Johansson, L. Ögren and B. Olsson, Anal. Chim. Acta, 145 (1983) 71.
5 B. Olsson, L. Ögren and G. Johansson, Anal. Chim. Acta, 145 (1983) 101.
6 K. G. Paul, in P. D. Boyer, H. Lardy and K. Myrbäck (Eds.), The Enzymes, Vol. 8, 2nd ed., Academic Press, New York, 1963, p. 2.
7 B. W. Griffin and P. L. Ting, Biochem., 17 (1978) 2206.
8 F. T. Nayler and B. C. Saunders, J. Chem. Soc., (1950) 3519.
9 A. J. Karabelos, T. H. Wegner and T. J. Hanratty, Chem. Eng. Sci., 26 (1971) 1581.
10 L. K. McCune and R. H. Wilhelm, Ind. Eng. Chem., 41 (1949) 1124.
11 B. J. Rovito and J. R. Kittrell, Biotech. Bioeng., 15 (1973) 143.
12 C. N. Satterfield, Heterogeneous Catalysis, M.I.T. Press, Cambridge, 1970, p. 129.
13 H. H. Weetall, in K. Mosbach (Ed.), Methods in Enzymology, Vol. 44, Academic Press, New York, 1976, p. 134.
14 A. S. Brill, in M. Florkin and E. H. Stotz (Eds.), Comprehensive Biochemistry, Vol. 14, Elsevier, Amsterdam, 1973, p. 447.
15 P. Thibault, P. Monsan and C. Jouret, Sci. Aliment., 1 (1981) 55.
16 C. Flemming, A. Gabert and H. Wand, Acta Biol. Med. Ger., 32 (1974) 135.
17 Kikutake Junichiro, Jpn. Pat., Jpn. Kokai Tokkyo Koho, 78, 104, 789 (1978).
18 R. Epton, G. Marr and R. G. Ridley, Polymer, 20 (1979) 1447.
19 R. A. Messing and H. H. Weetall, U.S. Pat. 3, 519, 538 (1970).
20 D. L. Eaton, in D. E. Leyden and W. T. Collins (Eds.), Silylated Surfaces, Gordon and Breach, New York, 1980, p. 201.
21 J. M. Reijn, Flow Injection Analysis, Doctoral Thesis, Utrecht, 1982, p. 100.

III

DETERMINATION OF HYDROGEN PEROXIDE IN A FLOW-INJECTION SYSTEM WITH IMMOBILIZED PEROXIDASE AND CHROMOGENIC REAGENTS

Bo Olsson
Department of Analytical Chemistry, University of Lund,
P.O.Box 124, S-221 00 Lund, Sweden

SUMMARY

A flow injection system with a reactor containing peroxidase immobilized on porous glass was used for the determination of hydrogen peroxide. A number of chromogenic reagents were studied in combination with different immobilization methods, in particular with regard to adsorption of the coloured product on the enzyme support. A f.i.a. manifold had a throughput of 210 samples h^{-1} and a detection limit of 0.1 μM H_2O_2 and could be used for at least 17 000 determinations with the same enzyme reactor. Systems with higher sensitivity or higher sample throughput are also described.

INTRODUCTION

Immobilized catalysts are finding an increasing number of applications in analytical chemistry, in particular in flow injection analysis (f.i.a.). Horseradish peroxidase (HRP) catalyzes reactions which form the basis for hydrogen peroxide determinations over a wide concentration range and with various detection principles. Hydrogen peroxide is produced in many enzymatic reactions including those of at least forty oxidases [1,2] and several important analytical methods involve detection of hydrogen peroxide as an indicator species. The initial step in the catalytic cycle [3] is a rather selective oxidation of HRP by hydrogen peroxide and it is followed by

reactions in which a cosubstrate is oxidized and the native enzyme regenerated. The latter reactions proceed with low selectivity and a great number of cosubstrates have been used for spectrophotometric detection, some of which form coloured products directly, whereas others form coloured adducts after coupling with a second compound. A good colour reagent should react rapidly with HRP and fulfill a number of general requirements [4].

It has been observed that adsorption of coloured reaction products to hydrophobic enzyme carriers result in severe peak tailing in f.i.a. [5]. This impair the performance of the method seriously and different immobilization procedures and reagent compositions were therefore tried in order to find useful combinations.

EXPERIMENTAL

Immobilization of peroxidase

Horseradish peroxidase, HRP, EC 1.11.1.7 (Sigma, Type VI) was immobilized onto glycerylpropyl derivatized controlled pore glass (Pierce, CPG/460 Glucophase G, pore diam 46 nm, particle size 37-73 μm) with different methods.

Tresyl coupling. The glass was activated by adding 100 μl tresyl chloride (2,2,2-trifluoroethanesulfonyl chloride, Fluka) to a slurry of 1 g glass in 1.3 ml acetone and 0.1 ml pyridine as described before [6]. The activated and washed glass was suspended in 2 ml cold 0.4 M phosphate buffer, pH 7.5, and 2 ml of a solution containing 20 mg HRP which had been dialyzed against 0.1 M phosphate buffer, pH 7.5, was added. The reaction was allowed to proceed over night; the enzyme-glass conjugate was then washed, soaked for 2 h in 0.2 M Tris-HCl, pH 7.5, washed with 0.5 M NaCl and stored in 0.1 M phosphate buffer, pH 7.0.

Diazo coupling. The glass was acylated by refluxing it for 4 h in chloroform containing 3% p-nitrobenzoyl chloride (BDH, p.a.) and 5% triethylamine (Fluka, p.a.) as described before for alkylamino glass

[7]. A modification of this procedure was also used. One gram glass was acylated in 10 ml pyridine containing 1 g p-nitrobenzoyl chloride at room temperature for 14 min, washed with chloroform and dried.

The two acylated glasses were treated with dithionite to reduce the nitro group and the resulting arylamino glasses were activated with HCl and nitrite as described before [7]. Four milliliter of a solution containing 20 mg peroxidase, which had been dialyzed against 0.25 M phosphate buffer, pH 8.5, was added to each portion of activated arylamino glass. The reaction was allowed to proceed over night whereafter the glass was washed with buffer and salt solutions and stored in 0.1 M phosphate buffer, pH 7.0.

Activity measurements

The apparent activity of the immobilized-enzyme preparations was measured by pumping (1.1 ml min^{-1}) a reagent containing 4 mM DCPS, 0.2 mM 4-AP and 0.05 mM H_2O_2 through reactors (volume 17 µl, i.d. 2.5 mm) packed with the material. The apparent concentration of HRP in the reactor was calculated by correlating the absorbance obtained during the known time of passage to an absorbance-time curve obtained separately with a known concentration of dissolved peroxidase.

Colour reagents

MBTH (3-methyl-2-benzothiazolinone hydrazone hydrochloride), DMAB (3-dimethylaminobenzoic acid) and DCPS (2,4-dichlorophenol-6-sulphonate) were obtained from Janssen. DCPS was also synthetized from DCP [8] for use in the stability tests. Phenol and DCP (2,4-dichlorophenol) were from Merck, 4-AP ("4-aminophenazone", 4-amino-1,2-dihydro-1.5-dimethyl-2-phenyl-3H-pyrazole-3-one) from BDH, ABTS (2,2'-azino-di-[3-ethylbenzthiazolin-6-sulphonate]) from Boehringer and CTA ("Chromotropic acid", 4,5-dihydroxynaphthalene-2,7-disulphonic acid) was obtained from Sigma. ESPA (N-ethyl-N-sulphopropyl-aniline) was synthetized according to Tamaoku et al. [9]. Reagent solutions were made up in 0.1 M sodium citrate buffer, pH 6.0, containing 1 mM EDTA, and used the same day.

The flow injection system

A diagram of the f.i.a. system is shown in Fig. 1. The samples were introduced into an aqueous carrier stream by means of a pneumatically actuated slide injection valve (Cheminert CSVA and SVA 8031 for 1.5 and 20 μl sample volumes respectively). The carrier and reagent streams were pumped (Gilson Minipuls 2) with flow rates of 0.9 and 0.45 ml min^{-1} respectively and a single bead string reactor (length 10 cm, i.d. 0.8 mm, bead diameter 0.5 mm) was inserted after the confluence point for thorough mixing. A guard column containing about 200 μl unactivated arylamino glass was inserted into the reagent line to adsorb impurities. The enzyme reactor consisted of a PTFE tubing (i.d. 1.5 mm, length 31 mm) filled with enzyme-treated glass and fitted with Altex screw couplings and retaining nets of polypropylene. The absorbance was monitored in a 10 μl flow-through cell (LKB, model 2151) connected to the reactor outlet by 20 cm of a 0.5 mm i.d. PTFE tubing.

RESULTS AND DISCUSSION

Immobilization of peroxidase HRP

It is well known that HRP can be immobilized to e.g. porous glass with different methods [10-14]. The common glutaraldehyde coupling produces catalysts with poor activity and low stability, whereas very good yields are reported with a diazo coupling of the enzyme to arylamino glass [7]. A major problem with the immobilized catalyst is that the common colour reagents for spectrophotometric determinations give products which adsorb on the hydrophobic support [5].

Nonspecific adsorption in affinity chromatography has been reduced by coating of the porous glass surface with a hydrophilic layer of glycerylpropyl groups [15]. Different methods for coupling of HRP to glycerylpropyl glass were tried and the activity and stability of some conjugates are shown in Fig. 2.

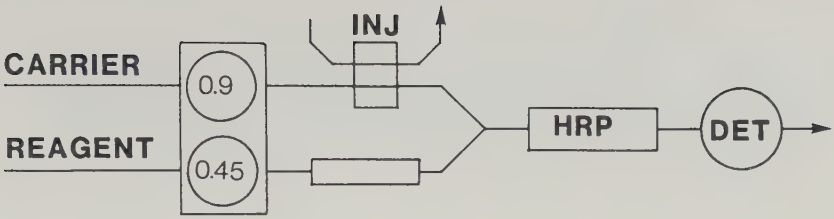

Fig. 1. Diagram of the f.i.a. system. For details, see text.

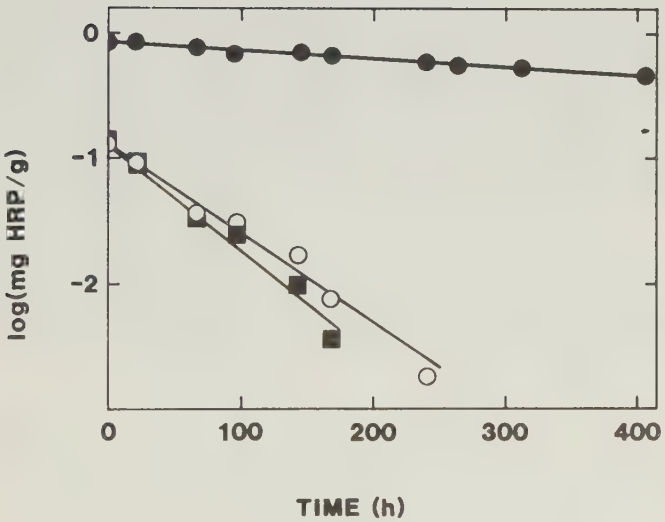

Fig. 2. Apparent enzyme concentration and time stability of HRP-glass conjugates immobilized with, (●) diazo coupling (acylation in pyridine), (■) diazo coupling (acylation in chloroform), and (○) tresyl coupling.

The initial activity with the tresyl coupled HRP (the middle curve) corresponds to a coupling yield of 0.17 mg enzyme g^{-1} glass, i.e. a very low coverage. The activity decreased with time and the apparent half-life time was 47 h under conditions of continuous feed of substrates.

The diazo coupling to the arylamino support which had been acylated in chloroform produced a conjugate with much the same activity and stability (the lower curve) as that obtained with the tresyl coupling. A spot test with 2,4,6-trinitrobenzene sulphonate as colour indicator for amines [16] showed that the yield of the acylation step was low and that most of the hydroxy groups of the glycerylpropyl coating remained underivatized.

Acylation in pyridine, which is a strong base, resulted in a more or less complete reaction as indicated by the spot test, and the hydrophilic properties of the glass surface are thus not retained. From a determination of the amount of unbound HRP it was indicated that the coupling yield was 17 mg/g glass, i.e. in the same order as that of diazo coupling to similar arylamino supports obtained from acylation of alkylamino glass [7]. The activity of this preparation (Fig. 2, upper curve) is very high and it is in fact limited by the rate of mass-transfer of the hydrogen peroxide from the bulk of the solution to the enzyme within the porous glass. Deactivation of the enzyme with time will consequently only result in that the remaining enzyme is used more efficiently and the apparent stability is therefore very good as can be seen in Fig. 2. The apparent half-life time was estimated to be 540 h.

Enzyme coupling via aldehydes produced from the hydroxy groups of the glycerylpropyl coating [17] and via carbonyl diimidazole [18] were also tried since these methods retain the hydrophilic character of the surface, but the yields were extremely low. Immobilization of HRP to hydrophilic surfaces with ordinary methods that couples through the protein moiety of the enzyme therefore seems to result in low yields generally, in line with the assumption [10] that the immobilization reaction preferentially involves the hydrophobic zones of HRP. Coupling of HRP through oxidation of the carbohydrate moiety of

the enzyme on the other hand is expected [19] to result in a low recovery of activity.

The presented stability curves (Fig. 2) were obtained with a continuous feed of hydrogen peroxide containing reagent solution to the reactors between the activity measurements. The stability was found to be much better when a hydrogen peroxide-free reagent solution was used and if stored in buffer under non-flow condition the preparations are stable for years. Hydrogen peroxide or products of the enzyme reaction are thus probably involved in the deactivation of the enzyme; cf. the irreversible change of peroxidase at high peroxide concentrations [3].

Adsorption

The extent of adsorption of some coloured reaction products on the enzyme support was studied by examining the peak profiles obtained for injections of a standard hydrogen peroxide sample into the flow system. Some peaks are shown in Fig. 3 and Table I gives the peak width at 10% of the maximum height, normalized with that obtained for a non-adsorbed solute (8.4 s), for various combinations of colour reagents and HRP-preparations.

The hydrophobic arylamino glass gives rise to severe peak broadening with the reagents containing 4-AP or MBTH as cosubstrate and an aromatic amine (ESPA, DMAB) or a phenol (phenol, DCPS) as coupler. The products obtained with an amine as coupler are particularly troublesome and they even adsorb somewhat to the hydrophilic support materials. The ABTS reagent and the reagents containing DCPS or CTA as couplers give products with negligible adsorption to the hydrophilic supports and the tresyl coupled material is particularly good. The coloured products obtained from reagents containing CTA, a sulphonated hydroxynaphthalene, show negligible adsorption to all the enzyme preparations. Unfortunately, the molar absorptivity of the product with 4-AP is rather low and in combination with MBTH the reagent is very unstable and not very useful in practice.

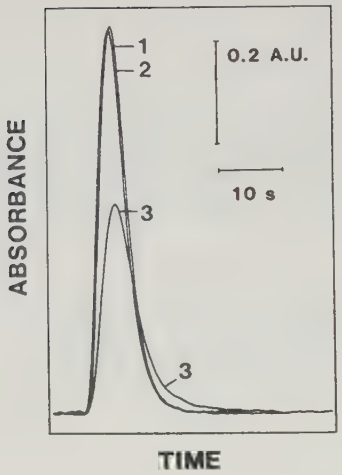

Fig. 3. F.i.a. peaks obtained with ABTS and different HRP-glass conjugates, (1) tresyl coupled, (2) diazo coupled (acylation in chloroform), (3) diazo coupled (acylation in pyridine).

TABLE I

Effect of adsorption on the width of f.i.a. peaks. Values given are the width at 10% of the maximum height normalized by division with the corresponding width of a non-adsorbed solute (8.4 s)

Reagent		Immobilization method		
cosubstrate	coupler	tresyl	diazo	diazo
ABTS	-	1.06	1.06	1.5
4-AP	ESPA	1.14	1.21	221
4-AP	DCPS	1.06	1.12	3.7
4-AP	phenol	1.14	1.14	8.2
4-AP	CTA	1.00	1.02	1.04
MBTH	DMAB	1.43	1.50	36
MBTH	CTA	1.00	1.01	1.04

a) 2 mM b) 0.1 mM c) 10 mM d) glass acylated in chloroform
e) glass acylated in pyridine.

Design of the enzyme reactor

The advantages of using reactors which give a quantitative conversion of the substrate of interest to the product have been discussed elsewhere [20]. The reactor size required to obtain full conversion depends of course on factors such as flow rate, enzyme loading, and activity of the catalyst under the conditions of use (type and concentration of cosubstrate, pH, etc.) and detailed discussions on enzyme reactor kinetics can be found in the literature, see e.g. [21].

The kinetics followed by peroxidase can, for a constant concentration of cosubstrate, be considered to be of the Michaelis-Menten type. For a typical concentration of the cosubstrate 4-AP (around 1 mM), the Michaelis constant, K_M, and the maximum reaction rate are both rather low (K_M = 12 uM H_2O_2 [7]) and the enzyme is therefore utilized with a low efficiency. It has been found [22] that certain very efficient auxiliary substrates for peroxidase, e.g. 2,4-dichlorophenol (DCP), can be used to promote the rate of colour reagent oxidation. With a millimolar concentration of DCP in the reagent the Michaelis constant becomes of the order of 0.1 mM H_2O_2 and the maximum rate becomes approximately 25 times higher than with 1 mM 4-AP alone. The promoting effect of DCP is illustrated in Fig. 4 which shows the fractional conversion (X) as a function of the mean residence time (τ) in the reactor, plotted according to the pseudo-first order approximation of the Michaelis-Menten equation for a plug-flow reactor [7].

$$\ln(1-X) = K' \cdot \tau \qquad (1)$$

Extrapolation of the linear curve obtained with DCP in the reagent predicts that a conversion of 99.99% will be obtained for a residence time of 3.3 s in this reactor with tresyl coupled HRP. This corresponds to a reactor volume of 60 μl at a flow rate of 0.9 ml min^{-1}.

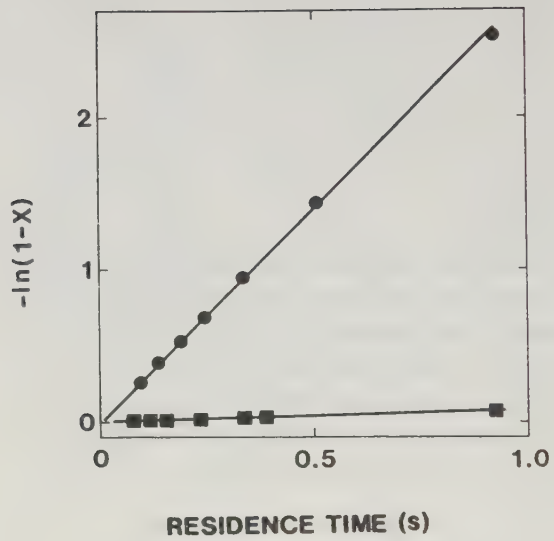

Fig. 4. The fractional conversion (X) in a reactor with tresyl immobilized HRP as a function of the residence time (τ) in the reactor (volume 5 µl).
Reagents:
(■) 0.2 mM 4-AP, 4 mM DCPS, 100 µM H_2O_2
(●) 0.2 mM 4-AP, 4 mM DCPS, 1 mM DCP, 100 µM H_2O_2

TABLE II

Properties of f.i.a. methods for hydrogen peroxide. The flow system in Fig. 1 was used with a 55 µl reactor containing tresyl coupled HRP.

Reagent[a]		baseline noise (Abs)	Sensitivity (Abs/M)	linear range (µM)
ABTS	414	$0.2\ 10^{-3}$	10 000	0.04-200
4-AP/DCPS	514	$0.2\ 10^{-3}$	3 600	0.1-500
4-AP/CTA	600	$0.3\ 10^{-3}$	690	0.8-1000

[a] concentrations as in Table I. The reagents also contained 1 mM DCP.

Determination of hydrogen peroxide

Table II shows some properties of three f.i.a. methods, differing in the reagent composition used. The flow injection system shown in Fig. 1 was used with 55 µl of tresyl coupled HRP-glass conjugate and all reagents contained 1 mM DCP. It can be seen that the ABTS reagent and the 4-AP/DCPS reagent both result in sensitive methods, where the upper limit of the linear span is set by the range of the spectrophotometer. The reagent with 4-AP and CTA is an order of magnitude less sensitive but this is still sufficient for many applications.

The tabulated values were obtained with an injection volume of 20 µl which gives a total dilution of the sample of 6 times at the peak maximum. As usual in f.i.a. the methods are easily adapted to more concentrated samples by selection of a smaller injection volume. The peakwidth at 1% of the maximum height was 17 s which corresponds to a maximum throughput of 210 samples h^{-1} if 1% carry-over is accepted. All three reagent mixtures are stable for many days if stored in dark bottles.

The stability of a system with the tresyl coupled enzyme and with the 4-AP/DCPS reagent was studied by injections of 1.5 µl samples of 0.5 mM hydrogen peroxide at a rate of 180 samples per hour until 17 000 samples had been processed in all. The relative standard deviation within groups of 50 peaks was 1% or better but there was a 10% variation in the response over the period due to wear of the tubings (PVC) of the peristaltic pump. When the pump tubings were renewed the same peak height was obtained after 17 000 injections as in the beginning. The effect of reactor ageing was thus negligible, which is probably due both to the initial overcapacity of the reactor and to the discontinuous supply of hydrogen peroxide inherent with a f.i.a. method, cf. the middle curve in Fig. 2 which reflects the stability of the enzyme with a continuous supply of hydrogen peroxide. There was, however, an accumulation of polymeric material in the reactor with time which finally may result in an excessive back-pressure. Some coloured material could be removed by flushing the reactor with acetone without loss of activity but this treatment was not completely effective.

The 4-AP/CTA reagent can be used with HRP preparations made by diazo coupling to hydrophobic arylamino glass. The required reactor size for full conversion is very small. A reactor of 14 μl was used with 1.5 ul injetions directly into the reagent stream. The system produced reproducible peaks with less than 1% carry-over at injection frequences of up to 600 h^{-1}.

Interferences

It is known that hydrogen peroxide measurements with colour reagents are subject to interferences by reducing agents, e.g. uric acid [23]. The susceptibility of some reagent combinations towards interference from uric acid is shown in Table III. ABTS is in essence a redox indicator and a decreased peak height is observed already at sub-stoichiometric concentrations of uric acid. The 4-AP-containing

TABLE III

Effect of uric acid in the sample on the response from 9 μM H_2O_2. The response is normalized by division with that obtained from 9 μM H_2O_2 alone. Conditions and reagent composition as in Table II.

Uric acid (uM)	relative response		
	ABTS	4-AP/DCPS	4-AP/CTA
3	0.88	1.00	1.00
30	0.55	0.94	1.00
300	-	0.56	0.91

reagents form coupled products with the hydroxyaromates (DCPS, CTA) which, once formed, are relatively resistent towards reduction. The interfering reactions probably involves reduction of the oxidized 4-AP intermediate formed in the enzyme reaction [24]. The lower interferences obtained with CTA as coupler as compared to that obtained with DCPS is most likely due to the very fast coupling between CTA and the oxidized 4-AAP [25]. Reagents with MBTH and CTA are also relatively resistant towards interferences from reductants [26].

ACKNOWLEDGEMENTS

The author thanks Professor Gillis Johansson for valuable discussions.

REFERENCES

1. L.C. Clark Jr, in "Methods in Enzymology", Vol. 56, Academic Press, New York, 1979, p. 448.
2. T.E. Barman, Enzyme Handbook, Vol. 1, Springer-Verlag, New York, 1969.
3. H.B. Dunford and J.S. Stillman, Coord. Chem. Rew., 19(1976)187.
4. T.T. Ngo and H.M. Lenhoff, Anal. Biochem., 105(1980)389.
5. B. Olsson, L. Ögren and G. Johansson, Anal. Chim. Acta 145(1983)101.
6. K. Nilsson and P.O. Larsson, Anal. Biochem., 134(1983)60.
7. B. Olsson and L. Ögren, Anal. Chim. Acta, 145(1983)87.
8. D. Barham and P. Trinder, Analyst, 97(1972)142.
9. K. Tamaoku, Y. Murao, K. Akiura, and Y. Ohkura, Anal. Chim. Acta, 136(1982)121.
10. P. Thibault, P. Monsan and C. Jouret, Sci. Aliment., 1(1981)55.
11. C. Flemming, A. Gabert, and H. Wand, Acta Biol. Med. Ger., 32(1974)135.
12. Kikutake Junichiro, Jpn. Pat., Jpn. Kokai Tokyo Koho, 78, 104, 789 (1978).
13. R. Epton, G. Marr and R.G. Ridley, Polymer, 20(1979)1447.
14. R.A. Messing and H.H. Weetall, U.S. Pat. 3, 519, 538 (1970).
15. F.E. Regnier and R. Noel, J. Chrom. Sci., 14(1976)316.
16. W.E. Hornby and H. Filippusson, Biochem. J., 120(1970)215.
17. G.P. Royer, F.A. Liberatore, and G.M. Green, Biochim. Biophys. Res. Commun., 64(1975)478.
18. G.S. Bethell, J.S. Ayers, W.S. Hancock, and M.T.W. Hearn, J. Biol. Chem., 254(1979)2572.
19. I. Weinryb, Biochim. Biophys. Res. Commun., 31(1968)110.
20. G. Johansson, L. Ögren, and B. Olsson, Anal. Chim. Acta, 145(1983)71.
21. P.W. Carr and L.D. Bowers, "Immobilized Enzymes in Analytical and Clinical Chemistry" (Chemical Analysis, Vol. 56), John Wiley & Sons, New York, 1980.
22. H. Lundbäck and B. Olsson, in manuscript.
23. W.J. Blaedel and J.M. Uhl, Clin. Chem., 21(1975)119.
24. D.L. Witte, L.F. Brown, and R.D. Feld, Clin. Chem., 24(1978)1778.
25. B. Olsson and H. Lundbäck, in manuscript.
26. R.H. White-Stevens and L.R. Stover, Clin. Chem., 28(1982)589.

IV

Analytica Chimica Acta, 145 (1983) 71—85
Elsevier Scientific Publishing Company, Amsterdam — Printed in The Netherlands

ENZYME REACTORS IN UNSEGMENTED FLOW INJECTION ANALYSIS

GILLIS JOHANSSON*, LARS ÖGREN[a] and BO OLSSON
Analytical Chemistry, University of Lund, P.O. Box 740, S-220 07 Lund (Sweden)
(Received 20th August 1982)

SUMMARY

The design of immobilized-enzyme reactors for use in flow injection analysis is discussed. The reactors should be optimized for a short residence time and a very high (>99.9%) conversion of substrate to products. Selection of carrier and immobilization method is important in order to increase the amount of active enzyme per unit volume. The efficiency of the reactor can be increased by decreasing the particle size in packed-bed reactors and the radius of open tubular reactors. The maximum inherent rate constant that can be obtained under optimal conditions is estimated for a number of enzymes of analytical interest; it is shown that with high rate constants and small particle diameters, residence times less than seconds can be obtained. Some applications of immobilized-enzyme reactors in flow systems are reviewed.

A combination of the flow injection technique described by Růžička and Hansen [1] and Stewart [2] with enzymatic methods of analysis should be able to produce useful solutions to a broad range of problems. It is advantageous to merge the speed and simplicity of flow injection analysis (f.i.a.) with the selectivity of the enzymatic methods, especially with immobilized-enzyme reactors optimized for the technique.

Reactor design has been studied in chemical engineering, both from theoretical [3, 4] and practical points of view. Enzyme reactors constitute a special case of a more general theory. Only liquid moving phases and solid unshrinkable, incompressible supports for the catalyst have to be considered. The reactions occur isothermally, because of the small reactor dimensions and the low substrate concentrations.

Analytical reactors should be able to process an impulse or a short plug of substrate with little dispersion and preferably with close to 100% conversion of substrate to products. The dispersion is normally of secondary importance in the bio-engineering field and high conversions are often avoided in order to improve production economy. The rate of conversion in a reactor depends on the rate of the chemical reaction as well as on the rate of the mass transfer. The chemical rate depends on the intrinsic kinetics of the immobilized enzyme and on the amount of catalyst. The dispersion can be reduced by appropriate reduction of reactor dimensions. It is thus necessary to con-

[a]Present address: AB Draco, P.O. Box 1707, S-221 01 Lund, Sweden.

0003-2670/83/0000-0000/$03.00 © 1983 Elsevier Scientific Publishing Company

centrate the enzyme into a smaller volume or to increase the efficiency of mass transfer. With surface-bound enzymes, the amount of enzyme will depend on the total surface area and on the number of molecules per unit surface. Carr and Bowers [5] have recently reviewed the literature on analytical enzyme reactors and summed up the work in the field. The discussion in this paper will be restricted to packed-bed reactors with the enzyme immobilized in particles of porous support and to open tubular reactors with a thin enzyme layer on the walls.

SURFACE AREA PER UNIT VOLUME

A packed-bed reactor will develop dead volumes unless it is filled with a pressure-resistant support material. Porous glass seems to be one of the most suitable supports commonly used. It is available as chips of various sizes and pore diameters. The enzyme loading is to a first approximation proportional to the surface area [6], provided that the pore diameter is larger than the effective enzyme diameter. Table 1 shows how the surface area increases with a decreased pore diameter. The conclusion to be drawn at this stage is that the smallest possible pore diameter should be used in order to compound as much enzyme as possible into each unit volume.

The geometrical areas of open tubular reactors are several orders of magnitude less, compared on the basis of equal volumes (Table 1). Direct immobilization on the wall would give an enzyme loading of 0.1—1 mg m^{-2} and the amount of enzyme would thus be too low for analytical purposes even if the mass transfer were very fast. Some surface enlargement technique is therefore necessary in order to increase the enzyme loading. Nylon and other plastic tubings have been etched or hydrolyzed [7—14] or the enzyme has been immobilized in a porous silica layer or in a polyanionic gel on the tube wall [14, 15]. With the latter type, the inside area could be increased by irregularities in the coating, the "fuzzy wall" reactor, a design which enhanced the mass transfer. The surface area of glass capillaries can be enlarged very greatly by growing whiskers on the inside [16].

TABLE 1

Surface areas of some enzyme reactors all with a void volume of 100 μl (100 μl of CGP-10 ≈ 40 mg, total void fraction ≈ 0.8)

Packed-bed (CPG-10)		Open tubular		
Pore diameter (nm)	Area (m^2)	I.d. (mm)	Length (m)	Area (m^2)
24	5.5	0.1	12	0.004
35	3.8	0.2	3.2	0.002
50	2.5	0.5	0.5	0.0008
100	1.3	1.0	0.12	0.0004

ENZYME ACTIVITY PER UNIT SURFACE

A wealth of literature is available about methods for enzyme immobilization [17—19] and for each type of support material several possibilities have been worked out. Glass can be silylated giving alkylamino or arylamino derivatives to which enzyme can be bound by means of, e.g., glutaraldehyde, isothiocyanate, carbodiimide, triazine or azo coupling [5, 17, 19]. No one method is generally superior, for the loading and the stability will vary depending on the enzyme. For example, it was found that azo coupling is superior to glutaraldehyde coupling for immobilizing peroxidase [20, 21]. The opposite was true when lactate dehydrogenase was immobilized to the same type of support [22].

The type of linkage, the support material and the method of immobilization will influence the hydrophobicity and charge around the active center of the enzyme. Such factors may have pronounced effects on the substrate binding constant and the maximum rate of reaction, as well as on the pH optimum and sensitivity towards changes in ionic strength. The Michaelis constant may thus be altered by more than one order of magnitude [23].

Enzymes are normally not very pure as received and the impurities may interfere in several ways. They may be immobilized and thus compete with the active enzyme for sites on the support, and they may even be bound preferentially [21]. Impurities may deactivate the enzyme (proteolytic enzymes), and they may interfere with the reaction (catalase in reactions producing hydrogen peroxide) or lower the selectivity by forming products which are sensed by the detector.

An enzyme is bound to a support with many covalent bounds so that the stability towards shear forces becomes high [24]. Some of the enzyme remaining on the carrier after the immobilization is only physically adsorbed, however. Unless removed by thorough washing, it will desorb when the reactor is put into use and give rise to a fast initial loss of activity. Several other factors may contribute to a rapid deactivation with time. The most dramatic is bacterial growth which results in a sudden loss of activity. The sensitivity towards infection varies; e.g., peroxidase is almost immune, and even has a bactericidal effect [25]. Precautions include boiling of reagents, especially deionized water, dialysis or sterile filtration of samples, or addition of preservatives.

Heavy metals may be bound very tightly to an enzyme and inhibit its catalytic action. Metal contamination may occur during the immobilization or through the feed stream to the reactor [26]. Reactivation by treatment with a strong complex-former or on-line purification with a chelating resin may remove the metals [27]. Soluble chelating reagents will deactivate some enzymes [28].

In summary, it can be concluded that the activity of a preparation will vary widely depending on the immobilization. Half-life times of almost two years have been reported [29]. The new ceramic controlled-pore supports [30] may in many cases result in better stability than silica glass.

CONVERSION EFFICIENCY

Flow injection analysis is a dynamic method and the detector signal seldom reaches the steady-state level. It might therefore seem logical that enzyme reactors for f.i.a. should operate with incomplete conversion. There is a difference, however, in that the reactor performs a chemical conversion, whereas dispersion is a purely physical process. The success of the f.i.a. concept is due to the precise control of the mixing process and any chemical reactions have to be controlled to the same degree or the overall performance will be degraded.

A reactor capable of high conversion will provide a good immunity towards changes which affect the reaction rate. This is illustrated in Fig. 1 for two reactors having initial conversions of 99.9 and 30%, respectively. The effect of mass transfer was neglected in the calculations. The enzyme activity may be decreased by denaturation or losses of enzyme or binding of inhibitors, but also by changes in pH, ionic strength or sample composition (Fig. 1a). The more efficient reactor is only slightly affected whereas the conversion and therefore also the analytical signal are significantly reduced with the less efficient reactor. The next plot (Fig. 1b) shows that the more efficient

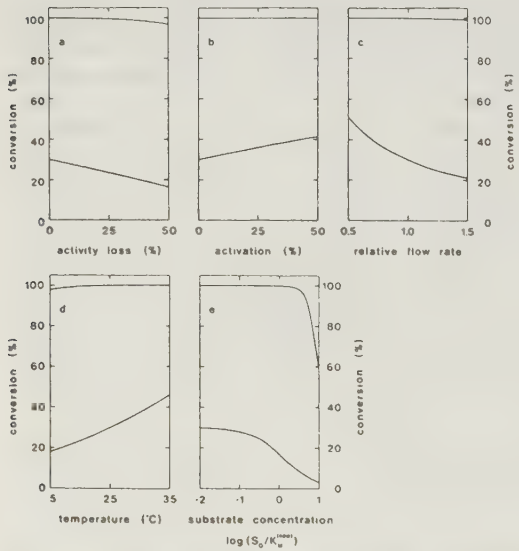

Fig. 1. Fractional conversion of substrate in reactors with negligible mass transfer resistance. The dependence on the parameters was calculated with first-order kinetic expressions except for the substrate concentration where Michaelis—Menten kinetics was assumed. The two reactors had initially a conversion of 99.9 (upper lines) and 30.0% (lower lines).

reactor is unaffected by factors which increase the activity. The effects of changes in flow rate and temperature are outlined in Fig. 1(c) and (d) and again are seen to be negligible for the more efficient reactor. The final plot (Fig. 1e), which assumes Michaelis—Menten kinetics, shows that the less efficient reactor will start to give non-linear calibration plots at substrate concentrations almost two orders of magnitude lower than the Michaelis constant.

With real reactors, there is also some mass transfer resistance which is a physical process and as such will be less affected by changes in the parameters mentioned above. When the mass transfer resistance becomes appreciable, the total reaction rate is controlled jointly by the physical and chemical processes and even an inefficient reactor will show an improved behaviour.

RATE OF REACTION IN A REACTOR

Kinetics

The Michaelis—Menten kinetics

$$S + E \rightleftharpoons ES \rightarrow P + E \tag{1}$$

expresses a mechanism by which the substrate, S, is bound reversibly to the enzyme, E, to form a substrate—enzyme complex, ES, which decomposes irreversibly to the product, P, and the enzyme. The rate of reaction is

$$-\mathrm{d}s/\mathrm{d}t = V_{max}\, S/(K_M + S) \tag{2}$$

where V_{max} is the maximum rate when $S \gg K_M$. K_M is the Michaelis constant with the dimension of concentration. If $S \ll K_M$, Eqn. (2) simplifies to a first-order expression.

Many enzymes show a much more complicated reaction scheme than that shown in Eqn. (1). For example, glucose oxidase requires oxygen as a cosubstrate, whereas alcohol dehydrogenase requires a coenzyme and also works reversibly. Nevertheless, the Michaelis—Menten kinetics has proved to be a very useful approximation when the cosubstrate or coenzyme is in excess. The further approximation with a first-order expression may at first seem to be less useful as the analytical concentrations quite often are larger than K_M (see Table 2). As discussed in detail by Goldstein [31], the effective substrate concentration in reactors with mass transfer resistance is less at the catalyst site than in the bulk. The reactor can therefore be represented by a first-order expression even at concentrations that are well above K_M of the soluble enzyme:

$$-\mathrm{d}s/\mathrm{d}t = K_{ps}^{(app)}\, S \tag{3}$$

with the apparent rate constant, $K_{ps}^{(app)}$, identical to $V_{max}/K_M^{(app)}$. Integration yields

$$-\ln [S_t/S_0] = K_{ps}^{(app)}\, \tau \tag{4}$$

TABLE 2

Estimated inherent rate constants, K, for some enzymes immobilized on porous glass

Enzyme	Pore diam. (nm)	IU mg^{-1}	K_M (M)	K (s^{-1})
Alcohol dehydrogenase	26	300	1.3×10^{-2}	2
L-Alanine dehydrogenase	29	30	1.7×10^{-3}	2
Asparginase	24	80	6×10^{-6}	1000
Carboxypeptidase A	15	35	1.9×10^{-3}	2
Creatine kinase	20	25	1.6×10^{-2}	0.2
Creatininase	30	70	3.3×10^{-2}	0.2
β-Galactose dehydrogenase	23	5	3.7×10^{-3}	0.1
β-Galactosidase	39	30	3.9×10^{-3}	0.7
Glucose oxidase	28	210	3.3×10^{-2}	0.6
Hexokinase	23	300	1×10^{-4}	300
Invertase	31	150	9×10^{-3}	2
Lactate dehydrogenase	25	550	6.7×10^{-3}	8
Malate dehydrogenase	19	1100	5.5×10^{-5}	2000
Peroxidase, horse radish	16	160	1.2×10^{-5}	1000
Urease	38	100	1.9×10^{-2}	0.5
Uricase	23	8	1.7×10^{-5}	50
Xanthine oxidase	31	0.4	1.3×10^{-6}	30

where S_0 and S_t are, respectively, the concentrations at the inlet and the outlet of the reactor and τ is the mean residence time

$$\tau = \pi R^2 L \epsilon_t / Q = L/F \tag{5}$$

where Q is the volumetric flow rate, R the radius, L the length of the reactor, ϵ_t the total void fraction and F the linear flow velocity.

If X is the fraction of substrate which has reacted during the transit ($X = 1 - S_t/S_0$) then

$$\tau = -[\ln(1-X)]/[K_{ps}^{(app)}] \tag{6}$$

This equation relates the two most important parameters in the design of analytical reactors, namely the fractional conversion and the mean residence time which in turn is related to the dispersion. If the apparent rate constant of the reactor can be increased sufficiently, the mean residence time can be kept low while almost complete conversion ($-\ln(1-X) = 6.9$ for 99.9% conversion) is still achieved.

Because of the chemical reaction there will be a depletion of substrate around as well as inside the enzyme support (see Fig. 2 [32]). At the limit when the catalyst becomes very efficient, the reaction will go to completion already at the surface and the enzyme in the interior will not be used at all. The utilization of the enzyme can be expressed by the effectiveness factor, η_t

$$\eta_t = \text{Rate with finite mass transfer/Rate with infinite mass transfer} \tag{7}$$

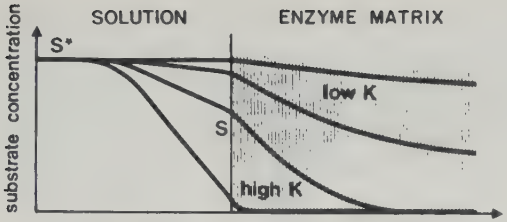

Fig. 2. Variation of the substrate concentration inside and outside a matrix with immobilized enzyme.

The total effectiveness factor, η_t, can be split up into effectiveness factors for external, η_e, and internal, η_i, mass transfer

$$\eta_e \, \eta_i = \eta_t \tag{8}$$

The effectiveness factors are given by the ratio of the rates which for first-order kinetics is equal to the ratio of the rate constants:

$$\eta_e = K_{ps}^{(app)}/K_{ps} \text{ and } \eta_i = K_{ps}/K \tag{9}$$

where K_{ps} is the rate constant in the absence of external mass transfer limitation and K the rate constant in the absence of all mass transfer resistances.

External mass transfer

The transport of substrate up to the enzyme bed is proportional to the concentration difference according to Fick's first law. At steady state, it will also be equal to the reaction rate

$$h(S^* - S) = K_{ps} S \tag{10}$$

where h is the transport coefficient and S^* and S are the substrate concentrations in the bulk and at the surface, respectively. The transport coefficient will take different forms depending on the flow pattern and the bed geometry [33]. An expression has been given [34] which has proved to be valid for reactors packed with porous glass [21, 35]

$$h = BF^{1/2} d_p^{-3/2} \tag{11}$$

where B is a constant, F the linear flow velocity and d_p the mean particle diameter. Because

$$K_{ps}^{(app)} S^* = K_{ps} S \tag{12}$$

the rate constants for packed-bed reactors will be related by

$$1/K_{ps}^{(app)} = (d_p^{3/2}/BF^{1/2}) + (1/K_{ps}) \tag{13}$$

Expressions for open tubular reactors have been derived by Kobayashi and Laidler [36] and tested experimentally on L-asparaginase attached to nylon tubing [37]. In the case of a diffusion-controlled reaction

$$h = B' F^{1/3} R^{-1/3} L^{-1/3} \tag{14}$$

where B' is another constant, R the radius and L the length of the tube. The dependence on L is a result of changes in concentration profile along the tube. Equation (14) is valid for a 2-m long tube (i.d. 1.0 mm) but not for very short or very long and thin tubes. The relations between $K_{ps}^{(app)}$ and K_{ps} take different forms depending on the conditions [36]. When the rate of reaction is low compared to the rate of mass transfer, the apparent rate constant will be equal to the inherent rate constant. The original paper [36] should be consulted for other cases.

Equations (11) and (14) show that the transfer of substrate will become more efficient as the linear flow velocity increases. This reflects the fact that the diffusion layers around the particles or at the tube wall become thinner. A decrease in particle size is very important for increased mass transfer in a packed-bed reactor. A reduction in radius is similarly of importance for improving the performance of tubular reactors although the precise mathematical form of the influence is unknown for small diameters.

Internal mass transfer

The internal mass transfer in a porous particle or in a layer can be expressed with the Thiele modulus, ϕ,

$$\phi = (\text{volume/external surface})\,(K/D_{eff})^{1/2} \tag{15}$$

where D_{eff} is the effective diffusivity in the pores. The volume/surface ratio becomes $d_p/6$ for a spherical particle and d, the thickness, for a layer on the inside of a tube ($d \ll R$). For a packed-bed reactor [4]

$$\eta_i = (1/\phi_s)\,[(1/\tanh 3\phi_s) - (1/3\phi_s)] \tag{16}$$

and for an open tubular reactor [3]

$$\eta_i = \tanh \phi_L / \phi_L \tag{17}$$

For large values of the Thiele modulus (i.e., large K and large d or d_p) the equations can be simplified to

$$\eta_i = (6/d_p)\,(D_{eff}/K)^{1/2} \text{ and } \eta_i = (1/d)\,(D_{eff}/K)^{1/2} \tag{18}$$

The equations state that η_i increases, i.e., the enzyme is utilized more efficiently, as d or d_p is decreased. A very large K results in a very small η_i and the enzyme in the interior will be little used (cf. Fig. 2). Equation (16) has been used to illustrate this in a quantitative way (see Fig. 3).

The compounded effect of internal and external mass transfer for packed-bed reactors can be calculated by means of Eqns. (8), (9), (13), and (16), as shown in Fig. 4. The apparent rate constant should be large in order to achieve a short residence time as well as a high fractional conversion (cf. Eqn. 6). The external mass transfer is the principal rate-limiting factor for large K values. It can be seen from the figure that a higher linear flow velocity will increase $K_{ps}^{(app)}$ but that the highest $K_{ps}^{(app)}$ values are attained only with very small particles.

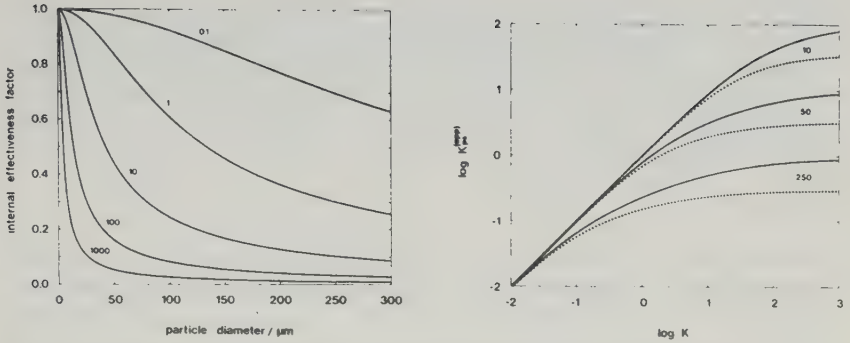

Fig. 3. The internal effectiveness factor as a function of the particle diameter, d_p, and the inherent rate constant, K, indicated on the curves. The calculation was made for spherical particles using Eqn. (16), with $D_{eff} = 2 \times 10^{-6}$ cm^2 s^{-1}.

Fig. 4. The apparent rate constant of packed-bed reactors plotted as a function of the inherent rate constant for particle diameters of 10, 50 and 250 μm and two linear flow velocities: (—) 1 cm s^{-1}; (---) 0.1 cm s^{-1}. $D_{eff} = 2 \times 10^{-6}$ cm^2 s^{-1}; $B = 3.8 \times 10^{-5}$ m s$^{-1/2}$.

Another paper from this laboratory [21] shows that the rate constants can be determined by varying the linear flow rate and the particle diameter. The above equations were found to describe the experiments quite well.

Michaelis—Menten kinetics

Enzyme preparations with K values of less than 1 s^{-1} are little influenced by mass transfer resistances. Integration of Eqn. (2) gives an expression for τ for reactions with Michaelis—Menten kinetics [38—40]:

$$\tau = [S_0 X / V_{max}] - [(K_M^{(app)} / V_{max}) \ln (1 - X)] \qquad (19)$$

with the same notations as above. If $S_0 \ll K_M^{(app)}$, the equation will simplify to Eqn. (6) and if $S \gg K_M^{(app)}$, the first term dominates and the reaction order becomes zero. Values of V_{max} and $K_M^{(app)}$ can be determined from the Lineweaver—Burke or Eadie—Hofstee plots [5], which are linear if the mass transfer influence can be neglected. The procedures for designing reactors when the constants are known has been discussed before [39].

A reactor with an appreciable mass transfer resistance shows an apparent Michaelis constant which becomes higher as the importance of mass transfer increases [41]. The validity of the first-order approximation will thus depend on the reactor design, but the Michaelis—Menten equation will have to be used sooner or later as S_0 is increased. Equations for reactors with mass transfer resistance and Michaelis—Menten kinetics are frequently difficult to solve in closed form.

A reactor operating with zero-order kinetics ($S_0 \gg K_M^{(app)}$) is obviously useless analytically because the amount of product is independent of the

substrate concentration. Even reactors operating in the Michaelis—Menten region ($S_0 \simeq K_M^{(app)}$) have disadvantages analytically because the output is a non-linear function of the input (cf. the lower curve in Fig. 1e). The linear range can be made to approach or even pass $K_M^{(app)}$ if the fractional conversion is made very high, $K_M^{(app)}$ can be increased by making the mass transfer resistance larger.

OPTIMIZATION

The inherent rate constant is a conditional constant and it can be increased by increasing the loading of enzyme on the surface and by increasing the surface area of the carrier. It is of interest to consider the magnitude of the inherent rate constant for various enzymes if an optimal enzyme packing is assumed. The intrinsic kinetic constants of an immobilized enzyme molecule will be affected by a number of factors [31]. For the purpose of this discussion, it will nevertheless be assumed that the K_M values of immobilized and soluble enzymes are equal; other assumptions are that the available surface area can be covered to 10% and that such a coverage can be obtained within pores which are twice as large as the diameter of the enzyme molecules. The specific activities (IU mg^{-1}) were taken from catalogues of commercially available chemicals and the purest product was selected. It was assumed that the impurities have the same molecular weight as the enzyme and are immobilized with the same probability. Table 2 shows the results of such calculations made for some enzymes of interest for applications of f.i.a. As a check the K value for peroxidase was also calculated for 72.9-nm pores, and was found to be 300 s^{-1}, which agrees fairly well with the value of 150 s^{-1} found experimentally [21] for aged reactors.

The results in Table 2 are informative about several aspects. With larger molecules, a larger pore size has to be selected which results in a smaller surface area per gram of glass (cf. Table 1). The result is that the supposed loading becomes close to 18 mg of enzyme per gram of glass irrespective of the molecular weight of the enzyme. The first-order rate constant equals the ratio of V_{max} and K_M. Urease has a high activity per mg of enzyme but its large K_M value will force the first-order rate constant to become low. Urease and glucose oxidase both have low rate constants but nevertheless both have performed well in flow injection systems [42—44]. Because the rate constants of most enzymes are larger than those mentioned, the prospects should be bright for making high-performance reactors for other applications. All diagrams in this paper were calculated using a diffusion coefficient of 0.7×10^{-5} cm^2 s^{-1}, which is an intermediate value for substrates of the enzymes listed in Table 2.

The residence time is a function of K as well as of the particle size (Fig. 5). The calculations were made for a reactor with a fractional conversion of 99.9%, a flow rate of 1 ml min^{-1} and a diameter of 2.0 mm. The length varies over several orders of magnitude; its size can be obtained from Eqn. (5)

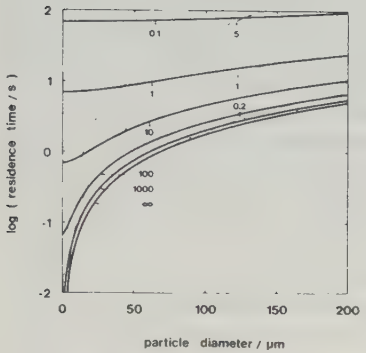

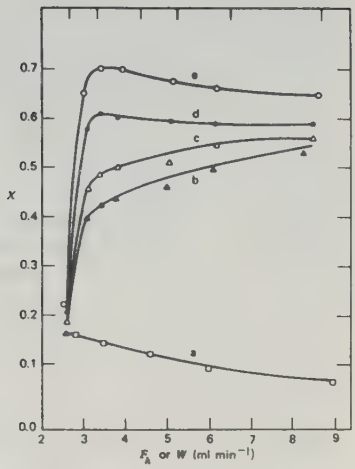

Fig. 5. The residence time, τ, in a packed-bed reactor (2.0 mm i.d., flow rate 1 ml min^{-1}, 99.9% conversion) plotted as a function of particle diameter for inherent rate constants between 0.1 and ∞ s^{-1}. The feint lines show where the pressure drop over the reactor equals 0.2, 1 and 5 atm. D_{eff} and B as in Fig. 4.

Fig. 6. Fractional conversion as a function of flow rate for an open tubular reactor: (a) straight tube, unsegmented flow; (b) straight tube, segmented flow; (c—e) coiled tubes, segmented flow. Reproduced, from Horvath et al. [46], with permission.

by inserting the τ value read from the figure. Figure 5 shows that the particle size is fairly unimportant for K values around 0.1 s^{-1}. The larger the rate constant, the greater the further decrease in mean residence time that can be obtained by decreasing d_p. In practice, there is little to be gained by increasing K much above 100 s^{-1}.

The pressure drop was also calculated by using Darcy's equation and various limits are marked in Fig. 5. With a small K value, the particle size can be increased above 200 μm in order to decrease the pressure drop with very little increase in residence time. Of course, the diameter can be increased to reduce the pressure drop further; the relative increase in dispersion will be small at first. A smaller conversion factor might have to be selected in order to decrease τ, but as the mass transfer resistance is negligible for small K values the full disadvantage of parameter dependence then has to be accepted (cf. Fig. 1).

Even if the smallest particle sizes must be excluded for practical reasons, quite a number of enzymes should be capable of giving reactors which convert 99.9% of the substrate to products in less than one second. The lengths of these reactors will approach the diameter used in the calculation. If the diameter had been decreased to say 1.0 mm, the linear flow velocity would

have increased, which in turn would have decreased τ further at the expense of an increased pressure drop. The striking conclusion is that it should be feasible to produce packed-bed reactors with volumes of a few microliters and with residence times in the millisecond range.

Such extremely short residence times may be of little practical interest at present. The system might therefore be optimized with some additional properties in mind. The plot in Fig. 1(a) shows that a reactor giving high conversion is little affected by activity losses. This property can be exaggerated by designing the reactor with say 99.9999% conversion efficiency. The length would only be twice as long but it could lose half of its activity before its performance decreased to that of a reactor giving 99.9% conversion.

It has been reported in several cases that enzyme stability improves for larger support particles. If the particle diameter is increased, the effectiveness factor will decrease, but as some enzyme is deactivated, the K value will decrease and the effectiveness factor will increase. Some of the enzyme in the center of the particles, which was little used at first, will thus be available as a reserve when the preparation ages. The conclusion is that, with enzymes which have high K values, the unnecessarily short residence times may be traded for an increased useful lifetime.

APPLICATIONS

Immobilized enzyme reactors have found numerous applications since their introduction almost twenty years ago [45]. They can easily be interfaced with almost any type of detector which can record the concentration of the substrate, a product, a cosubstrate or a coenzyme. Their utility can be increased by mounting different enzyme reactors in series or by co-immobilization of two or more enzymes. The detection methods used include spectrophotometry, chemiluminescence, fluorescence, amperometry, conductometry, thermometry and potentiometry with ion-selective electrodes or gas sensors.

Open tubular reactors are well suited for use in air-segmented analyzers. The tubes usually have a diameter of 1 mm and a length between 0.5 and 2 m. Air segmentation is very important for radial mixing. Further improvements result from the use of tight coiling, intermediate flow rates and short slug lengths, as shown in Fig. 6 [46]. When the same coils were operated with a homogeneous flow, the fractional conversion decreased drastically (curve a). The reactors are usually operated with intermediate fractional conversions. Carr and Bowers [5] estimated that the coil used by Hornby et al. [13] would have reached 99% conversion if it had been 210 cm long and operated with the shortest slug length of those studied. Typical operating conditions are illustrated in a recent paper with coiled 1-mm nylon tubes with immobilized creatininase [47]. The conversion was 23—28 and 53—60% for 0.5- and 1-m tubes, respectively, when the residence time was 30 s.

The open tubular reactors used so far are not well suited for flow injection applications. The sensitivity becomes too low and the dispersion too high with continuous flow, because of the large diameters of the tubes. Further development could result in more appropriate designs which might have advantages over packed-bed reactors for samples which could clog the latter.

Thermal detection methods require specially designed reactors in order to maximize the temperature transfer to the sensor [5, 48]. A thermistor can be placed in the effluent from a reactor or in the bed of immobilized enzyme. In order to increase the sensitivity, the heat capacity of the bed should be kept as low as possible if short pulses of substrate are to be measured. The maximum sensitivity will thus be obtained at less than complete conversion. The improved designs reported during the last few years have resulted in an increased sample throughput and a decreased sample volume. Danielsson et al. [49] injected 5—20 μl samples of serum directly into the buffer stream.

Cremonesi and Bovara [50] seem to have been the first to use immobilized enzymes together with a flow injection system. They reported on the determination of glucose, ethanol, and testosterone with enzymes immobilized on cellulose. They concluded that cellulose is to be preferred to, e.g., Sepharose because it is deformed less easily, but that further improvement in the matrix was desirable. Nevertheless, they obtained good linearity of response, high sensitivity and a sample capacity of 60 h^{-1} with h.p.l.c. equipment including a spectrophotometer which was not optimized for the purpose.

Glucose determinations have received much attention because of their clinical importance as can be seen by the list of references given by Carr and Bowers [5]. Watson et al. [42] developed a glucose analyzer for 2-μl sample injections, using a packed-bed reactor containing glucose oxidase immobilized on porous alumina. The mean residence time in the reactor was 15 s and the conversion was "100%". The detection was based on electrochemical oxidation of the hydrogen peroxide. In another flow injection method for glucose determinations [43], glucose oxidase and peroxidase were immobilized on porous glass and used in successive reactors with a photometric detector (555 nm); 45 samples per hour could be processed with negligible carry-over and with 25- or 100-μl samples depending on the desired range. This example also illustrated the use of an on-line dialyzer to keep the reactors free from large molecules, particles and bacteria. At a flow rate of 1 ml min^{-1} on both sides of the dialysis membrane, 16% of a test substance (catechol) passed across the membrane. Some sensitivity is thus lost in the dialyzer but it is still adequate for glucose determinations in both serum and urine.

Adams and Carr [51] observed serious adsorption in their flow injection system for urea determination. Proteins visibly coated the hydrophobic non-porous glass. The peak shape differed substantially when urea and

ammonia samples were injected. Gorton and Ögren [43] also used urease immobilized on porous glass; and employed an on-line dialyzer which passed 27% of the urea or ammonia into the buffer fed to the reactor. No interferences arose from adsorption, but a small difference was noted between the peak shapes produced by urea and ammonia samples. A dialyzer may thus reduce interferences from sample components, but will not remedy adsorption of products or dialyzable components. Such adsorption can be affected by changes in the immobilization method [21, 51].

REFERENCES

1 J. Růžička and E. H. Hansen, Anal. Chim. Acta, 78 (1975) 145.
2 K. K. Stewart, G. R. Beecher and P. E. Hare, Anal. Biochem., 70 (1976) 167.
3 O. Levenspiel, Chemical Reaction Engineering, 2nd edn., Wiley, New York, 1972.
4 C. N. Satterfield, Mass Transfer in Heterogeneous Catalysis, M.I.T. Press, Cambridge, 1970.
5 P. W. Carr and L. D. Bowers, Immobilized Enzymes in Analytical and Clinical Chemistry, Wiley, New York, 1980.
6 D. L. Eaton in D. E. Leyden and W. T. Collins (Eds.) Silylated Surfaces, Gordon and Breach, New York, 1980, p. 201.
7 W. E. Hornby and H. Filippuson, Biochim. Biophys. Acta, 220 (1970) 343.
8 H. Filippusson and W. E. Hornby, Biochem. J., 120 (1970) 215.
9 P. V. Sundaram and W. E. Hornby, FEBS Lett., 10 (1970) 325.
10 D. J. Inman and W. E. Hornby, Biochem. J., 129 (1972) 255.
11 J. P. Allison, L. Davidson, A. G. Hartman and G. B. Kitto, Biochem. Biophys. Res. Commun., 47 (1972) 66.
12 D. J. Inman and W. E. Hornby, Biochem. J., 137 (1974) 25.
13 W. E. Hornby, J. Campbell, D. J. Inman and D. L. Morris, in E. K. Pye and L. B. Wingard, Jr. (Eds.), Enzyme Engineering, Vol. 2, Plenum Press, New York, 1974, p. 401.
14 C. Horvath and B. A. Solomon in E. K. Pye and L. B. Wingard, Jr. (Eds.), Enzyme Engineering, Vol. 2, Plenum Press, New York, 1974, p. 259.
15 C. Horvath and B. A. Solomon, Biotechn. Bioeng., 14 (1972) 885.
16 H. A. Mottola, Anal. Chim. Acta, 145 (1983) 27.
17 K. Mosbach (Ed.), Methods in Enzymology, Vol. XLIV, Immobilized Enzymes, Academic Press, New York, 1976.
18 O. R. Zaborsky, Immobilized Enzymes, CRC Press, Cleveland, OH, 1973.
19 H. H. Weetall and S. Suzuki (Eds.), Immobilized Enzyme Technology, Plenum Press, New York, 1975.
20 P. Thibault, P. Monsan, O. C. Jouret, Sci. Aliment., 1 (1981) 55.
21 B. Olsson and L. Ögren, Anal. Chim. Acta, 145 (1983) 87.
22 J. E. Dixon, F. E. Stolzenbach, J. A. Berenson and N. O. Kaplan, Biochem. Biophys. Res. Commun., 52 (1973) 905.
23 L. Goldstein, Y. Levin and E. Katchalski, Biochemistry, 3 (1964) 1913.
24 H. H. Weetall, N. B. Havewala, H. M. Garfinkel, W. M. Buehl and G. Baum, Biotechn. Bioeng., 16 (1974) 169.
25 S. Henry, J. Koczan and T. Richardson, Biotechn. Bioeng., 16 (1974) 289.
26 R. P. Chambers, G. A. Swan, E. M. Walle, W. Cohen and W. H. Baricos, in H. H. Weetall and S. Suzuki (Eds.), Immobilized Enzyme Technology, Plenum Press, New York, 1979, p. 199.
27 L. Ögren and G. Johansson, Anal. Chim. Acta, 96 (1978) 1.
28 W. G. Bardsley, R. E. Childs and M. J. C. Crabbe, Biochem. J., 137 (1974) 61.

29 J. R. Ford and W. H. Pitcher, in H. H. Weetall and S. Suzuki (Eds.), Immobilized Enzyme Technology, Plenum Press, New York, 1975, p. 17.
30 H. H. Weetall in K. Mosbach (Ed.), Methods in Enzymology, Vol. XLIV, Immobilized Enzymes, Academic Press, New York, 1976, p. 134.
31 L. Goldstein in K. Mosbach (Ed.), Methods in Enzymology, Vol. XLIV, Immobilized Enzymes, Academic Press, New York, 1976, p. 397.
32 J. M. Engasser in P. Dunhill, A. Wiseman and N. Blakebrough (Eds.), Enzymic and Non-Enzymic Catalysis, Horwood, Chichester, 1978, p. 174.
33 A. J. Karabelos, T. H. Wegner and T. J. Hanratty, Chem. Eng. Sci., 26 (1971) 1581.
34 L. K. McCune and R. H. Wilhelm, Ind. Eng. Chem., 41 (1949) 1124.
35 B. J. Rovito and J. R. Kittrell, Biotechn. Bioeng., 15 (1973) 143.
36 T. Kobayashi and K. J. Laidler, Biotechn. Bioeng., 16 (1974) 99.
37 P. S. Bunting and K. J. Laidler, Biotechn. Bioeng., 16 (1974) 119.
38 L. Goldstein and E. Katchalski, Fresenius Z. Anal., Chem., 243 (1968) 375.
39 G. Johansson and L. Ögren, in E. Pungor and I. Buzas (Eds.), Ion Selective Electrodes, Akademiai Kiado, Budapest 1977, p. 93.
40 W. E. Morf, Mikrochim. Acta, (1980 II) 317.
41 T. Kobayashi and K. J. Laidler, Biotechn. Bioeng., 15 (1973) 47.
42 B. Watson, D. N. Stifel and F. E. Semersky, Anal. Chim. Acta, 106 (1979) 233.
43 L. Gorton and L. Ögren, Anal. Chim. Acta, 130 (1981) 45.
44 B. Olsson, L. Ögren and G. Johansson, Anal. Chim. Acta, 145 (1983) 101.
45 E. Reisel and E. Katchalski, J. Biol. Chem., 239 (1964) 1521.
46 C. Horvath, B. A. Solomon and J. M. Engasser, Ind. Eng. Fundam., 12 (1973) 431.
47 M. Mascini and G. Palleschi, Anal. Chim. Acta, 136 (1982) 69.
48 B. Danielsson, B. Mattiasson and K. Mosbach, Appl. Biochem. Bioeng., 3 (1981) 97.
49 B. Danielsson, K. Gadd, B. Mattiasson and K. Mosbach, Clin. Chim. Acta, 81 (1977) 163.
50 P. Cremonesi and R. Bovara, Biotechn. Bioeng., 16 (1976) 1487.
51 R. E. Adams and P. W. Carr, Anal. Chem., 50 (1978) 944.

V

Analytica Chimica Acta, 145 (1983) 101—108
Elsevier Scientific Publishing Company, Amsterdam — Printed in The Netherlands

AN ENZYMATIC FLOW INJECTION METHOD FOR THE DETERMINATION OF OXYGEN

BO OLSSON, LARS ÖGREN[a] and GILLIS JOHANSSON*

Department of Analytical Chemistry, University of Lund, P.O. Box 740, S-220 07 Lund (Sweden)

(Received 24th July 1982)

SUMMARY

An enzymatic flow injection method for the determination of dissolved oxygen is described. Oxygen from the sample is reduced quantitatively to hydrogen peroxide in a packed-bed reactor containing immobilized glucose oxidase. β-D-Glucose is used as a cosubstrate. The effluent is mixed with a stream containing chromogens and fed into a second reactor containing immobilized peroxidase. The coloured product formed is monitored spectrophotometrically. The response is linear from the detection limit (2—5 μM O_2) to air-saturated samples (0.3 mM O_2) when the peak areas are plotted versus the O_2 content in the samples (50 μl). The maximum speed for 1% carry-over is 60 samples per hour and the results are available 25 s after the start of sampling. Broadening of the peak is caused by adsorption of the coloured product in the peroxidase reactor.

Dissolved oxygen is an important co-substrate in many enzyme reactions. Usually the oxygen is in excess, e.g., when glucose oxidase is used for determination of β-D-glucose. The reaction works equally well when β-D-glucose is in excess and the dissolved oxygen is the limiting substrate. It should be possible to utilize any of a number of oxidoreductases for determination of dissolved oxygen. There appears to be only one earlier study in which oxygen was determined enzymatically [1].

The selectivity of glucose oxidase for the oxidant is high [2], the stability of the enzyme is also good and it is readily available in high purity at low cost. The reaction involves the coenzyme FAD (flavine adenine dinucleotide) which is permanently bound in the enzyme.

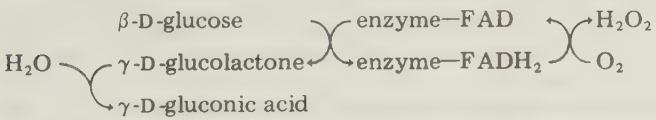

(1)

With β-D-glucose in excess, the flavine will be present in the reduced form, $FADH_2$. Reoxidation of $FADH_2$ with oxygen produces hydrogen peroxide quantitatively.

[a]Present address: AB Draco, P.O. Box 1707, S-221 01 Lund, Sweden.

0003-2670/83/0000-0000/$03.00 © 1983 Elsevier Scientific Publishing Company

Numerous methods are available for determination of hydrogen peroxide [3] and an electrochemical method has already been developed for flow injection analysis [4]. An enzymatic method was selected because of its high selectivity. Possible interferents are substances (e.g., phenolic compounds and some aromatic amines) which will react with or substitute the co-reactant. The enzymatic method involves peroxidase-catalyzed coupling of hydrogen peroxide with chromogens to a coloured product. Such reactions have been studied extensively because of their importance for determination of β-D-glucose and at least 35 reagents have been investigated more or less thoroughly. 4-Aminophenazone and *N*,*N*-dimethylaniline were selected for the present study

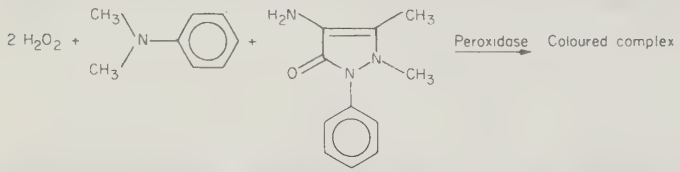

(2)

The detailed reaction mechanism is not known. It has been observed in this laboratory that the absorbance is somewhat less with immobilized peroxidase than with the soluble enzyme.

In the method described by Ghosh et al. [1] oxygen was reacted with a known excess of β-D-glucose as in Eqn. (1). The hydrogen peroxide was simultaneously destroyed by catalase which was present as an impurity. The enzymes were next destroyed by boiling. The remaining β-D-glucose was then determined spectrophotometrically with oxygen in excess in the usual way (Eqns. 1 and 2). In the method proposed here, the hydrogen peroxide formed in the reaction with glucose oxidase is determined directly on-line with the peroxidase-catalyzed colorimetric method (Eqn. 2). The glucose oxidase should be essentially free of catalase in order to prevent decomposition of the hydrogen peroxide.

EXPERIMENTAL

Flow injection system

A buffer containing β-D-glucose is pumped through the injector to a reactor with immobilized glucose oxidase as shown in Fig. 1. Chromogens are pumped in a second channel to a confluence point where the stream mixes with the sample stream. The colour-forming reaction takes place in a reactor with immobilized peroxidase and the product is monitored at 555 nm with a variable-wavelength flow-through spectrophotometer (LKB model 215). The sample is drawn into the sample loop (50 μl) by a second pump (LKB Varioperpex) operated for 5 s at 3.0 ml min^{-1} for each sample. The slide injection valve (Cheminert SVA 8031) was operated by two pneumatic actuators controlled by a desk-top computer (ABC 800, Luxor, Sweden). The computer

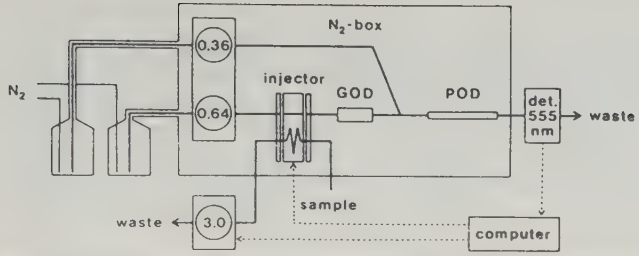

Fig. 1. Flow injection system for detection of oxygen. GOD, glucose oxidase reactor; POD, peroxidase reactor. For a detailed explanation, see text.

also controlled the sampling pump and collected absorbance values from the spectrophotometer. The computer evaluated the data and displayed the peak and operational parameters on the screen.

The reagents were contained in glass bottles which were connected to the pump tubings with 0.9 mm i.d. teflon for the liquid lines and coaxially with 2.5 mm i.d. nylon tubing for the gas line. The flow rates were 0.64 and 0.36 ml min^{-1} for the glucose and chromogen buffers, respectively. The connection to the spectrophotometer was through 0.3 mm i.d. teflon tubing.

The head of the reagent pump (Gilson, Minipuls 2) was fitted with a polycarbonate gas-tight box (volume 4 l) which also housed the injection valve and the enzyme reactors. Purified nitrogen (<10 ppm O_2), delivered by pressure regulators with steel membranes through steel and nylon tubing, was bubbled through the reagent bottles. The nitrogen passed into the gas-tight box via the coaxial connection and was vented through a safety valve in the box set for a slight overpressure. Oxygen exchange with the atmosphere has to be prevented up to the glucose oxidase reactor. After that it will not influence the results. The sample inlet tube was of thick-walled nylon (0.8 mm i.d., 2.5 mm o.d.). The permeation rate of oxygen through teflon and PVC is 250—500 times faster than through nylon-6. As there are no pump tubings available in oxygen-tight materials, it was necessary to resort to a gas-tight box for the pump head. The measures undertaken for the prevention of oxygen exchange and contamination were fully adequate.

Reagents

The injection line contained a 0.01 M phosphate buffer, pH 6.0, with 1 mM β-D-glucose (Pharmacia Fine Chemicals). The chromogen line contained a 0.14 M phosphate buffer, pH 6.0, with 2.14 mM 4-aminophenazone (BDH Chemicals), 6.92 mM *N,N*-dimethylaniline (99.5%; Riedel-de Haën) and 2.25% triethylamine (Fluka, p.a.). Selection of reagents is critical for the stability. Chemicals from some other manufacturers were not of sufficient purity. The chromogen buffer was renewed daily.

Enzyme reactors

Glucose oxidase from *Aspergillus niger* (EC 1.1.3.4) with less than 1.7% catalase activity (Serva) was azo-coupled to porous glass CPG-10 (Electro-nucleonics; pore diameter 72.9 nm, 120—200 mesh). A portion (0.25 ml) of 0.1 M phosphate buffer, pH 7.0, was added to 0.75 ml of enzyme solution (14 mg ml^{-1}); 0.9 ml of the resulting solution was added to 0.1 g of arylamino glass. The coupling gave a yield of 48%, i.e., 43 mg of glucose oxidase per g of glass. The enzyme-glass was wet-packed in a teflon reactor (2.7 mm i.d., 14.7 mm long, volume 84 μl).

Peroxidase from horse radish (EC 1.11.1.7; Sigma Type VI, P6140) was also azo-immobilized to porous glass [5] with the same pore and particle size. The immobilization gave a yield of 36%, i.e., 28 mg of peroxidase per g of glass. The enzyme-glass was wet-packed in a teflon tubing (1.0 mm i.d., 28 mm long, volume 22 μl). The packing was retained in the reactor by two nickel screens which were sealed against the flanged tube endings and held in place by Altex screw couplings.

Calibration

A three-necked 500-ml flask was fitted with an oxygen electrode (Beckman Monitor System 123305) in the center and a thermometer (±0.05°C) in one side port. The sampling line and tubings for air or nitrogen were fitted into the remaining port. The flask was filled with air-saturated 0.01 M phosphate buffer, pH 6.0. The oxygen electrode was calibrated by using the tables given by Hitchman [6]. The barometric pressure was read to ±1 mm Hg. Samples were also drawn into the sample loop and injected into the system described above. Other oxygen levels were produced by gas bubbling and determined with the oxygen electrode.

Hydrogen peroxide was standardized by visual titration with potassium permanganate.

RESULTS AND DISCUSSION

Properties of the method

Samples with various amounts of dissolved oxygen were injected into the system. The peak absorbances and peak integrals were plotted versus the sample oxygen concentration as determined by the electrode (Fig. 2). A straight line passing the origin is obtained when the peaks are integrated; peak height measurements resulted in a curved plot.

The colour-forming reaction in the peroxidase reactor can be tested separately if samples of hydrogen peroxide are injected. The β-D-glucose is of course excluded from the reagent pumped through the injection line during this test. The results are again plotted in Fig. 2. The peak absorbances fall exactly on the same line as those for the oxygen determination. This shows that the bend in the calibration is due to the colour-forming reaction and also that the reaction in the glucose oxidase reactor (Eqn. 1) is quantitative.

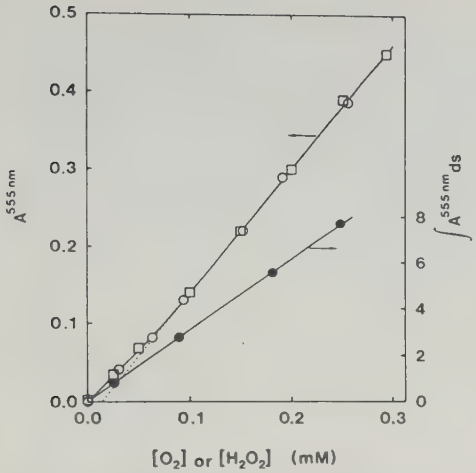

Fig. 2. Calibration curves for oxygen (○, •) and hydrogen peroxide (□). Open symbols correspond to peak heights, and filled symbols to peak integrals.

Figure 3A shows the peak form when various amounts of dissolved oxygen were injected. There is a pronounced tailing in the peaks which is especially severe for small amounts of oxygen. A larger proportion of the coloured product is delayed in the system at low levels which explains the need to integrate the peaks in order to achieve a linear calibration plot.

In order to assess the physical dispersion of the system, catechol solution was used as a sample and monitored at 275 nm. Table 1 gives the peak widths at various heights for the catechol sample compared to an oxygen

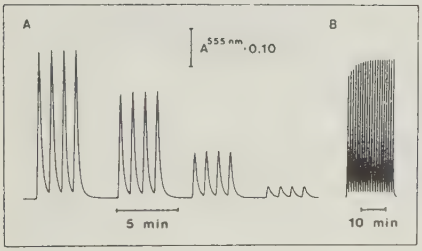

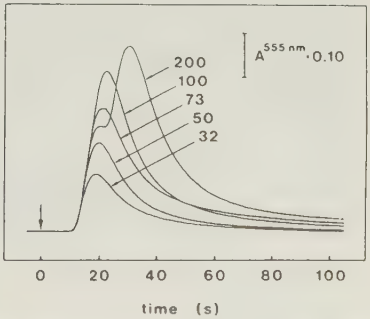

Fig. 3. Peak shapes. A, aged reactor with samples containing 0.248, 0.181, 0.089 and 0.026 mM O_2; B, new reactor, air-saturated samples.

Fig. 4. Variation in peak shape with sample volume (200, 100, 73, 50 and 32 µl) of air-saturated samples.

TABLE 1

Peak width(s) at half ($t_{w\,1/2}$), a tenth ($t_{w\,1/10}$), and hundredth ($t_{w\,1/100}$) of the peak height (Sample volume 50 μl, flow rate 1 ml min^{-1})

	Sample		
	Catechol	O_2 [a]	O_2
$t_{w\,1/2}$	5	13	25
$t_{w\,1/10}$	11	31	69
$t_{w\,1/100}$	18	60	>120

[a] With triethylamine added to the reagent solution.

sample. It can be concluded from the data that the peak broadening during oxygen determination is due to adsorption of the coloured product in the peroxidase reactor. An amine was therefore added to the final reagent in order to repress the adsorption and the effect of the addition can also be seen in Table 1. These data show that sixty oxygen samples can be processed per hour if a carry-over of 1% is acceptable. In the absence of adsorption, the system should have been able to process 200 samples per hour.

The colour of the peroxidase reactor can be seen through the teflon wall; it darkens permanently with use, probably because of polymerization and irreversible adsorption of the product. For a new reactor, the peak heights will increase with successive injections when a solution containing a high level of oxygen is sampled (Fig. 3B). The effect disappears completely with ageing of the reactor.

It is known that some of the available reagents for peroxidase-catalyzed colorimetric determination of hydrogen peroxide adsorb to porous glass [7, 8]. The present reagents were used before in this capacity without undue adsorption [8]. In the present study, peroxidase was azo-coupled to arylamino-glass whereas alkylamino-glass and glutaraldehyde coupling were used earlier. The reason for sticking to the former immobilization method in spite of its larger adsorption is that it gives a product with superior activity and stability [5].

The peak-to-peak noise corresponds to 0.001 absorbance unit. The detection limit, however, is set by the adsorption and is estimated as 2—5 μM oxygen. The peaks are evaluated relative to the base-line so that the background will be subtracted automatically. Nevertheless, the reagent blank should be reasonably low, otherwise the accuracy will be degraded. When the chromogen reagent was fresh, its absorbance was negligible (<0.001) but it increased during the day. The rate of increase varied from one batch of reagents to another.

The system was designed for a maximum oxygen level corresponding to 50 μl of air-saturated sample. The range may be adjusted, as usual in flow injection analysis, by adjusting the sample size. Oxygen-saturated solutions can be analyzed with 10-μl sample volumes.

Design of the flow injection system

The glucose oxidase reactor is the main dispersing element in the system if non-adsorbed compounds are considered. The actual peak shapes are determined mainly by adsorption in the peroxidase reactor and there is therefore little to be gained by attempting to reduce dispersion in the glucose oxidase reactor. The reactor size is large enough to convert essentially all the substrate to product, which is advantageous for an analytical system [9].

The optimization of peroxidase reactors is discussed separately [5]. Immobilization to 25-nm pore diameter glass was found to give the most active preparation. However, as the product adsorbs to the glass surface, it is here essential to optimize the activity with respect to surface area. A larger pore diameter will give a lower loading but with a better utilization of the enzyme. Although the volume of the reactor will be larger, the surface area will be lower, resulting in less adsorption. The reactor geometry was designed in accordance with the theory presented [5] to give 99.9% conversion with as small volume as possible.

In determining the size of the glucose-oxidase reactor, the difference between steady-state and f.i.a. measurements with large samples must be considered. When the β-D-glucose buffer was air-saturated and pumped through the reactor, the conversion of oxygen was essentially 100% up to 3.5 ml min^{-1}. The over-capacity seems to be 3.5 times (if the effect of increased mass transfer by increased linear flow is neglected). The dynamic properties of the reactor for various sample volumes are shown in Fig. 4. The peak height first increases with sample volume as usual, but at 200 μl a plateau is formed on the rising part of the curve. The level coincides with the amount of reduced coenzyme in the reactor (14 nmol equivalent to 60 μl of air-saturated sample). The amount was calculated from the known enzyme loading. The plateau appears because the sample plug is so long that the amount of β-D-glucose is insufficient in the middle. All the reduced $FADH_2$ in the reactor is then oxidized by oxygen and the sample then passes through without reaction.

A practical consequence of the limited capacity to reduce oxygen is that the amount of oxygen in large samples should not exceed 14 nmol. With small sample volume, β-D-glucose is mixed with the sample and more oxygen can be reduced.

Glucose oxidase was previously immobilized using glutaraldehyde coupling [8] whereas azo coupling was used in this study. Both methods yield active and stable reactors and no grounds for preference of one over the other have appeared so far.

Properties of the new method

The enzymatic method measures the amount of dissolved oxygen in the sample, in contrast to the oxygen electrode which measures the partial pressure. For standardized conditions like those used above, the information is independent of the principle but this is not so generally [6].

The injected sample volume is 50 μl but another 200 μl is required before the sample loop is completely flushed. Still, this is a moderate requirement compared to the usual oxygen methods. The result is available at the computer 25 s after the start at the sampling pump which again compares favourably with existing methods. If the glucose reactor has 100% conversion efficiency, the method can be calibrated with hydrogen peroxide samples. Some of the advantages are due to the f.i.a. principle and some to the chemical reaction scheme utilized.

The prospects for further development of the method seems to be good. If the peak broadening caused by adsorption could be remedied, the peak height and thus the sensitivity could be increased. The sample volume could then be reduced correspondingly or the detection limit could be decreased, and the sample throughput could be increased. Several routes are open for further work in order to reduce adsorption (e.g., different reagents, supports or immobilization method).

REFERENCES

1 A. Ghosh, V. Janic and H. A. Sloviter, Anal. Biochem., 38 (1970) 270.
2 M. Dixon, Biochim. Biophys. Acta, 226 (1971) 269.
3 G. G. Guilbault, Handbook of Enzymatic Methods of Analysis, Clinical and Biochemical Analysis Vol. 4, Dekker, New York, 1976.
4 H. Lundbäck, Anal. Chim. Acta, 145 (1983) 000.
5 B. Olsson and L. Ögren, Anal. Chim. Acta, 145 (1983) 000.
6 M. Hitchman, Measurement of Dissolved Oxygen, Wiley-Interscience, New York, 1978.
7 P. Thibault, P. Monsan and C. Jouret, Sci. Aliments, 1 (1981) 55.
8 L. Gorton and L. Ögren, Anal. Chim. Acta, 130 (1981) 45.
9 G. Johansson, L. Ögren and B. Olsson, Anal. Chim. Acta, 145 (1983) 71.

VI

Analytica Chimica Acta, 167 (1985) 123—136
Elsevier Science Publishers B.V., Amsterdam — Printed in The Netherlands

GALACTOSE DETERMINATION IN AN AUTOMATED FLOW-INJECTION SYSTEM CONTAINING ENZYME REACTORS AND AN ON-LINE DIALYZER

BO OLSSON, HANS LUNDBÄCK and GILLIS JOHANSSON*

Department of Analytical Chemistry, University of Lund, P.O. Box 124, S-221 00 Lund (Sweden)

(Received 17th July 1984)

SUMMARY

D-Galactose is oxidized in a reactor containing immobilized galactose oxidase to give hydrogen peroxide, which is determined spectrophotometrically after an oxidative color-forming reaction in a peroxidase reactor. On-line treatment in a dialyzer, a metal-chelate column and a catalase reactor makes the method essentially free from interferences for serum samples, for example. The effect of catalase impurities in the galactose oxidase preparation is illustrated. The linear range for the determination of D-galactose was from 10 μM to 14 mM, and the recovery from spiked serum samples, at low galactose levels, was close to 100%. The sample frequency was 45 h^{-1} and the sample volume was 160 μl. The sampler, the pump and the valves in the flow system were controlled by a personal computer which also collected and analyzed the data.

Determination of D-galactose is of interest in medicine, e.g., for liver tests [1], a test for galactosemia [2], and for the study of glucose intolerance in newborns [3]. It is usually determined through a catalytic reaction involving galactose oxidase. The enzyme also acts on a range of substrates with terminal D-galactopyranosyl residues, e.g., raffinose, lactose and other compounds of interest in the food industry [4, 5]. The efficiency of its oxidation of dihydroxyacetone [6] might be utilized for biotechnical process control [7].

Galactose oxidase (GalOD) catalyzes the reaction between D-galactose and oxygen

$$\text{D-galactose} + O_2 \xrightarrow{\text{GalOD}} \text{D-galactohexodialdose} + H_2O_2 \qquad (1)$$

in a fairly complex reaction, the details of which are only partially understood [8, 9]. The enzyme contains copper [10], which seems to change between copper(III) and copper(I) during the course of reaction (1) [11]. An infrequent side-reaction produces an inactive form of the enzyme with an intermediate oxidation state which may be copper(II). The enzyme can be reactivated by a number of oxidants, including hexacyanoferrate(III). The transition between the copper(III) and copper(II) forms of the enzyme is mediated by certain redox couples like hexacyanoferrate(III) and hexacyanoferrate(II). An induction period which is observed in phosphate buffers is

0003-2670/85/$03.30 © 1985 Elsevier Science Publishers B.V.

eliminated in the presence of, for example, hydrogen peroxide and hexacyanoferrate(III).

The enzyme may lose its copper and become an inactive apoenzyme but the activity can be restored by treatment with a copper(II) solution [12]. A number of substances can inhibit the enzyme; the most important in practice are high concentrations of chloride, hydrogen peroxide and hexacyanoferrate(III). Hydrogen peroxide, which is formed during turn-over, may thus, depending on the conditions, act as an activator or an inhibitor. The enzyme is reported to be stable at room temperature over extended periods of time, especially in phosphate buffers. It has a good natural resistance towards bacterial attacks, elevated temperatures and organic solvents.

Galactose oxidase is the most commonly used enzyme for galactose determinations, although galactose dehydrogenase also seems to work well [13]. The reaction (1) can be followed by monitoring the consumption of oxygen [12] or the production of hydrogen peroxide which can be detected amperometrically [2, 14], fluorimetrically [1] or spectrophotometrically [15, 16]. Of special interest in connection with this work is a determination by flow injection analysis (f.i.a.) based on an earlier method in which immobilized galactose oxidase and a Clark electrode were used [12].

EXPERIMENTAL

Preparation of the galactose oxidase reactor

Galactose oxidase (EC.1.1.3.9; Sigma Chemical Co.) was obtained as both type IV and type V, which differ in purity. Attempts to immobilize the crude enzyme were unsuccessful and a purification was therefore undertaken. The enzyme (400 Sigma units) was dissolved in 1 ml of buffer and dialyzed against phosphate buffer, pH 7.0, overnight and against 20 mM sodium acetate, pH 5.0, for 30 min. The dialyzed solution was injected directly into a preparative high-performance liquid chromatographic (h.p.l.c.) system containing a 5 mm i.d. Mono-S HR 5/5 cation-exchanger column (Pharmacia Fine Chemicals, code no. 17-0547-01) and a spectrophotometric detector. Elution (1 ml min^{-1}) was done with a gradient of 0—0.5 M sodium chloride in the sodium acetate buffer. The gradient (20 mM min^{-1}) was applied after all the unretained material had been eluted. The galactose oxidase fraction (0.8 ml) contained about 90% of the oxidase activity of the injected sample and the specific activity (units per absorbance at 280 nm) had increased 32 times. The fraction was immediately dialyzed against 0.25 M phosphate buffer, pH 8.5.

The dialyzed galactose oxidase fraction was added to 50 mg of arylamino glass activated as described before [17, 18] and allowed to react overnight at room temperature. Almost 100% of the enzyme was retained on the support. The glass (Electronucleonics) had a pore size of 33 nm and a particle size of 75—125 μm. The enzyme-glass was packed into teflon tubing (i.d. 1.9 mm, volume 95 μl) fitted with retaining nets made of polypropylene. The reactor

was provided with Altex screw fittings for connection to other components in the flow system. The enzyme reactor was stored in a Tris buffer containing 2 mM copper sulphate and 0.1 mM EDTA.

Preparation of the other reactors in the flow-injection system

Peroxidase (EC.1.11.1.7, Sigma type VI, P-8375) was immobilized on diazotized controlled pore glass CPG-glucophase-G (Pierce Chemical Co.) with a pore diameter of 46 nm and a particle size of 37—74 μm. The support was diazotized by the same procedure as used earlier for alkylamino glass [18]; 2.5 mg of enzyme was added to 50 mg of glass and the coupling yield was 2%. The enzyme-glass was packed into a reactor (i.d. 2.4 mm, volume 180 μl). The apparent pseudo first-order rate constant for the reactor (K_{POD}) was 1.1 s^{-1} and the conversion of hydrogen peroxide to products should therefore be at least 99.99%. The low loading and large reactor volume is advantageous for the chromogenic reaction.

The colored products which form in the peroxidase reactor will absorb on normal hydrophobic porous glass and the adsorption may result in severe peak broadening [19]. Adsorption on the glucophase-G support is negligible under the conditions used in the flow-injection system. Extended experience with the peroxidase reactor indicates that it can be used for several months without visible deterioration.

Catalase (EC.1.11.1.6, Sigma C-40) was also coupled to diazotized CPG-glucophase-G support material by the same procedure as described for peroxidase; about 25% of the enzyme was retained on the support. The enzyme-glass was packed into a reactor (i.d. 1.9 mm, volume 70 μl). The apparent pseudo first-order rate constant for the reactor was >2 s^{-1}, corresponding to $>99.99\%$ destruction of the hydrogen peroxide.

Bond-Elut-NH_2 (Analytichem International, Harbor City, CA 90710), is a disposable column packing for sample clean-up. The material, which consists of propylamine silylated silica, was packed into a teflon tube (i.d. 1.9 mm, volume 70 μl) with methanol as solvent. The column was washed with water, saturated with copper ion (10 mM copper sulphate, 15 min), and washed with a salt solution (10 mM sodium chloride, 10 min) and 0.1 mM ascorbic acid (15 min) at a flow rate of 1 ml min^{-1}. The latter treatment removes loosely bound copper. The capacity for ascorbic acid removal after this treatment corresponds to 10 μmol as determined by breakthrough curves. A new reactor was taken each morning and the used reactors were discarded because of some slow irreversible inactivation.

Flow-injection manifold for galactose determination

The sample loop (160 μl) of a pneumatic injection valve (Cheminert SVA 8031) was filled by a suction pump from a sampler with test tubes or vials (Fig. 1). The sample was injected into a carrier stream normally consisting of water, and dialyzed on-line in a home-made dialyzer [20] with channels of length 475 mm, width 1.5 mm, and height 0.25 mm. The dialyzer consisted

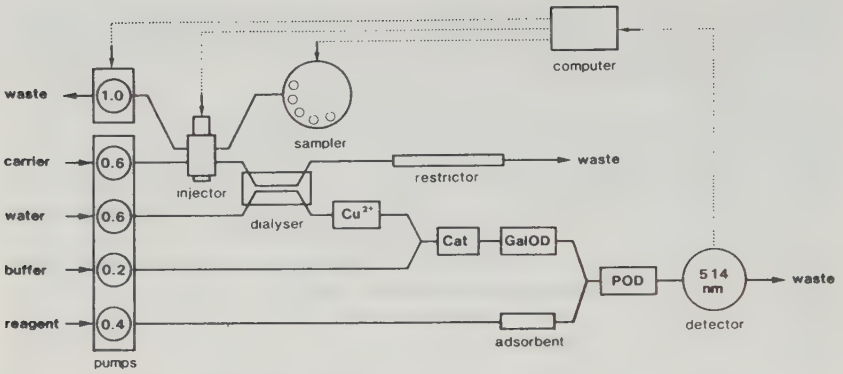

Fig. 1. Schematic diagram showing the flow-injection system for galactose determination with spectrophotometric detection. The flow rates given in the pump symbols are in ml min^{-1}. Reactors: Cu^{2+}, Bond-Elut-NH_2-Cu; Cat, catalase; GalOD, galactose oxidase; POD, peroxidase; adsorbent, arylamino porous glass.

of two equal perspex halves with cut channels, clamped together over a 0.025-mm thick cellulose acetate dialysis membrane (Elkay Products, Worcester, MA; cat. no. DM-C-2-157-0144). A restrictor was inserted at the waste outlet to match the back-pressure on the detector side of the dialyzer.

The channels of the dialyzer could be filled with solid glass beads (150—250 μm diameter) to reduce the dispersion. Filling was facilitated by wetting the channels with a water-soluble surfactant (Triton X-100). The filling was done with the dialyzer open and a dry membrane was placed between the halves before they were clamped together. Polypropylene nets were mounted at the outlets to retain the glass beads.

The dialyzer was followed by the Bond-Elut-NH_2-Cu column for the removal of interferences and by a catalase reactor for removal of hydrogen peroxide not only from the sample but produced by reactions in the Bond-Elut-NH_2-Cu reactor (Fig. 1). The hydrogen peroxide, which is produced by oxidation of galactose in the galactose oxidase reactor, was monitored through the colour which is formed in an oxidative coupling reaction in the peroxidase reactor. The final detection was done spectrophotometrically at 514 nm (LKB HPLC detector model 2051). A column containing about 200 μl of arylamine-activated porous glass was inserted into the reagent line to adsorb impurities. The carrier and the reagent streams were pumped by a 4-channel peristaltic pump (Gilson Minipuls 2). The confluence points were followed by short (5 cm) single-bead-string reactors [22] for efficient mixing. All tubing was of teflon (i.d. 0.5 mm).

The operation of the system was controlled from a personal computer (Luxor AB, model ABC 800, with high-resolution graphics) with interfacing cards for the sampling pump and for the pneumatics for the sampler and the

injector. The detector output was connected to an A/D converter so that single peaks could be displayed on the whole screen in parallel with the recorder. The peak heights and areas were evaluated and stored for further numerical handling.

Chemicals

Several reagents have been in common use for peroxidase-catalyzed detection of hydrogen peroxide. The reagent specifications differ in some respects when an immobilized or a soluble enzyme is used. The combination of 2,4-dichlorophenol-6-sulphonate (DCPS), and 4-aminoantipyrine seems to be well suited for applications in f.i.a. The DCPS was synthesized as described by Barham and Trinder [22]; it contains unreacted dichlorophenol (DCP) which acts as mediator in the peroxidase reaction. The reagent stream contained 20 mM DCPS/DCP, 0.8 mM 4-aminoantipyrine and 1 mM EDTA in 0.1 M phosphate buffer, pH 7.0. The EDTA improves the stability of the reagent against trace metal-catalyzed air oxidation so that the reagent can be used for up to a week. It was degassed in order to prevent formation of air bubbles in the cuvette.

The reaction conditions in the galactose oxidase reactor were controlled by mixing the dialyzed sample with a stream of pH 7.0 buffer. Two buffers were used, 0.3 M phosphate or 0.5 M *N*-2-hydroxyethylpiperazine-*N'*-2-ethane sulfonic acid (HEPES) to which redox-controlling reagents were added as described later. Many buffer ions, including Tris and acetate, inhibit the enzyme, but a zwitterionic buffer made with *N,N*-bis(hydroxyethyl)glycine (Bicine) has been reported to be favorable because it eliminates the induction period of galactose oxidase observed in phosphate buffers [8]. The zwitterionic buffer HEPES was preferred here because it has a more favorable pK_a value and a weaker copper chelating strength than Bicine.

RESULTS AND DISCUSSION

Column activity of the galactose oxidase reactor

Inadvertently co-immobilized catalase in the galactose oxidase reactor will decompose some of the hydrogen peroxide formed in reaction (1) and decrease the final colour yield. Even small amounts of catalase will have large effects because of its very high turn-over rate compared to that of galactose oxidase.

Hydrogen peroxide decomposition is a pseudo first-order reaction. The conversion rate can be expressed by $-dC/dt = K_{catalase}C$, and the integral expression for a plug-flow reactor is

$$C/C_0 = \exp(-K_{catalase}\tau) \qquad (2)$$

where C_0 and C are the substrate (H_2O_2) concentrations at the inlet and outlet of the reactor, respectively, and τ is the mean residence time. $K_{catalase}$, which is the apparent pseudo first-order rate constant for the reactor, is

dependent on the concentration and the prevailing rate constant(s) of the enzyme and on factors that affect the utilization of the activity, such as the pore and particle size of the support [23].

The $K_{catalase}$ value for the galactose oxidase reactor was determined from Eqn. 2 by passing a constant flow of hydrogen peroxide through the reactor. The remaining fraction of substrate was measured at the outlet. The $K_{catalase}$ value was independent of the flow rate and thus of the mean residence time, confirming the validity of Eqn. 2.

The oxidation of D-galactose in the reactor should be of pseudo-first order for substrate concentrations well below K_m (K_m for galactose is 38 mM in air-saturated solutions [8]) and Eqn. 2 should also be followed for this reaction. The concentration of hydrogen peroxide at the outlet of the reactor, however, will depend on the activities of both galactose oxidase and catalase. If the hydrogen peroxide is treated as a metastable intermediate of two consecutive first-order reactions, the relative concentration at the outlet ($[H_2O_2]/C_0$) will be [24]

$$[H_2O_2]/C_0 = K_{GalOD}/(K_{catalase} - K_{GalOD}) \{\exp(-K_{GalOD}\tau) - \exp(-K_{catalase}\tau)\} \quad (3)$$

where C_0 is now the concentration of D-galactose at the inlet and K_{GalOD} is the pseudo first-order rate constant for galactose oxidation.

Because $K_{catalase}$ was determined separately and the mean residence time is known, K_{GalOD} is the only unknown variable. The value of K_{GalOD} was found by fitting Eqn. 3 to the experimental data (Fig. 2). The greatest weight was put on the data at the highest flow rate, where the effect of catalase was minimal. Figure 2, curve a, shows the response for a reactor with rather high

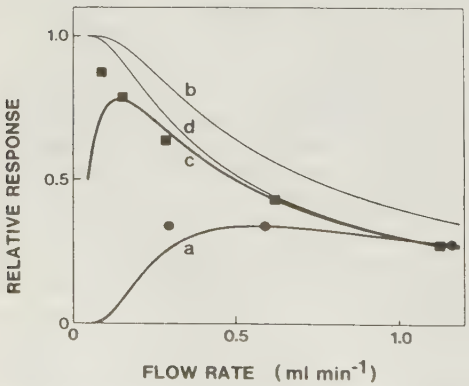

Fig. 2. The responses of a galactose oxidase reactor: (a) before treatment; (b) hypothetical response of the reactor in (a) at zero catalase activity; (c) the same reactor as in (a) after AT treatment; (d) hypothetical response of the reactor in (c) at zero catalase activity. K_{GalOD}: (a, b) 0.028 s^{-1}; (c, d) 0.020 s^{-1}. $K_{catalase}$: (a) 0.034 s^{-1}; (b, d) 0; (c) 0.002 s^{-1}.

catalase activity. Curve **b** represents a simulated case for the same reactor assuming no catalase activity. It can be seen that it is of importance for the sensitivity of the method to find methods of decreasing the catalase activity.

Normal inhibitors for catalase, like cyanide and azide, cannot be used because they will also inhibit galactose oxidase [5, 6, 25]. 3-Amino-1,2,4-triazole (AT) has been used as a ligand in studies of catalase and has been reported to bind irreversibly to the enzyme during turn-over [26]. The reactor used to obtain curve **a** in Fig. 2 was subjected to treatment with 0.1 M aminotriazole/2 mM H_2O_2 at pH 7.0 for 3 h, and the activity of catalase and galactose oxidase was measured again. Curve **c** in Fig. 2 is the fitted curve for the combined effects of the enzymes while curve **d** again is the simulated response of a hypothetical reactor with no catalase activity. It can be seen that the catalase activity of the reactor is decreased to a tolerable level by the aminotriazole treatment, but at the expense of a small loss of galactose oxidase activity (compare curves **b** and **d**). The net result is nevertheless an improved yield of hydrogen peroxide (compare curves **a** and **c**). It was generally found that the curves deviated from the experimental points at low flow rates. This could be due to a weak inhibition of catalase by a product formed in the enzymatic reactions.

The aminotriazole-inhibited catalase was found to regain its activity slowly. Because repeated treatment with the aminotriazole deactivates galactose oxidase, it should be more profitable to purify the enzyme preparation further.

Medium for the galactose oxidase reaction

The composition of the buffer is known to be important for the activity, stability and the type of kinetic behavior of the enzyme [8]. Two different buffer systems were selected for this study, namely HEPES and phosphate; additions of hexacyanoferrate(III) and hexacyanoferrate(II) were made to both. The HEPES buffer was by itself able to activate the enzyme from a low activity state. The enzyme could be brought up to full activity by soaking the reactor in 50 μM hexacyanoferrate(III) in HEPES buffer. In the presence of D-galactose (i.e., during turn-over), however, there was a slow deactivation with time. Yet, it was found that the presence of galactose could also raise the activity of the enzyme from a low level. A certain activity level was thus associated with each galactose concentration and it could be reached from the low or the high side depending on the previous history of the enzyme. Such behavior is not acceptable for a component in a system for quantitative measurements.

It is known that the enzyme activity depends on the redox state of the enzyme and that it can be controlled by mediating redox couples [11]. Attempts were made, therefore, to fix the activity at the high level by adding 5 μM hexacyanoferrate(III) to the HEPES buffer but the combination of hexacyanoferrate(III) and HEPES proved to be strongly inhibitory during turn-over. The activity could be restored completely by activation with

hexacyanoferrate(III) in the absence of D-galactose. Phosphate buffer was therefore selected for further studies. It was found that an enzyme which had been brought to full activity by soaking it in 50 μM hexacyanoferrate(III) in phosphate buffer behaved well in the analytical system. Slow deactivation (about 2% h^{-1}), however, made it necessary to reactivate the enzyme periodically. Hexacyanoferrate(III) (5 μM) was therefore added to the phosphate buffer; the enzyme could then be kept at a state close to full activity. Unfortunately, the activity level of the enzyme still changed when D-galactose was added and the level depended on the concentration of galactose. This method of keeping the enzyme activity high was therefore abandoned.

The next attempt involved fixing the redox potential of the solution by additions of both hexacyanoferrate(III) and hexacyanoferrate(II). The activity level was found to change with the redox potential as described before [11] and a mole ratio of 10:1 was finally selected. This corresponds to approximately 90% of full activity and additions of 4 μM hexacyanoferrate(III) and 0.4 μM hexacyanoferrate(II) were sufficient to make the response factor independent of the amount of galactose in the samples.

Optimization of the system components for f.i.a.

Good overall performance of a flow-injection system, and in particular one with several reactors and dispersing elements, requires optimization with a certain type of samples in mind. The galactose determination system shown in Fig. 1 was designed for sensitive measurements in complex matrices of biological origin. Both dialysis and means for controlling reducing interferences were therefore included. The peak broadening caused by each component individually was measured by injecting 20 μl of a tracer (catechol) when each component was alone in the manifold. The peak width is given at 10% of the peak height (see Table 1). The manifold includes the injector, the tubing and the spectrophotometer, and their dispersion is included in the peak widths given for the other components.

A dialyzer with fairly long channels was chosen in order to transfer a sizeable fraction of the galactose from the sample to the detector side of the membrane and this component will therefore contribute significantly to the overall dispersion. The dispersion in open channels can be decreased by introduction of elements which break up the laminar flow [27]. The dialyzer channels were therefore filled with solid glass beads, and it can be seen from Fig. 3 that this almost doubled the peak height and decreased the peak width (at 10% of the peak height) to two thirds of the previous value. The price to be paid is an added pressure drop in the dialyzer. The total pressure drop becomes high because of the large number of components, but it is still within the range of good peristaltic pumps (see Table 1). With the glass beads in the dialyzer channels, 11% of the galactose in the sample channel was transferred to the detector side.

The effect of various sample volumes on dispersion and peak height can be seen in Table 2. The sensitivity increased with sample volume up to 160 μl

TABLE 1

Dispersion and pressure drop for the individual components in the flow-injection system at the flow rates shown in Fig. 1. The peak widths were determined with a catechol solution (20-μl samples)

Component	Volume (μl)	Width[a] (s)	Pressure-drop (bar)
Injector, manifold and detector	160	10	0.4
Dialyzer, with glass beads	130[b]	18[c]	0.8
Bond-Elut-NH_2-Cu and catalase reactors	70 + 70	16[c]	0.5 + 0.5
GalOD reactor	95	12[c]	0.55
POD reactor	180	12[c]	0.45
Total system	715	33[c]	3.2

[a]Peak width of 10% of peak height. [b]Each channel. [c]Including the injector, manifold and detector.

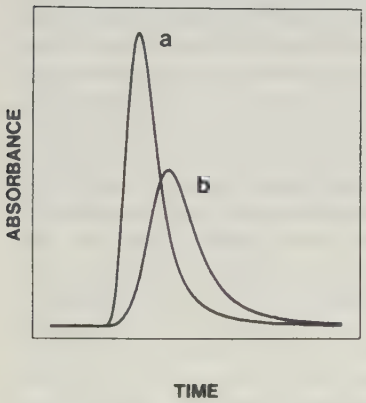

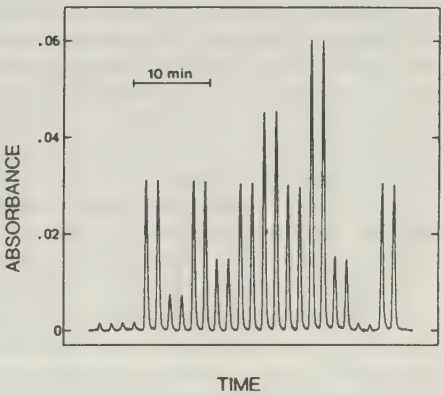

Fig. 3. The peak shape of a dialyzed hydrogen peroxide sample: (a) with solid glass beads in the dialyzer channels; (b) with open channels.

Fig. 4. Response for D-galactose standards. Concentrations from left to right: 10, 200, 50, 200, 100, 200, 300, 200, 400, 100, 10 and 200 μM.

without increased dispersion, and this sample volume was therefore selected for the following work. The sample frequency could be set to 45 samples h^{-1} with baseline separation for such a volume. The time from injection to the peak maximum was 68 s.

TABLE 2

Effect of injection volume on the peak heights and widths when measured in the complete system with catechol samples (flow-rates as in Fig. 1)

Injection volume (μl)	Normalized peak height	Width[a] (s)
20	0.16	34
40	0.29	33
80	0.57	34
160	1.00	38
300	1.43	47

[a]Peak width at 10% of peak height.

Removal of interferences

Reducing substances like ascorbic acid are well-known interferents in detection methods based on hydrogen peroxide. Ascorbic acid will react with an almost equimolar amount of the intermediates which are formed in the peroxidase reactor. The error is negative; less coloured compounds are obtained than in the absence of the interferent. Removal of the interfering substances by alkaline deproteinization with a heavy metal salt is often used for biological samples [28]. Oxidation by mercury(II) ions has also been described [29]. An off-line step, however, is less attractive than alternative on-line methods like oxidation by metal ions bound to an immobilized dithiocarbamate reactor [30].

Effective removal of interferences from added ascorbic acid was achieved by addition of mercury(II) ions (0.5 mM) in the water channel and EDTA (10 mM) in the buffer channel (in a system without the Bond-Elut-NH_2-Cu and the catalase reactors). Because of the waste disposal problem with mercury solutions, an immobilized chelate ion exchanger was next tried. The Bond-Elut-NH_2 was found to be equally effective in removing interferences from ascorbic acid with either mercury(II) or copper(II) metal ions. The latter metal was selected for the final system.

Ascorbic acid is oxidized quantitatively to dehydroascorbic acid in the Bond-Elut-NH_2-Cu reactor with the simultaneous formation of hydrogen peroxide. Hydrogen peroxide may also be present in the samples (e.g., as a result of aerobic oxidation). The catalase reactor will therefore increase the selectivity of the method independently of the method of reductant removal.

Determination of D-galactose

Some low-level galactose standards were run in the system described (Fig. 4). The results gave a linear calibration graph with a correlation coefficient of 0.9999. Standards with equal, intermediate concentrations (200 μM), which were interspaced between samples of lower and higher galactose contents (Fig. 4), show that no memory effects were present. The results

were obtained with a pure phosphate buffer (i.e., no added redox buffer) and they are therefore typical for a system for serum analyses (see below). It can be seen that the peak heights of the 200 μM series decrease very slowly owing to the formation of the inactive copper(II) form of the enzyme. The standard deviation calculated without regard to the successively lowered sensitivity was 1.7% (n = 10). The standard deviation of the peaks shown for 10 μM samples was 5% (n = 6).

The measurements were repeated with a system intended for non-serum samples, i.e., with phosphate and hexacyanoferrate(III)/hexacyanoferrate(II) in the buffer line. The sensitivity remained constant with time and the relative standard deviation at the 200 μm level was typically 0.3—0.5%.

The peak height absorbance for 14 mM galactose was ca. 2.0, which is close to the upper limit for most spectrophotometers. The fact that the calibration graph was linear up to this concentration indicates that the method has a very large linear operating range and could easily be extended upwards by decreasing the sample volume.

Interferences

The effect of some potential interferents was studied by injection of samples containing the substance with and without added D-galactose (Table 3). The interferences from the tested substances were negligible at concentrations well above those normally expected in serum samples. The reported normal range for, e.g., ascorbic acid is 0.01—0.1 mM and for total bilirubin 0.003—0.03 mM with up to 0.5 mM bilirubin for newborns.

The effect of sodium chloride injection is due to refractive index changes in the spectrophotometric cell and it disappears if the carrier has the same refractive index as the sample. It is of little concern in practice, however, because the signal from this effect passes zero and changes sign at the position of the galactose peak maximum. It can be seen that the effect on the response for D-galactose is negligible. Only a negligible amount of bilirubin is transferred through the dialysis membrane and it is thus effectively kept out of the detection system. In a system without a dialyzer, bilirubin is expected to give both chemical and spectral interferences [31]. Glycerol and dihydroxyacetone give responses because they are oxidized catalytically in the presence of galactose oxidase. Dihydroxyacetone is not expected to be present in serum but normal glycerol concentrations are reported to be up to 0.1 mM. It may thus give a high galactose value if present in abnormal amounts in a sample of low galactose content. Various other substances which are reported to be substrates for galactose oxidase [4, 5] are not expected to be present in serum.

Table 4 gives the results obtained when two different sera were spiked with standard additions of D-galactose. One of the sera was measured in two different carrier streams. The recoveries are close to 100%, although slightly high. The enhanced response is probably due to the high viscosity of the serum samples compared to that of the aqueous standards used for calibration.

TABLE 3

Effect of interfering substances on the response when measured separately or when added to a standard solution containing 100 μM D-galactose

Substance	Concentration (mM)	Relative response[a] (%)	
		Alone	Added to galactose
None	—	0	100
Ascorbic acid	1	0	99
	5	0	100
	10	0	
Glutathione	1	—	100
	5	—	98
	10	0	
Uric acid	1	—	101
	2	0	
Bilirubin	1	0	99
L-Cysteine	1		98
Methionine	1		96
Mixture[b]			100
Glycerol	10		200
Dihydroxyacetone	0.1	>400	>400
Hydrogen peroxide	0.1	0	
Sodium chloride	120	5	101

[a]Relative to 100 μM galactose. [b]1 mM each of ascorbic acid, uric acid, glutathione, L-cysteine and methionine.

TABLE 4

Recovery of standard additions of D-galactose to serum

D-Galactose added (μM)	Pathonorm B[a,b]		Pathonorm B[a,c]		Pooled serum[c,d]	
	Galactose found (μM)	Recovery (%)	Galactose found (μM)	Recovery (%)	Galactose found (μM)	Recovery (%)
0	5	—	9	—	20	—
10	—	—	18	90	—	—
50	57	104	57	96	72	104
200	216	106	215	103	226	103
400	406	100	418	102	419	100
600	617	102	640	105	600	97

[a]Reference serum (Nyegaard & Co., Oslo). [b]0.12 M NaCl in the carrier line (see Fig. 1). [c]Water in the carrier line. [d]Obtained from a local hospital.

The galactose levels of the two sera were both very low and close to the limit of the method. Serum galactose levels that are clinically significant are much higher. A further test was made by removing the galactose oxidase reactor from the system and repeating the measurements of the unspiked sera. No response except for the refractive index effect was observed in the absence of the reactor. The salt effect is absent with the saline carrier and a better low-level response is therefore obtained.

The results given above were obtained with a phosphate buffer. With a buffer also containing hexacyanoferrate(III) and hexacyanoferrate(II), there was a negative response when a serum sample was injected. Several minutes were then required before the normal baseline was regained. The explanation may be that an unknown dialyzeable component of the serum reacts with one or both of the ions of the redox couple. A buffer containing phosphate alone should therefore be used for serum samples and possibly other clinical samples. The only disadvantage is that more standards have to be included so that corrections can be made for the slowly decreasing galactose oxidase activity. Phosphate buffers with redox buffering ions give a stable response and may be preferred in non-clinical applications. The background absorbance, which is less than 0.001 with phosphate alone, rises to about 0.015 with the given concentrations of hexacyanoferrate(III) and hexacyanoferrate(II), which may give a somewhat more noisy baseline for low-level measurements.

REFERENCES

1 J. M. Henderson and F. W. Fales, Clin. Chem., 26 (1980) 282.
2 P. J. Taylor, E. Kmetec and J. M. Johnson, Anal. Chem., 49 (1977) 789.
3 G. J. Burrone, J. M. Johnson, S. A. Lewis and J. W. Sparks, Clin. Chem., 26 (1980) 339.
4 G. Avigad, D. Amaral, C. Asensio and B. L. Horecker, J. Biol. Chem., 237 (1962) 2736.
5 R. A. Schlegel, C. M. Gerbeck and R. Montgomery, Carbohydr. Res., 7 (1968) 193.
6 G. T. Zancan and D. Amaral, Biochim. Biophys. Acta, 198 (1970) 146.
7 H. Lundbäck, G. Johansson and O. Holst, Anal. Chim. Acta, 155 (1983) 47.
8 G. A. Hamilton, J. DeJersey and P. K. Adolf, in T. E. King, H. S. Mason and M. Morrison (Eds.), Oxidases and Related Redox Systems, (Proc. 2nd Int. Symp.), University Park Press, Baltimore, MD, 1973, p. 103.
9 R. D. Bereman, M. J. Ettinger, D. J. Kosman and R. J. Kurland, Adv. Chem. Ser., 162 (1977) 263.
10 D. J. Kosman, M. J. Ettinger, R. E. Weiner and E. J. Massaro, Arch. Biochem. Biophys., 165 (1974) 456.
11 G. R. Dykacz, R. D. Libby and G. A. Hamilton, J. Am. Chem. Soc., 98 (1976) 626.
12 S. K. Dahodwala, M. K. Weibel and A. E. Humphrey, Biotechnol. Bioeng., 18 (1976) 1679.
13 G. G. Guilbault, Handbook of Enzymatic Methods of Analysis, Clinical and Biochemical Analysis, Vol. 4, M. Dekker, New York, 1976, p. 262.
14 H. L. Pardue and C. S. Fringes, J. Electroanal. Chem., 7 (1964) 398.
15 H. Roth, S. Segal and D. Bertoli, Anal. Biochem., 10 (1965) 32.
16 M. Hjelm, Clin. Chim. Acta, 14 (1967) 87.
17 H. H. Weetall, in K. Mosbach (Ed.), Methods in Enzymology, Vol. 44, Academic Press, New York, 1976, p. 134.
18 B. Olsson and L. Ögren, Anal. Chim. Acta, 145 (1983) 87.

19 B. Olsson, L. Ögren and G. Johansson, Anal. Chim. Acta, 145 (1983) 101.
20 B. Bernhardsson, E. Martins and G. Johansson, Anal. Chim. Acta, 167 (1985) 111.
21 J. M. Reijn, W. E. van der Linden and H. Poppe, Anal. Chim. Acta, 126 (1981) 1.
22 D. Barham and P. Trinder, Analyst (London), 97 (1972) 142.
23 G. Johansson, L. Ögren and B. Olsson, Anal. Chim. Acta, 145 (1983) 71.
24 M. F. Dunn and S. A. Bernhard, in E. S. Lewis (Ed.), Investigation of Rates and Mechanisms of Reactions, (Techniques of Chemistry, Vol. 6), part 1, 3rd edn., Wiley, New York, 1973, p. 660.
25 J. A. D. Cooper, W. Smith, M. Bacila and H. Meding, J. Biol. Chem., 234 (1959) 445.
26 E. Margoliash, A. Novogradsky and A. Schejter, Biochem. J., 74 (1960) 339.
27 W. E. van der Linden, Anal. Chim. Acta, 151 (1983) 359.
28 R. J. Henry, D. C. Cannon and J. W. Winkleman, Clinical Chemistry, Principles and Techniques, 2nd edn., Harper & Row, Hagerstown, MD, 1974, p. 398.
29 R. H. White-Stevens, Clin. Chem., 28 (1982) 578.
30 T. Yao, Anal. Chim. Acta, 153 (1983) 175.
31 D. L. Witte, L. F. Brown and R. D. Feld, Clin. Chem., 24 (1978) 1778.

VII

ANALYTICAL LETTERS, 18(B7), 871-889 (1985)

AMPEROMETRIC DETERMINATION OF GALACTOSE, LACTOSE AND DIHYDROXYACETONE USING GALACTOSE OXIDASE IN A FLOW INJECTION SYSTEM WITH IMMOBILIZED ENZYME REACTORS AND ON-LINE DIALYSIS

KEY WORDS: Flow Injection Analysis, Amperometric Detection, Flow-Through Dialyzer, Immobilized-Enzyme Reactor, Galactose Oxidase, Peroxidase, Galactose, Lactose, Dihydroxyacetone, Hydrogen Peroxide

Hans Lundbäck and Bo Olsson

Department of Analytical Chemistry, University of Lund, P.O. Box 124, S-221 00 Lund, Sweden

ABSTRACT

A flow injection manifold containing a dialyzer and reactors with immobilized galactose oxidase and peroxidase was used for the determination of galactose in urine, lactose in milk and dihydroxyacetone in a biotechnological reaction medium. The hydrogen peroxide which is formed by the galactose oxidase reaction was detected by amperometric reduction of a mediator. The latter had been produced from hydrogen peroxide in a peroxidase catalyzed reaction. The hydrogen peroxide detection step was studied with several mediators and hexacyanoferrate (II) was selected. An ion exchange HPLC procedure was used to purify the galactose oxidase, in particular from catalase, and the kinetics and the selectivity of a reactor containing the immobilized enzyme was investigated. Columns for removal of certain interferents such as ascorbic acid were used in the determination of galactose in urine. The response to galactose standards was linear from the detection limit of 2 μM to 60 mM. The throughput was 45 samples per hour and the relative standard deviation 0.4%.

Copyright © 1985 by Marcel Dekker, Inc. 0003-2719/85/1807-0871$3.50/0

INTRODUCTION

The recent progress in the techniques of enzyme immobilization and of flow injection analysis (f.i.a.) can both be utilized in methods for the determination of sugars and some carbohydrates in various types of samples. The enzymes provide the selectivity and the f.i.a. the speed, the automation, and the ruggedness. With a sensitive detector the method can be used over a large concentration interval since the sensitivity can be adjusted by selection of different sample volumes and by changing the dispersion or the dilution.

The flow system concept lends itself to a sectioning of the task into analytical unit operations e.g. dialysis, sample pretreatment, chemical reactions, and final detection. This paper reports on development of components to be used in a flow manifold for determination of galactose, lactose, and dihydroxyacetone.

Galactose oxidase (GalOD) catalyzes the oxidation of D-galactose with the release of hydrogen peroxide[1].

$$\text{D-galactose} + O_2 \xrightarrow{\text{GalOD}} \text{galactohexodialdose} + H_2O_2 \qquad (1)$$

A number of compounds with D-galactopyranosyl residues are also oxidized, e.g. raffinose and lactose, as well as some other polyols, e.g. dihydroxyacetone and glycerol[1-3]. The enzyme is very stable at room temperature in phosphate buffers[4] and it is therefore well suited for immobilization and for use in analytical reactors in flow systems [5,6].

Hydrogen peroxide can be determined amperometrically by direct oxidation[7-9] or by reduction of mediators which previously have been oxidized by the peroxide[10-13]. The reduction of the oxidized form of mediators such as iodide, hexacyanoferrate(II), catechol, and hydroquinone, will take place at weakly reducing electrode potentials. This approach seems attractive since very low background currents can be obtained and since low applied potentials should decrease the probability of electrochemical interferences.

The reaction between hydrogen peroxide and mediators requires a catalyst and peroxidase is well suited since its reaction with hydrogen peroxide is both very fast and selective. The back-reduction of the oxidized peroxidase is not particu-

larly selective[13] and it is therefore necessary to use a large excess of the chosen mediator in order to promote its oxidation over the oxidation of other components emanating from the samples.

Many real samples require some pretreatment before entering the main enzyme reactors. On-line dialysis can remove particulate, macromolecular as well as some low molecular weight compounds and dialyzers have proved to be very useful in analytical flow systems if appropriately designed[6,14]. Some reducing substances which pass the dialyzer may interfere with the detection and an on-line oxidizing reactor[6,15], has therefore also been added in one of the applications.

EXPERIMENTAL

Amperometric Detection

The cell used in this work was of the confined wall-jet type, see Fig. 1. The working electrode was made by pressing rods of spectrographic graphite (type RW 003 from Ringsdorff-Werke, GmBH, diam 3.0 mm) into a Teflon holder. The circular end surface was polished on fine, wet emery paper. Carbon film electrodes were made by vapor deposition from hydrocarbons as described by Lundstroem[16]. Both electrode materials were pretreated by oxidaiton at +1.5 V for 30 s in a pH 7.0 buffer. The distance between the working electrode and the inlet nozzle was 1.0 mm.

An Ag/AgCl reference electrode was inserted into a small chamber in the inlet Teflon block. It was filled with 0.1 M KCl from a reservoir consisting of a syringe. Contact with the sample solution was through four very fine holes located symme-

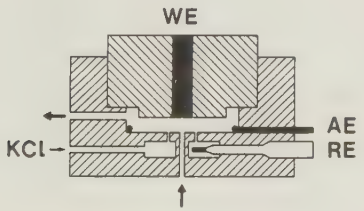

FIG. 1. Diagram of the amperometric flow cell. WE = working electrode, EA = auxiliary electrode, RE = reference electrode. KCl = reservoir of RE solution. For details see text.

trically around the inlet nozzle. The reference electrode was found to be 39 mV more positive than the saturated calomel electrode. The auxiliary electrode was a platinum wire wrapped around the circumference of an annulus in the outlet part of the cell. A PAR m-174 potentiostat was used and its output was connected in parallel to a potentiometric recorder and a personal computer.

Purification of Galactose Oxidase

Galactose oxidase (EC 1.1.3.9, Sigma Chemical Co., type V, from D a c t y l - i u m d e n d r o i d e s, 1200 U) was dissolved in 1.2 ml 0.1 M sodium phosphate, pH 7.0 and dialyzed against the same buffer for four hours. It was next dialyzed for 30 min against 20 mM sodium acetate pH 4.6 and this treatment caused some impurities to precipitate.

The supernatant was injected into an HPLC-system containing a cation exchange column (Mono-S, HR 5/5, Pharmacia Fine Chemicals) and a spectrophotometric detector set at 280 nm. Isocratic elution (1 ml min^{-1}) with a 20 mM sodium acetate pH 4.6, mobile phase, was used to rinse the column from unretained material. A salt gradient (0-0.5 M sodium chloride in the acetate buffer with a gradient slope of 20 mM sodium chloride min^{-1}) was next applied. Fractions were collected and their

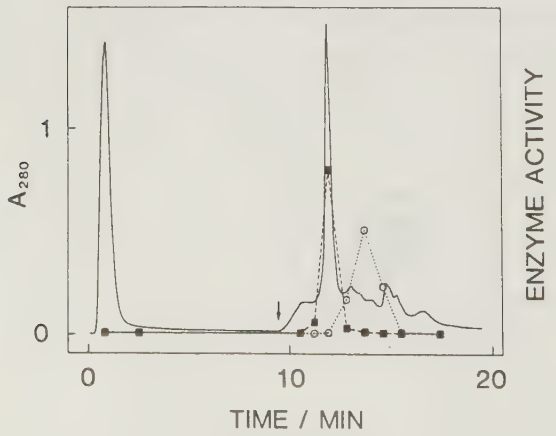

FIG. 2. Separation of galactose oxidase by cation exchange chromatography (—) A 280; (■-■) galactose oxidase activity; (⊙··⊙) catalase activity. The arrow indicates the start of the salt gradient.

catalase and galactose oxidase activities were determined. A chromatogram with the enzyme activities plotted on the same time scale is shown in Fig. 2. The most prominent peak (1.6 ml) contained 90% of the galactose oxidase activity and less than 1% of the total catalase activity. The specific activity (U/A^{280}) had increased six times in the chromatographic procedure. The catalase emerges later than the galactose oxidase as can be seen from the activity curves.

Preparation of Packed-bed Reactors

The oxidase fraction was dialyzed against 0.25 M sodium phosphate, pH 8.5 for 1.5 h and mixed with 50 mg arylamino derivatized controlled-pore glass (CPG-10, Electro-Nucleonics Inc., pore diam. 33 nm, particle size 75-125 μm) prepared and activated as described before[17]. The reaction was allowed to proceed overnight and the supernatant then contained less than 1% of the enzyme activity. The immobilized enzyme was packed into a reactor, i.d. 1.9 mm, volume 135 μl, made of a Teflon tubing fitted with retaining nets of polypropylene and Altex screw fittings. The reactor was activated each day by flushing it with a solution of 50 μM hexacyanoferrate(III) for one minute. The reactor was stored in phosphate buffer, pH 7.0, when not in use.

Peroxidase (EC 1.11.1.7, Sigma Chemical Co., type VI, from horse radish) was immobilized to arylamino derivatized controlled-pore glass (CPG-10, Electro-Nucleonics Inc., pore diam. 73 nm, particle size 75-125 μm) as described before[17], and packed into a reactor (i.d. 1.5 mm, volume 50 μl).

Catalase (EC 1.11.1.6, Sigma Chemical Co., C-40, from bovine liver) was immobilized to arylamino derivatized glycophase G controlled-pore glass (CPG/460, Pierce, pore diam. 46 nm, particle size 37-74 μm) as described before[6]. The enzyme-glass was packed into a reactor (i.d. 1.9 mm, volume 70 μl).

Bond-Elut-NH_2 (Analytichem International), which is a propylamine silylated silica, was packed into a reactor (i.d. 1.9 mm, volume 70 μl), and the amine groups were saturated with copper(II) as described before[6].

Flow-through Dialyzers

Dialyzer A consists of two perspex halves (85 x 65 x 12 mm) with rectangular grooves (widths 1.5 mm, depths 0.25 mm, lengths 475 mm) cut in the surfaces in a

folded pattern. The two halves were clamped together with a cellulose acetate dialysis membrane (Elkey Products Inc., Cat. no DM-C-2-157-0144, thickness 0.025 mm) in between. The liquid volume of each channel was 180 µl.

Dialyzer B was identical to A except that the channels were filled with solid glass beads (diam. 150-250 µm) to increase the radial mixing and hence to decrease the axial dispersion. The free volume then decreased to 130 µl on each side.

Dialyzer C was made by cutting a straight channel in each of two small perspex pieces. The channels were 4.6 mm long, 1.5 mm wide and 0.5 mm deep. The dialysis membrane was identical to those used in dialyser A and B.

A restrictor was inserted at the waste outlet to match the back pressure on the detector side of the dialyzer.

Flow Injection Manifold

A diagram of the flow injection manifold is shown in Fig. 3. The sample was introduced with a computer-controlled pneumatic injector (Cheminert SVA 8031) and the sample loop (10-160 µl) was filled by a peristaltic suction pump. A slide injector (Cheminert CSVA) with an injection volume of 1.5 µl was used in the determination of dihydroxyacetone. The carriers, the buffer and the reagent were pumped with a four-channel peristaltic pump (Gilson, Minipuls 2). The buffer was 0.5 M sodium phosphate, pH 7.0, and the reagent was a deaerated solution containing 5 mM potassium hexcyanoferrate(II) and 0.1 M sodium phosphate, pH 7.0. All connections were made with Altex screw fittings and 0.5 mm i.d. Teflon tubings. Short single bead string reactors[18] (i.d. 0.8 mm, length 50 mm, bead diam. 0.5 mm) were inserted after each confluence point to improve the mixing.

An injected sample is carried into the dialyzer where fractions of the dialyzable components pass through the membrane. The transferred solutes are carried to the galactose oxidase reacor in which substrates of the enzyme are oxidized through the reaction represented by eqn.(1). The hydrogen peroxide which is formed will enter the peroxidase reactor where a corresponding amount of oxidized mediator will be produced. The enzymatically oxidized mediator is then carried to the amperometric detection cell.

Reactors for sample pretreatment were incorporated in the flow system for the determination of galactose in urine. A copper(II) saturated Bond-Elut column was

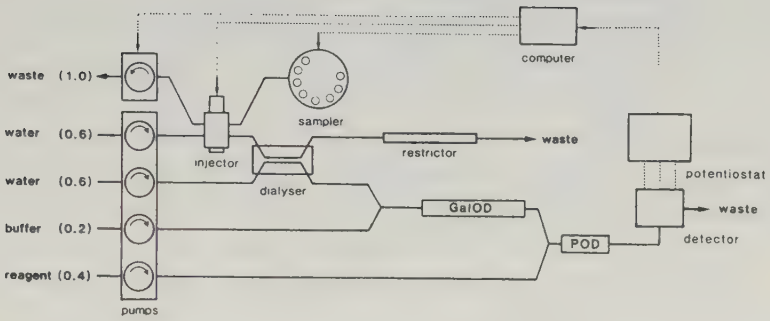

FIG. 3. The f.i.a. manifold. The flow-rates given in the figure are in ml min^{-1}. GalOD;Galactose oxidase reactor, POD; peroxidase ractor. For details see text.

inserted between the dialyzer and the buffer confluence point to remove certain reducing compounds[6]. Ascorbic acid will thus be retained on the column and there be oxidized to dehydroascorbate. Hydrogen peroxide is evolved in the process and a catalase reactor was therefore inserted between the buffer confluence point and the galactose oxidase reactor to decompose the peroxide. Copper ions which may be released from the Bond-Elut column interfere with the amperometric detection and 5 mM EDTA was therefore added to the buffer when this column was present.

Chemicals

D-galactose (G 0750), D-raffinose (R 0250), and α-lactose (L 3625) were obtained from Sigma Chemical Co. Dihydroxyacetone (98%, Merck) was dissolved in water and allowed to monomerize over night. Stock solutions of hydrogen peroxide (Perhydrol, Merck) were standardized by titration with permanganate which in turn had been standardized against oxalate. 4-methyl catechol (Aldrich) was recrystallized from cyclohexene. All other chemicals were of p.a. quality.

RESULTS AND DISCUSSION

Amperometric Determination of Hydrogen Peroxide

A simplified flow manifold consisting of the injector, the peroxidase reactor

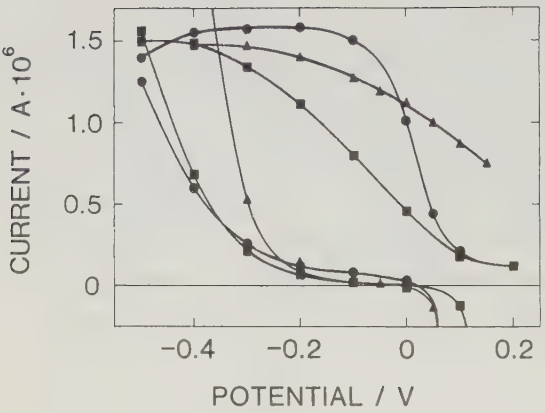

Fig. 4. Current-potential relations in f.i.a. for: (●) oxidized 4-methylcatechol on a graphite electrode; (▲) hexacyanoferrate(III) on a graphite electrode; (■) hexacyanoferrate(III) on a carbon film electrode. Lower curves; background currents; upper curves; baseline corrected peak currents for 80 µl injections of 100 µM hydrogen peroxide.

and the amperometric cell was used to study the hydrogen peroxide detection step. Hydrogen peroxide was injected and the current-potential relations were determined for two electrode materials and two mediators (Fig. 4).

The reduction of enzymatically oxidized 4-methylcatechol was kinetically well behaved at the graphite electrode as can be seen from the steep rise in current with decreasing potential. The background currents were rather high which was probably due to the presence of reducible impurities in the fresh 4-methylcatechol solution. This, together with the observation that the solution is unstable and degrades even if deaerated, renders this mediator less suitable.

It can be seen in Fig. 4 that the background currents with hexacyanoferrate(II) are very low in a potential range around -50 mV vs the reference electrode at both the graphite and carbon film electrodes. Deaerated solutions of hexacyanoferrate(II) were quite stable and the drift in the background current was negligible over a day. The reduction of hexacyanoferrate(III) was quite irreversible at both electrode materials and rather reductive potentials were needed to reach thelimiting current plateau. The response with the graphite electrode was very reproducible and this electrode material was used with hexacyanoferrate(II) as

mediator for most of the measurements reported below. The quality of the graphite used in this study was quite even and the pretreatment did not seem to be critical. The carbon film electrode, on the other hand, was quite sensitive to the pretreatment.

Some other mediators were also tested. Hydroquinone was found to behave similarly to 4-methylcatechol, whereas resorcinol showed much slower electrode kinetics. A gradual passivation of the electrode surface was also observed and resorcinol was therefore rejected. Iodide was excluded because of adsorption in the peroxidase reactor. A binding of iodine to peroxidase has been reported[19].

The efficiency of the peroxidase reactor was tested by comparing the responses from injections of hexacyanoferrate(III) and hydrogen peroxide. A precise stoichiometry of 1:2 was found which indicates that the conversion of hydrogen peroxide to hexacyanoferrate(III) in the reactor is quantitative. The peroxidase reactor is very stable and it can be used for at least several months without noticeable degradation.

The described flow injection system was operated with the hexacyanoferrate(II) solution and a graphite electrode polarized at -50 mV vs the reference. The response was linear in the range 10^{-7} - 10^{-3} M hydrogen peroxide with a detection limit of 30-50 nM. The upper limit was set by the limit above which the peroxide was no longer quantitatively reacted with the mediator in the peroxidase reactor.

The Immobilized Galactose Oxidase Reactor

The oxidation of substrates by galactose oxidase can be described by Michaelis-Menten kinetics[4], which can be simplified to a pseudo first order expression for substrate concentrations well below K_M

$$- \frac{dC}{dt} = K \cdot C \qquad (2)$$

The integral expression for a plug-flow immobilized-enzyme reactor at a steady state feed of substrate is

$$\frac{C}{C_o} = \exp\ (-K \cdot \tau) \qquad (3)$$

where C_o and C are the substrate concentrations at the inlet and the outlet of the reactor respectively, τ is the mean residence time, and K is the apparent pseudo first order rate coefficient of the reactor. The conditional coefficient K, depends on e.g. the enzyme concentration and the effects of immobilization.

The production of hydrogen peroxide by eqn.(1) in the reactor can be expressed by

$$\frac{H_2O_2}{C_o} = 1 - \exp(-K \cdot \tau) \qquad (4)$$

where $[H_2O_2]$ is the concentration of hydrogen peroxide at the outlet of the reactor. Catalase impurities will decompose some of the hydrogen peroxide and reduce the net yield of hydrogen peroxide. The rate of decomposition is directly proportional to the peroxide concentration, and eqn.(3) should be followed for a steady-state feed of hydrogen peroxide to the galactose oxidase reactor. When the hydrogen peroxide is produced in situ it can be treated as a metastable intermediate of two consecutive first order reactions, namely the production of peroxide by the oxidase reaction and the destruction of peroxide by the catalase reaction. The solution[20], adapted to a plug flow reactor, is

$$\frac{[H_2O_2]}{C_o} = \frac{K_{GalOD}}{K_{catalase}-K_{GalOD}} \left\{ \exp(-K_{GalOD} \cdot \tau) - \exp(-K_{catalase} \cdot \tau) \right\} \qquad (5)$$

where K_{GalOD} and $K_{catalase}$ are the apparent pseudo first order rate coefficients of the oxidase and catalase reactions respectively.

Inspection of eqn.(5) shows that good yields of hydrogen peroxide can be obtained only if $K_{catalase}$ is significantly lower than K_{GalOD} and then only if the residence times are not excessively long.

In a previous study[6], the catalase activity was reduced from an initially high value by periodical treatments with 3-amino-1,2,4-triazole. Some of the galactose oxidase was also deactivated so that the value of K_{GalOD} decreased somewhat after each treatment. Normal inhibitors for catalase, like cyanide and azide, also deactivate galactose oxidase[2,3,21]. The strategy used in this paper was to increase the purity of the galactose oxidase preparation by a more efficient chromato-

graphic procedure before the immobilization. The catalase content of the reactor was thereby reduced to a very low level.

The two rate coefficients in eqn.(5) can be evaluated from measurements of $[H_2O_2]/C_o$ at different residence times. A simplified flow system without dialyzer was used for the measurements and large injection volumes were used so that a steady-state response was reached. The flow rate was changed by varying the speed of the pump motor so that the relative flow rates of the channels remained the same. The cell was calibrated with hexacyanoferrate(III) at each flow rate to compensate for the flow dependence of the amperometric detectors. It can be seen in

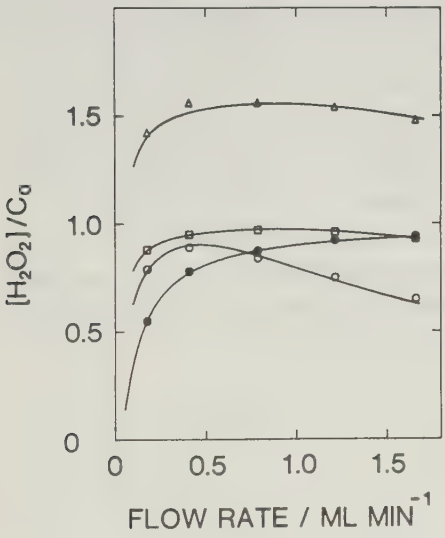

FIG. 5. Yield ($[H_2O_2]/C_o$) of hydrogen peroxide from the galactose oxidase reactor at various flow rates (flow rate through the galactose oxidase reactor) for: (●) hydrogen peroxide; (○) galactose; (□) raffinose; (△) dihydroxyacetone. Solid lines are drawn from: (●) eq(3) with K = 0.013 s^{-1}; (○) eq(5) with K_{GalOD} = 0.20 s^{-1} and $K_{catalase}$ = 0.006 s^{-1}; (□) eq(5) with K_{GalOD} = 0.50 and $K_{catalase}$ = 0.003 s^{-1}
The initial concentration of substrates was 100 μM.

Fig. 5 that the ratio between detected and injected hydrogen peroxide decreases with decreasing flow rate as the residence time and thus the time for decomposition increases. The recovery of hydrogen peroxide follows eqn.(3) very precisely and the solid line represents this first order equation with a fitted value of $K_{catalase}$ = 0.013 s^{-1}. For galactose and raffinose the yield of hydrogen peroxide increases with decreasing flow rate since the longer residence times allow a larger fraction of the sugars to be oxidized. The yield passes a maximum and then starts to decrease as the decomposition of the formed hydrogen peroxide grows in importance. The solid lines for raffinose and galactose in Fig. 5 are drawn from eqn.(5) with the fitted values of $K_{catalase}$ and K_{GalOD} as given in the figure. The presence of substrate in the reactor apparently decreased the rate of hydrogen peroxide decomposition as indicated by the very low $K_{catalase}$ values obtained in these cases. The experiments were repeated with galactose and raffinose at ten times lower concentrations. The values of K_{GalOD} were unaffected which demonstrates the validity of the first order assumption. The values of $K_{catalase}$ were closer to the value obtained with hydrogen peroxide alone. The precise value of $K_{catalase}$ has no analytical consequence since only about 2% of the formed hydrogen peroxide will decompose during the passage through the reactor in the analytical system.

The behaviour of dihydroxyacetone differs from that expected from a simple kinetic and stoichiometric scheme. It is immediately apparent from Fig. 5 that more than one mole of hydrogen peroxide is produced from one mole of dihydroxyacetone. The high yield of hydrogen peroxide is most likely due to a successive oxidation of the two hydroxy groups of hydroxyacetone. The yield (H_2O_2/C_o) of 1.5 at the highest flow rate should in the simiplest case lead to a yield of almost 2 at the lower flow rates. The weak dependence on the flow rate, however, suggest that at most 1.6 mole of hydrogen peroxide can be formed per mole of dihydroxyacetone under the present conditions. The non-stoichiometric behaviour of dihydroxyacetone does not reduce the analytical usefulness of the method since the relative yield of hydrogen peroxide is independent of the initial substrate concentration.

The stability of the galactose oxidase reactor was very good. No noticeable decrease in activity was detected after storage in a refrigerator for one month. The response of the analytical system was quite stable but a small decrease in the response (0.3% per day) was calculated after the reactor had been con tinuously used

for one month. The stability of the immobilized enzyme was considerably better than the less purified preparation used earlier[6]. No loss of copper from the enzyme was observed and treatments with a copper(II) solution[5,6] had therefore no effect.

Selectivity of the Flow Injection System and the Effect of Dialysis

The concentration normalized peak heights, obtained without a dialyzer in the f.i.a. manifold, are given in Table 1 for some compounds. The sensitivity towards a given carbohydrate is affected by the degree of conversion of the compound in the galactose oxidase reactor which in turn is dependent on e.g. the activity of galactose oxidase towards the particular substrate, the activity state of the reactor and the residence time. The relative sensitivities of the various compounds are therefore a conditional measure of the analytical selectivity of the present system. With the dialyzer inserted into the flow system the response (Table 1) depends on the selectivity of the dialyzer as well as on the selectivity of the enzyme reactor. The last row in Table 1, which gives the ratio of the sensitivites obtained with and without the dialyzer, shows the lowering of the analytical response due to dialyzer A, which thus varies for the different compounds.

The peak heights depend on the dispersion caused by the flow components and on the diffusion coefficients of the injected species. Peak area measurements were therefore made with the computer simultaneously with the peak height measurements in order to obtain results which are independent of the peak profile. The net yield of

TABLE 1

Selectivity of the System with and without Dialyzer A in the Flow Manifold. Injection Volume 20 ul. Flow rates as in Fig. 3. The peak currents are normalized by division with the concentration of the injected substrate.

Compound	i /C (μA/mM)		
	without dialyzer	with dialyzer	ratio
hydrogen peroxide	2.65	0.250	0.094
galactose	2.33	0.075	0.032
lactose	0.22	0.0041	0.019
raffinose	2.78	0.034	0.012
dihydroxyacetone	4.60	0.278	0.060
glycerol	0.032	0.0018	0.056

hydrogen peroxide in the galactose oxidase reactor can thus be estimated from the area responses obtained without a dialyzer by correlation to the response obtained from injections of hexacyanoferrate(III), see Table 2. Very good agreements between the net yields found with the flow injection system and those found with the steady-state measurements (at the same flow rate) were noticed, compare Fig. 5. The number of coulombs per millimole of injected substrate obtained with dialyzer A in the flow system is also given in Table 2. The ratio between the quantitites of electricity obtained with and without the dialyzer which corresponds to the dialysis factor, is given in the last row. The high efficiency of the on-line dialyzer is demonstrated by the fact that 16% of the hydrogen peroxide and 6.1% of the galactose pass from the sample to the detector channel in a flow system able to process 45 samples per hour. The dialysis factors (as well as the ratio in the last row in Table 1) were independent of the concentration of analyte as shown by the linearity of the calibration curves obtained both with and without a dialyzer. The size of the dialysis factor decreases with increasing molecular size as expected from theory[22]. The type of compound is also important as shown by the observation that only a very small fraction of hexacyanoferrate(III) passes the membrane.

It was found that 11% of the galactose passes the membrane in dialyzer B at 0.6 ml min^{-1} in both channels. This indicates that the more efficient radial mixing caused by the beads in the flow path, apart from reducing the axial dispersion in the dialyzer, also enhances the dialysis factor. The membrane position in dialyzer B

TABLE 2

Net Yields of Hydrogen Peroxide and Dialysis Factors in Dialyzer A obtained with the Flow System. Injection Volume 20 ul. Flow Rates as in Fig. 3. The peak areas are normalized by division with the amount of injected substrate.

Compound	Peak area (As/mmole) without dialyzer	Net yield[a] of H_2O_2	Peak area (As/mmole) with dialyzer	Dialysis factor
hydrogen peroxide	1.62	0.87	0.255	0.157
D-galactose	1.56	0.80	0.096	0.061
lactose	0.15	0.078	0.0058	0.038
raffinose	1.90	0.98	0.048	0.025
dihydroxyacetone	3.05	1.57	0.315	0.103
glycerol	0.022	0.011	0.0021	0.096

a) calculated from the peak area obtained from hexacyanoferrate(II) injection

was stabilized by the filling and pressure differences between the channels of up to 0.5 bar did not affect the signal. In certain applications it is desirable to have a very low transfer of analyte through the dialysis membrane, e.g. when highly concentrated solutions are to be analyzed. An efficient method of reducing the dialysis factor is to shorten the residence time in the dialyzer and to decrease the membrane area exposed to the flow paths. With the very small dialyzer C only 0.4% of the dihydroxyacetone will pass the membrane at the flow rates stated in Fig. 3.

Determination of D-galactose in Urine

A flow injection manifold which also contained the copper(II) saturated Bond-Elut column and the catalase reactor was used for determinations of D-galacose in urine. With dialyzer B and 10 ul injections of galactose standards the response was linear from the detection limit of 2 uM up to 60 mM. This sample volume produces a response corresponding to 7% of the steady-state value obtained with very large injection volumes. The axial dispersion was fairly independent of the sample size up to about 150 ul. With injections of 160 ul the detection limit became 0.2 uM galactose. With samples of this size or smaller 45 samples could be analyzed per hour, with a carry-over of less than half a percent. The relative standard deviation for 80 μl injections of 100 μM galactose standards was 0.4% (n=25). The evaluation was made in the computer from baseline corrected peak heights.

TABLE 3

Determination of Galactose in Urine. For details see text.

Sample	matrix effect[a] (mM)	galactose response (mM)	recovery of added galactose (%)
1[b]	0.02	0.79	104[c]
2[b]	-	0.43	102[c]
3[b]	0.02	0.20	97[d]
4[b]	0.01	0.24	100[d]
ascorbic acid (10 mM)	0.00	0.00	100[d]
uric acid (2 mM)	0.00	0.00	100[d]

a) response of the sample with the galactose oxidase reactor removed from the flow manifold (galactose equivalents)
b) urine samples from non fasting individuals
c) 1 mM galactose
d) 0.2 mM galactose

Galactose is not present in the urine from fasting healthy individuals. Most of the galactose derived from food intake is converted in the liver but approximately 10% of the galactose is eliminated by renal excretion[23].

The galactose concentration of urine, collected from non fasting individuals, was determined by injection of undiluted samples. The recovery of standard additions of galactose to the samples was also determined (Table 3). The good recoveries indicate that the response factor remains the same in the urine matrix as in the aqueous standards. No interferences were produced by ascorbic acid at about the highest co ncentration reported for urine, or by uric acid, at a level set by the solubility.

The electrochemical response from unknown sample constituents was measured with the galactose oxidase reactor removed from the flow manifold so that no hydrogen peroxide could be formed from the galactose. A small response was obtained from the urine samples (Table 3). Temporary exclusion of the mediator from the reagent indicated that the effect was both due to direct reduction at the electrode and to chemical oxidation of the mediator.

Determination of Lactose in Milk

The normal concentration of lactose in cow milk is approximately 140 mM and only small amounts of non-lactose carbohydrates have been found [24]. Galactose is not present, which makes it possible to use the present method for lactose determinations, although the response factor (including dialysis) was 16 times lower for lactose than for galactose (see Table 1). The determinations were made with dialyzer A in the flow system shown in Fig. 3. Milk containing 0.5% and 3.0% fat were analyzed by injecting the undiluted samples. The lactose contents as determined from a calibration graph were found to be 136 and 137 mM respectively. The recovery of lactose added to the milk samples was 98-102% for both types of milk. There was no interference from the matrix and the result was the same for determinations of the lactose concentration in undiluted milk and in milk diluted ten times with water. The linear range of the method with 20 µl injections was 0.05-300 mM.

Determination of Dihydroxyacetone in the Presence of Glycerol

Dihydroxyacetone is produced enzymatically from glycerol in a biotechnological process with free[24] or immobilized[25] microorganisms. The initial concentration of glycerol is typically 0.5 M and it decreases as the product dihydroxyacetone accumulates. The yield is good and approximately one mole of dihydroxyacetone is obtained from each mole of glycerol.

The flow manifold (Fig. 3) was used with dialyzer C and the small volume injection valve. A single bead string reactor was inserted after the injector to ensure thorough mixing before the sample entered the dialyzer. The resulting dilution of the sample with the carrier is necessary to avoid changes in the dialysis factor due to high but variable viscosity of the samples. The small injection volume, 1.5 µl, in combination with the dialysis of the sample gave a total dilution of 17 000 times.

The response to dihydroxyacetone alone (Fig. 6) was strictly linear in the

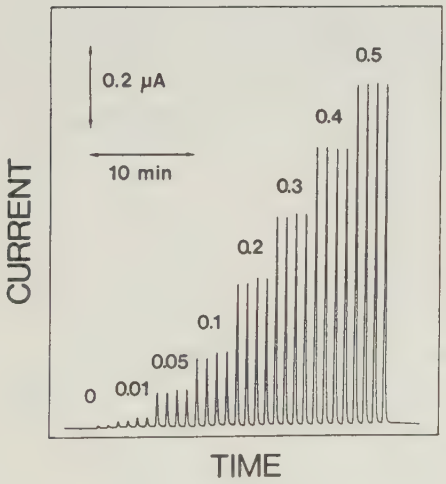

FIG. 6. Flow injection analysis of dihydroxyacetone in the absence and presence of glycerol. The number above the peaks indicates the concentration (M) of dihydroxyacetone. For each concentration a duplicate of dihydroxyacetone alone was injected, followed by a duplicate of dihydroxyacetone with glycerol added to a total carbohydrate concentration of 0.5 M.

range 0-0.5 M with a slope of 1.62 μA/M. A series of solutions with dihydroxyacetone concentrations from 0 to 0.5 M and with glycerol concentrations from 0.5 to 0 M was prepared so that the total carbohydrate concentration was 0.5 M in each solution. The other constituents of a process reaction medium[27], 50 mM succinate buffer, pH 5.0, and 10 mM $CaCl_2$ were also present in the solutions. The same linear range was obtained (Fig. 6) and the slope became 1.61 μA/M dihydroxyacetone. The slightly different slope is due to a slow oxidation of glycerol in the galactose oxidase reactor. The response to a solution of 0.5 M glycerol alone corresponds to 4.5 mM dihydroxyacetone and the selectivity of the method against glycerol is thus better than 100:1, compare Table 1. Calibration with standards containing both glycerol and dihydroxyacetone should give a correct calibration curve for dihydroxyacetone in the reaction medium since the concentration profiles cross in a well defined manner during the course of the biotechnical process. About seventy samples per hour could be processed with negligible carry-over and with a relative standard deviation of less than 0.5%.

ACKNOWLEDGEMENTS

The authors thank Professor Gillis Johansson for valuable help with the manuscript.

REFERENCES

1. G. Avigad, D. Amaral, C. Asensio, and B.L. Horecker, J. Biol. Chem. 237(1962)2736.
2. R.A. Schlegel, C.M. Gerbeck, and R. Montgomery, Carbohyd. Res. 7(1968)193.
3. G.T. Zancan and D. Amaral, Biochim. Biophys. Acta 198(1970)146.
4. G.A. Hamilton, J. DeJersey, and P.K. Adolf in T.E. King, H.S. Mason, and M. Morrison (Eds.), Oxidases and Related Redox Systems, (Proc. 2nd Int. Symp.), University Park Press, Baltimore, Md., 1973, p. 103.
5. S.K. Dahodwala, M.K. Weibel, and A.E. Humphrey, Biotech. Bioeng. 18(1976)1679.
6. B. Olsson, H. Lundbäck, and G. Johansson, Anal. Chim. Acta, in press.
7. G.G. Guilbault and G.J. Lubrano, Anal. Chim. Acta 64(1973)439.
8. M. Watson, D.N. Stiefel, and F.E. Semersky, Anal. Chim. Acta 106(1979)233.
9. H. Lundbäck, Anal. Chim. Acta, 145(1983)189.
10. H.L. Pardue and C.S. Frings, J. Electroanal. Chem. 7(1964)398.

11. W.J. Blaedel and C.L. Olson, Anal. Chem. 34(1964)445.
12. C. Toshio, Y. Shigeru, and H. Shingo, Bunseki Kagaku 32(1983)6.
13. C. Walsh, Enzymatic Reaction Mechanisms, W.H. Freeman and Co., San Francisco, 1979, p. 488.
14. L. Gorton and L. Ögren, Anal. Chim. Acta 130(1981)45.
15. T. Yao, Anal. Chim. Acta 153(1983)175.
16. K. Lundstroem, Anal. Chim. Acta 146(1983)97.
17. B. Olsson and L. Ögren, Anal. Chim. Acta 145(1983)87.
18. J.M. Reijn, W.E. van der Linden, and H. Poppe, Anal. Chim. Acta 126(1981)1.
19. J. Pommier, L. Sokoloff, and J. Nunez, Env. J. Biochem. 38(1973)497.
20. M.F. Dunn and S.A. Bernhard in E.S. Lewis (ed.), Investigation of rates and mechanisms of reactions, (Techniques of chemistry, vol. 6) part 1, 3rd Ed., John Wiley & Sons, New York, 1973, p. 660.
21. J.A.D. Cooper, W. Smith, M. Bacila, and H. Meding, J. Biol. Chem. 234(1959)445.
22. P.C. Farrell and A.L. Babb, J. Biomed. Mater. Res. 7(1973)275.
23. C.B. Laurell, B. Lundh, and B. Nosslin, Angewandte klinische Chemie, Bratt-Institut für neues Lernen, Goch, 1980, p. 436.
24. D.A.T. Southgate, Determination of food carbohydrates, Applied Science Publisher Ltd., Essex, 1976, p. 86.
25. S.R. Green in H.J. Peppler (ed.), Microbiol. Technol., Reinhold Publishing Corp., New York, 1967, p. 360.
26. O. Holst, S.O. Enfors, and B. Mattiasson, Eur. J. Appl. Microbiol. Biotechnol. 14(1982)64.
26. O. Holst, H. Lundbäck, and B. Mattiasson, to be published.

VIII

DETERMINATION OF SUCROSE IN THE PRESENCE OF GLUCOSE IN A FLOW INJECTION SYSTEM WITH IMMOBILIZED MULTIENZYME REACTORS

Bo Olsson, Berit Stålbom, and Gillis Johansson
Department of Analytical Chemistry, University of Lund,
P.O.Box 124, S-221 00 Lund, Sweden

SUMMARY

Sucrose was determined by its reactions in a packed-bed enzyme reactor containing coimmobilized invertase, mutarotase, and glucose oxidase. The produced hydrogen peroxide was measured spectrophotometrically after a chromogenic reaction. Glucose in the samples was decomposed in a pre-reactor containing coimmobilized mutarotase, glucose oxidase, and catalase. The response was linear over more than three decades. The detection limit was 0.1 μM sucrose for injection volumes of 80 μl. The sample frequency was 80 h^{-1} with and RSD of 0.3%. The response for glucose was 0.7% of that for sucrose.

Sucrose can be determined by a number of different methods, e.g. by polarimetry, density or refractive index measurements, chromatography, or by chemical reactions [1]. The physical methods are very fast and precise but may be less correct due to the presence of other compounds. Most samples contain e.g. optically active interferants but it is often tacitly assumed that plus and minus errors will balance. Corrections can be made by measuring the difference in polarization before and after inversion of the sucrose. Determination by gas chromatography relies on an inprecise derivatization and determination by liquid chromatography would benefit from further development of columns and detection methods.

The chemical methods for sucrose can be made very selective by using enzymatic reagents, but they are at present less reproducible than the physical ones and most of them give at least the same response for glucose as for sucrose. A separate glucose determination is therefore often made so that a correction can be applied. A direct determination with an enzyme electrode with an outer glucose eliminating layer has been described [2].

A flow injection method (f.i.a.) with immobilized enzymes should be able to provide both increased speed, precision and convenience compared with previous enzymatic procedures. Immobilized enzymes have been used in flow systems for sucrose determinations [3-6] and a recent report also uses the f.i.a. methodology [7].

EXPERIMENTAL

Chemicals

Invertase, EC.3.2.1.26, from Candida utilis (Sigma grade X, 500 IU mg^{-1}), mutarotase, EC.5.1.3.3, from porcine kidney (Sigma, 5700 IU mg^{-1}), glucose oxidase, EC.1.1.3.4, from Aspergillus niger (Serva, 300 IU mg^{-1}), catalase, EC.1.11.1.6, from bovine liver (Sigma 65000 U mg^{-1}), and peroxidase, EC.1.11.1.7, from horseradish (Sigma, type VI, 300 U mg^{-1}) were used as received. DCPS (2,4-dichlorophenol-6-sulphonate) was synthesized as described before [8]; it contains unreacted dichlorophenol which acts as mediator in the colour-forming peroxidase reaction. The reagent contained 20 mM DCPS, 1 mM 4-amino-antipyrine (BDH) and 1 mM EDTA in 0.1 M citrate buffer, pH 6.0. It can be used for up to a week if it is kept in a dark bottle. The buffer used in the flow system was 0.1 M citrate, pH 6.0. The azide buffer contained 60 mg sodium azide L^{-1}.

Preparation of the sucrose reactor

Controlled pore glass (Serva, CPG-10, pore diam; 66.8 nm, particle size 75-125 μm) was alkylamino derivatized and activated with glutaraldehyde as described before [9]. Invertase (8.6 mg), mutarotase (0.5 mg) and glucose oxidase (5.2 mg) was dissolved in 2.4 ml 0.1 M sodium

phosphate buffer, pH 7.0, and thoroughly dialyzed against the same buffer. The activated glass (0.20 g) was suspended in the chilled enzyme solution and the reaction was allowed to proceed over night at 8°C. The preparation was packed into a nylon tubing (i.d. 2.4 mm; length 80 mm) provided with retaining polypropylene nets and Altex screw fittings. A solution of 0.5 M NaCl was pumped through the reactor for 1 h and it was stored filled with phosphate buffer.

Preparation of the glucose-eliminating reactor

Mutarotase (0.5 mg), glucose oxidase (5.2 mg) and catalase (0.5 mg) were coimmobilized on controlled pore glass (0.20 g) with the same procedure as described above. The salt solution was pumped through the nylon tubing reactor (length 90 mm) for 12 h to desorb any loosely bound catalase.

Preparation of the peroxidase reactor

Peroxidase (5 mg) was diazocoupled to 0.10 g arylamino derivatized controlled pore glass CPG-glucophase-G (Pierce, pore diam. 46 nm, particle size 37-74 μm) as described before [10] and the preparation was packed into a nylon tubing reactor (length 40 mm).

The flow injection system

A four-channel peristaltic pump (Gilson Minipuls 2) was used to deliver the solutions to the manifold at the flow rates indicated (in ml min^{-1}) in Fig. 1. The sample, normally 80 μl, was introduced into the carrier stream by means of a pneumatically actuated loop injector (Cheminert SVA 8031). Each confluence point was followed by a short single bead string reactor (length 50 mm, i.d. 0.8 mm, bead diameter 0.5 mm) to improve the mixing. All connecting lines were of 0.5 mm i.d. teflon tubings and made as short as possible. The flow-through spectrophotometer (LKB, model 2051) was set at 514 nm.

RESULTS AND DISCUSSION

Sucrose reactor

Enzymatic determination of sucrose is commonly made by a sequnece of reactions:

$$\text{sucrose} + H_2O \xrightarrow{\text{invertase}} \alpha\text{-D-glucose} + \text{D-fructose} \qquad (1)$$

$$\alpha\text{-D-glucose} \xrightleftharpoons{\text{(mutarotase)}} \beta\text{-D-glucose} \qquad (2)$$

$$\beta\text{-D-glucose} + O_2 + H_2O \xrightarrow[\text{oxidase}]{\text{glucose}} \text{D-gluconic acid} + H_2O_2 \qquad (3)$$

Invertase acts selectively on terminal, unsubstituted β-D-fructofuranosides [11]. Glucose oxidase is very selective for β-D-glucose and the combination will therefore only act on glucose and sugars which leave a free glucose after one or more fructose units are splitted off. The hydrolysis produces α-D-glucose which will mutarotate slowly ($T_{1/2}$ = 4 min, 30°C, pH 6.5 [12]) to β-D-glucose until an equilibrium with 27% in the alpha and 63% in the beta form is reached. The enzyme mutarotase will speed up the reaction rate so that the equilibrium can be reached in a very short time.

The immobilization and particularly the coimmobilization of the three enzymes necessary for sucrose determination has been studied in detail previously [12]. It has also been shown that the apparent first order rate coefficients of the three enzymes in a reactor should be of about the same size for optimum performance [13]. Glutaraldehyde immobilization was selected for this work and it was found that dialysis of the enzyme solution before coupling was an essential step. Each enzyme was first immobilized separately and filled into a reactor so that the rate coefficient of the preparation could be evaluated. The data were used to estimate the proportion of the enzymes necessary for a coimmobilization on porous glass.

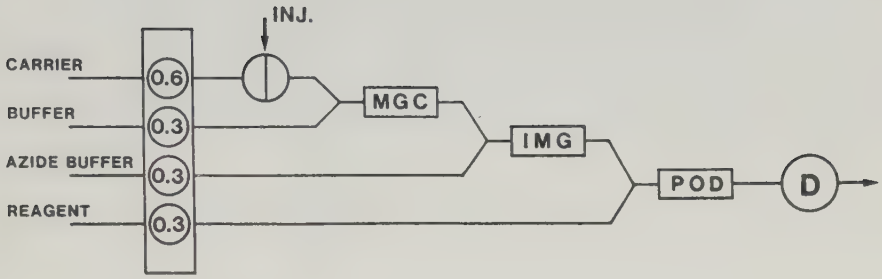

Fig. 1. Diagram of the flow injection system. MGC = glucose eliminating reactor; IMG = sucrose reactor, POD = peroxidase reactor. For details, see text.

TABLE 1

Conversion of sucrose to hydrogen peroxide in the sucrose reactor (360 µl) at various flowrates.

flowrate (ml min^{-1})	conversion (%)
0.2-1.0	100
1.2	100
1.4	96
1.6	93

The stoichiometry of the conversion of sucrose to hydrogen peroxide in the sucrose reactor was determined at different flow rates, see Table 1. The results show that a 360 µl reactor can produce hydrogen peroxide quantitatively at the flow rate used in the analytical system (1.2 ml min^{-1}). The conversion drops as the flow rate increases since the residence time in the reactor then becomes too short.

Experiments in which auxiliary reactors with a single enzyme also were inserted in the flow indicated that invertase and glucose oxidase were limiting the overall rate to about the same extent. There was an excess mutarotase activity in spite of the small amount taken in the coimmobilization.

Glucose eliminating reactor

Glucose is perhaps the most common sugar besides sucrose in food industry samples and it will also give hydrogen peroxide in stoichiometric amounts in the sucrose reactor, see eqns. (2)-(3). Two strategies are at hand for determination of sucrose in the presence of glucose, namely one in which the glucose is decomposed prior to the sucrose reactor and one using a simultaneous determination of glucose and glucose plus sucrose with a subsequent subtraction of glucose equivalents from the total [5,7]. Masoom and Townshend split the flow so that one half of the sample reached a glucose oxidase reactor directly and one half after passing an invertase/mutarotase reactor.

The approach used in this work was to decompose glucose in a reactor containing coimmobilized glucose oxidase, mutarotase and catalase, see eqns. (2)-(4).

$$H_2O_2 \xrightarrow{\text{catalase}} H_2O + 1/2\ O_2 \qquad (4)$$

A glucose eliminating reactor with a volume of 400 ul was inserted in the flow upstream from the sucrose reactor (Fig. 1). Glucose samples were injected and any α-D-glucose, β-D-glucose or hydrogen peroxide

TABLE 2

Error in the determination of 200 μM sucrose due to presence of glucose in the sample.

[glucose](μM)	peak absorbance (A^{514})	error (%)
0	0.480	-
100	0.480	0.0
300	0.488	1.7
500	0.493	2.7
700	0.496	3.3
900	0.498	3.8

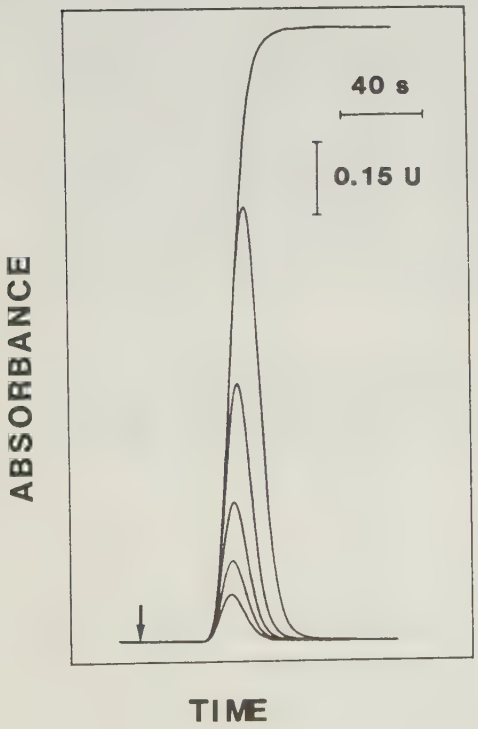

Fig. 2. Response for injections of 10, 20, 40, 80, 160 and 2000 μl.

which pass out from the first reactor will produce a detector response. It was found that 99.3% of the response to glucose was eliminated by the reactor at the flowrate of 0.9 ml min^{-1}.

Analytical results

The peak shape for injection of different volumes of a sucrose standard is shown in Fig. 2. The peak width at half maximum peak height remained almost constant, 15 s, up to a sample volume of 80 µl. The sample frequency at 1% carry-over was 80 samples h^{-1}.

Sucrose produced a linear calibration curve (Fig. 3) from the detection limit, 0.1 µM up to 500 µM, where the peak absorbance (1.5 A) became limiting. The sensitivity for glucose was 0.7% of that for sucrose up to at least 1 mM glucose (Fig. 3, lower curve).

Table 2, which reports on some sucrose determinations with samples also containing increasing amounts of glucose, verifies that the glucose elimination works equally well in the presence of sucrose. The compounded random and systematic errors in the sucrose determinations are given in the last column. The reproducibility was 0.3% RSD at a level of 200 µM sucrose (n=20). The mean systematic error due to glucose was less than 1% at equimolar concentrations of glucose and sucrose.

The enzyme reactors were stable during the course of this work and no measurable decrease in activity could be observed after 6 months in a refrigerator.

Properties of the method

Mutarotase should be present in a sucrose reactor intended for a fast analytical system because of the slowness of the spontaneous mutarotation; without mutarotase the signal became 5% of its previous value in the present system. The mutarotase will also make the response immune against factors (pH, temperature, etc.) which affect the rate of the spontaneous mutarotation. The robustness of the system is

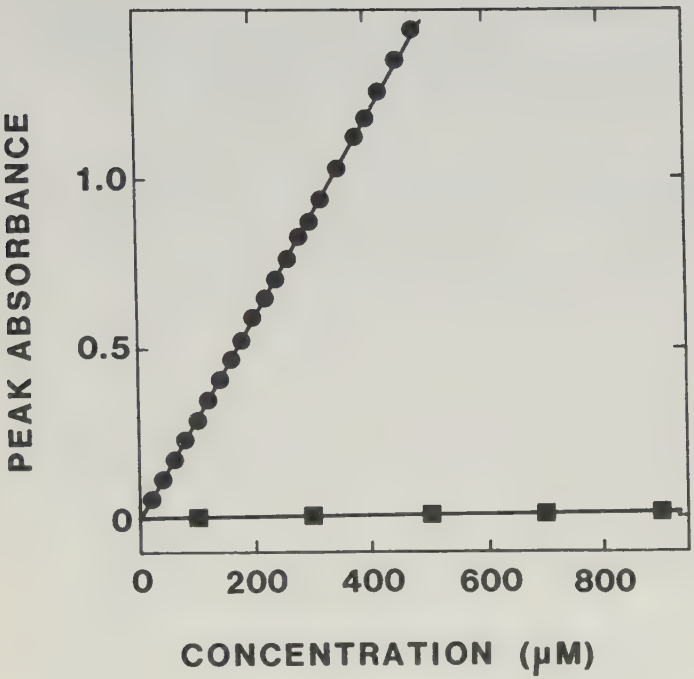

Fig. 3. Peak height as a function of sugar concentration.
(●) sucrose (■) glucose

greatly improved by the selection of reactors with essentially 100% conversion because it will make it more independent of such factors that affect the activity of the enzymes (pH, temperatures, ionic strength, inhibitors, and activators in the samples) [14].

Mutarotase in the sucrose reactor makes it necessary to include this enzyme also in the glucose eliminating reactor as α-D-glucose otherwise would pass and be converted to the beta form in the sucrose reactor. It is necessary to coimmobilize the mutarotase and the glucose oxidase so that the alpha form can be continuously transformed to the beta form as the latter is consumed.

Oxygen depletion through consumption in the enzymatic reactions will set an upper limit on both the glucose and sucrose contents of the samples. If the reaction rate or conversion decreases in the first reactor a break-through of glucose will occur which can give a large positive error. Lack of oxygen in the sucrose reactor may give negative errors. Table 2 shows that the present system has been designed so that no effects of oxygen depletion are noticeable within the specified range. The method has a large linear dynamic range and a decrease of the injection volume will make it possible to cover a higher range. The dilution in the f.i.a. system will automatically adjust the oxygen requirements in the reactors.

Many of the enzymatic methods for sucrose determinations which have been described in the literature have produced curved calibration graphs. The linearity of the present method arises both because the conversion is high and because the substrate concentrations in the enzyme reactors are well below the corresponding Michaelis constants [13] so that the reactions are of the first order [14]. The selectivity for sucrose over glucose can easily be improved by increasing the size of the glucose eliminating reactor. A doubling should theoretically reduce the interference level to the square of the present value, i.e. to $5 \cdot 10^{-3}$%. The increased reactor volume would cause additional peak broadening, and thus a reduced sample throughput, but would not impair the precision.

REFERENCES

1. Kirk-Othmer Encylcopedia of Chemical Technology, Vol. 21, 3rd ed., John Wiley & Sons, New York, 1983, p. 871.
2. F. Scheller and R. Renneberg, Anal. Chim. Acta, 152(1983)265.
3. J.W. Finley and A.C. Olson, Cereal Chem., 52(1974)500.
4. D.J. Inman and W.E. Hornby, Biochem. J., 137(1974)25.
5. J.A. Burns, Cereal Food World, 21(1976)594.
6. Y.Y. Kulis, E.V. Ralis, and R.S. Penkova, Appl. Biochem. Microbiol. , 15(1979)215.
7. M. Masoom and A. Townshend, Anal. Chim. Acta, 171(1985)185.
8. D. Barham and P. Trinder, Analyst (London), 97(1972)142.
9. G. Johansson and L. Ögren, Anal. Chim. Acta, 84(1976)23.
10. B. Olsson, H. Lundbäck, and G. Johansson, Anal. Chim. Acta, 167(1985)123.
11. S. Hestrin, D.S. Feingold, and M. Schramm in S.P. Colowick and N.O. Kaplan (Eds.), Vol. 1, Academic Press, New York, 1955, p. 251.
12. M.V. Morkyavichene, A.A. Dikchyuvene, A.B. Paulyukonis, and D.A. Kazlavskas, Appl. Biochem. Microbiol., 18(1982)557.
13. M.V. Morkyavichene, A.A. Dikchyuvene, A.B. Paulyukonis, and D.A. Kazlavskas, Appl. Biochem. Microbiol., 20(1984)60.
14. G. Johansson, L. Ögren, and B. Olsson, Anal. Chim. Acta, 145(1983)71.
15. H. Ooshima, M. Sakimoto, and Y. Harano, Biotech. Bioeng., 22(1980)2155.

IX

Theory and Application of Diffusion-Limited Amperometric Enzyme Electrode Detection in Flow Injection Analysis of Glucose

Bo Olsson, Hans Lundbäck and Gillis Johansson,
Analytical Chemistry, University of Lund, P.O. Box 124,
221 00 Lund, Sweden

Frieder Scheller and Jürgen Nentwig,
Akademie der Wissenschaften der DDR, Zentralinstitut fur Molekularbiologie, Bereich Angewandte Enzymologie, DDR-1115 Berlin-Buch, GDR

SUMMARY

A mathematical expression describing the transient response of a diffusion-limited amperometric enzyme membrane electrode in flow injection analysis is derived. The formula accounts for the injection volume, the dispersion in the flow manifold and for the diffusional characteristics of the enzyme membrane electrode. The maximum rate of sample throughput and the peak height sensitivity were calculated for a broad range of operating conditions and the design of an optimal system is discussed. The experimental characteristics of a glucose oxidase membrane electrode in a flow injection system were investigated and the behaviour of the system compared well with theory. A system optimized for high sample throughput was operated at 300 samples per hour with a relative standard deviation of 0.5 % and with a carry-over of 1 %. The linear range of detection was 0.01-100 mM glucose with 1.5 µl sample volume.

INTRODUCTION

Enzyme membrane electrodes have been used for the analysis of a large number of substances (1,2). Theoretical work has been aimed at an understanding of the sensor per se. and several mathematical models have been presented with closed-form solutions for the steady-state

response (3-8). The dynamic response has been investigated mainly with numerical simulation methods (9-13) but explicite solutions have been derived for potentiometric sensors (14-15). Equations for membrane diffusion transients have been given for time lag experiments (10) and for potential step amperometry (17). A formula was recently derived for the transient behaviour of the concentration profiles in amperometric enzyme membrane electrodes using a reaction-diffusion model (18).

Flow injection analysis (FIA) is an easily automated technique which is capable of a high sample throughput in wet chemical processing. It is a dynamic process which produces a well defined and highly reproducible concentration transient at the detector site. Theoretical descriptions of FIA-peaks are available (19-23), which give the relation between peak shape and system dimensions. The models are made with the assumption that the detector response is instantaneous and they are therefore not directly applicable when the response time is significant (24). There is thus a need for a model that describes the effects of the most important parameters on the over-all response of FIA systems containing enzyme membrane electrodes. A few experimental results with such systems have been reported (25,26).

EXPERIMENTAL

The amperometric cell. An amperometric detector for hydrogen peroxide was made from an oxygen electrode (VEB Metra Radebeul, Berlin, GDR) with a 0.5 mm platinum disk indicator electrode. The electrode was covered with a glucose oxidase membrane and a steel capillary inlet (length 80 mm; i.d. 0,5 mm) was directed towards the membrane in a confined wall-jet arrangement. The distance between the nozzle and the membrane was approximately 1 mm and the diameter of the exposed membrane surface was 1.4 mm. The outlet was placed concentrically with respect to the inlet nozzle. A potentiostat (PAR mod. 174) was used to polarize the indicator electrode at +600 mV vs the Ag/AgCl/0.1 M KCl reference electrode. The steel capillary inlet was connected to the ground wire of the potentiostat to reduce the flow dependent background noise.

The enzyme membrane. The glucose oxidase membrane consisted of two cellulose dialysis membranes (thickness 0.02 mm) sandwiched around a polyurethane layer (thickness 0.02 mm) containing the entrapped glucose oxidase (EC 1.1.3.4.; 50 I.U. cm^{-2}) (27). The rate of the enzymatic reaction is completely controlled by the rate of the diffusion of glucose in the membrane because of the high content of glucose oxidase (28).

The flow injection system. A diagram of the flow injection manifold is shown in Figure 1. The sample was introduced with a pneumatic injector (Cheminert SVA 8031) with a sample loop (10 - 320 µl) which was filled by a peristalic pump. The injector was connected to the steel capillary inlet of the electrode assembly with a Teflon tubing (length 120 mm; i.d. 0.5 mm). Another slide injector (Cheminert CSVA) with an injection volume of 1.5 µl was used alternatively. The outlet Teflon tubing (length 80 mm; i.d. 0.8 mm) of this injector was filled with solid glass beads (diam. 0.5 mm) and connected directly to the steel capillary. The carrier was a 0.1 M phosphate buffer, pH 7.0, containing 0.1 M potassium chloride and 1 mM sodium azide, and it was pumped by a Gilson Minipuls 2 peristaltic pump. The flow rate was 1.1 ml min^{-1} unless otherwise stated. The sampling and the injection were controlled by a personal computer which was also used for the peak evaluation.

THEORY

The response curve of a flow injection system with an amperometric enzyme membrane electrode detector can be treated as the result of a series of independent processes acting on the injected sample. In particular the response is influenced by the injection volume, the dispersion of the solute during transport from the injection site to the membrane surface, and by the diffusional transport of substrate and product in the membrane. The combined response will be derived assuming a rectangular injection, a Gaussian dispersion, and a diffusion-limited electrode response. In order to find expressions for the response of the membrane electrode to a dispersed sample zone

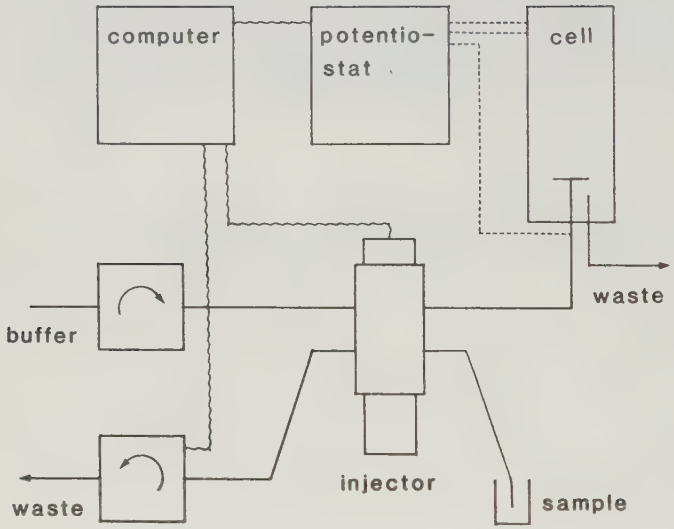

Figure 1 Schematic diagram of the FIA system. For details see text.

it is useful to first consider the response to an impulse of infinitely narrow width.

The membrane impulse response. The membrane electrode is assumed to consist of an infinite, plane sheet of membrane between the platium electrode surface and the external solution. The mass-transfer resistance is assumed to be negligible in the external solution so that the concentration at the membrane surface equals that in the bulk of the solution. Transport within the membrane occurs only through diffusion which is characterized by the effective diffusion coefficient in the porous structure, D_{eff}. It is assumed initially that no chemical reaction takes place in the membrane. The effect of an enzymatic reaction will be considered separately.

A general solution to the differential equation that describes the time dependent concentration profile in a plane membrane with constant concentrations at the interfaces and with an initially uniform concentration distribution is given by Crank (29). With the specific boundary conditions that the initial concentration is zero, that the solute is totally consumed at the electrode interface (x=0), and that the concentration in the external solution (x>l) is brought to C* in an instantaneous step at time t = 0, the solution simplifies to

$$\frac{C(x,t)}{C^*\epsilon} = \frac{x}{l} + \frac{2}{\pi} \sum_{n=1}^{\infty} \frac{(-1)^n}{n} \sin\left(\frac{n\pi x}{l}\right) \exp(-n^2\pi^2 t/\tau) \qquad (1)$$

where

$$\tau = \frac{l^2}{D_{eff}} \qquad (2)$$

τ is the characteristic diffusion time and ϵ is a factor which depends on the partition of solute between membrane and solution and which also takes the void fraction of the membrane into account. The other variables are defined in the List of Symbols.

The law of diffusion gives

$$J = - D_{eff}\left(\frac{\partial C}{\partial t}\right) \qquad (3)$$

The flux of solute per unit area at the electrode surface is obtained by inserting C(x,t) into eq 3 and evaluating the differential at x=0. The solution for a step input is

$$J^s(t) = J_{ss}[1+2 \sum_{n=1}^{\infty} (-1)^n \exp(-n^2\pi^2 t/\tau)] \quad (4)$$

where

$$J_{ss} = - \frac{C^* D_{eff} \epsilon}{l} \quad (5)$$

J_{ss} is the steady-state flux approached for large t. The sum converges rapidly for large t and for $t>0.15\ \tau$ only one term is needed for >99% accuracy.

The impulse response function can now be obtained by taking the time derivative of the step response function, eq. 4 (30). The solution is

$$\frac{\partial J^s(t)}{\partial t} = 2\ J_{ss} \sum_{n=1}^{\infty} (-1)^n \frac{n^2\pi^2}{\tau} \exp(-n^2\pi^2 t/\tau) \quad (6)$$

which describes a skewed peak with a maximum at $t = 0.092\ \tau$. The centralized second moment (the variance) was evaluated numerically to be $\tau^2/90$.

Effect of a chemical reaction in the membrane. An enzymatic reaction is now assumed to take place in the membrane and it is further assumed that the effective diffusivities of the substrate and the product are equal and that the product concentration is zero outside the membrane. The rate of reaction is taken to be proportional to the substrate concentration

$$- \frac{d[S]}{dt} = K[S] \quad (7)$$

where K is the pseudo-first order rate coefficient of the enzymatic reaction. K thus depends on the concentration and the rate parameters of the immobilized enzyme and possible cofactors.

The explicit finite difference method (31) was used to numerically simulate the time dependent flux of product formed in the membrane. The model membrane was divided into 20 equal segments and the diffusional transport was calculated for each solute by applying the proper difference equation for each segment in sequence. The chemical reaction condition was then applied within each segment and the sequence was repeated to describe the time dependence. The procedure follows essentially that of Mell and Maloy (9) and their paper may be consulted for details.

The dimensionless moduls K_τ , which is normally referred to as the enzyme loading factor, can be used as a measure of the degree of diffusional control. Simulations were first made with a very large enzyme loading factor so that the conversion of substrate to product went to completion within the model membrane. It was found that the simulated step response followed eq 4 exactly, i.e. the enzymatic conversion had no effect on the theoretical response curve. Similarly it was found that a pulse input generated a response according to eq 6. Simulations were next made with a number of enzyme loading factors. It can be seen (Figure 2) that the response is independent of the enzyme loading factor for $K_\tau > 30$, i.e. when the system is under complete diffusional control. Figure 3 shows the normalized time delay from the pulse imput to the response maximum for various enzyme loading factors. The normalized peak width is also given in the figure and it can be seen that the width increases substantially as the enzyme loading factor decreases. Simulations were also made with a model in which only the middle third of the membrane was chemically active to theoretically investigate the effect of confining the enzyme membrane between inactive dialysis membranes. Other models with inhomogeneous distribution of enzyme were also simulated. There was no effect on the size or the time dependence of the flux provided that the conversion of substrate to product was complete in the membrane and that the diffusivity of the solutes were equal throughout.

Equations 4 and 6 were derived under the assumption that the solute in the bulk was the electroactive species. The simulations have shown

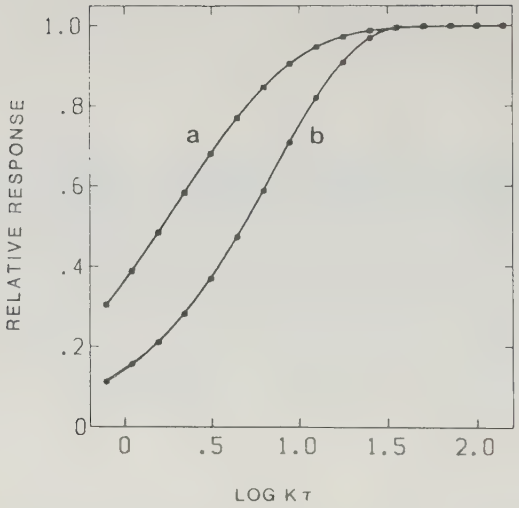

Figure 2 Simulated relative response as a function of the enzyme loading factor. (a) Steady-state flux after a step input; (b) peak height after a pulse input. The results are normalized by division with the values obtained at infinite enzyme loading factor.

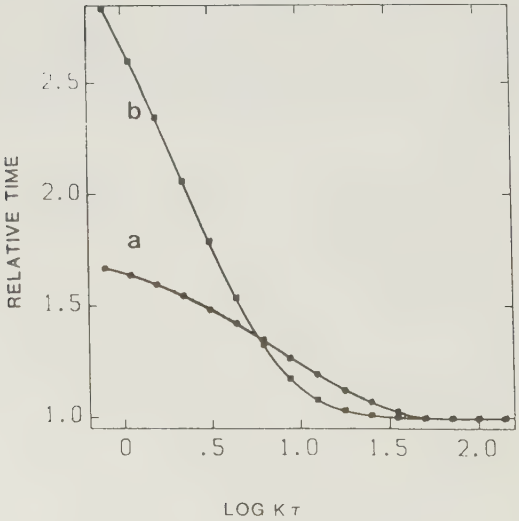

Figure 3 Simulated impulse response peak parameters as a function of the enzyme loading factor. (a) peak time; (b) peak width at 1% of maximum height. The results are normalized by division with the values obtained at infinite enzyme loading factor.

that the equations will describe also a case where the electroactive species is produced by an enzymatic reaction in the membrane. The equations are exactly valid only when the response is diffusion limited and when the diffusivity of the product equals that of the substrate.

Response to other input functions. The output response curve of the complete FIA system can be obtained by treating the concentration time profile to which the membrane is exposed as a sequence of infinitesimal impulses and adding up the membrane electrode response to each impulse. This approach is known as a convolution (32), and the convolution integral for an input function, f(t), combined with the membrane inpulse function eq 6, is,

$$J(t) = \int_0^t f(t_1) \frac{\partial J^S(t-t_1)}{\partial t} dt_1 \qquad (8)$$

where t_1 is a dummy variable.

The response to a nondispersed plug injection is obtained with a rectangular input function

$$f(t) = 1 \; ; \; t_r < t < t_r + \Theta$$
$$f(t) = 0 \; ; \; t < t_r, \; t > t_r + \Theta \qquad (9)$$

where Θ is the injection width in time units, and t_r is the mean residence time in the flow system. The step height is unity because the concentration term is included already in eq 6. The integral of eq 6 is of course eq 4, and the solution is

$$J^R(t) = J^S(t-t_r) - J^S(t-t_r-\Theta) \qquad (10)$$

For very small Θ, ($\Theta \ll \tau$), eq 10 reverts to the impulse response function, eq 6, multiplied with Θ. The superscripts R and S refers to the fluxes obtained with a rectangular and a step input respectively.

A more realistic model is obtained by including the effect of sample plug dispersion. Peak broadening caused by axial dispersion processes can, with some caution (23), be approximated by a Gaussian operator

$$\varphi(t_1) = \frac{1}{\sigma\sqrt{2\pi}} \exp(-\frac{t_1^2}{2\sigma^2}) \tag{11}$$

characterized by the standard deviation, σ, expressed in time units. The concentration profile at the site of detection is obtained by convoluting the Gaussian operator with the rectangular input function, eq 9. The solution is given by Sternberg (33) and in our notation it becomes

$$f(t) = \phi(\frac{t-t_r}{\sigma}) - \phi(\frac{t-t_r-\Theta}{\sigma}) \tag{12}$$

where $\phi(t_1)$ is the integrated normal distribution function which can be evaluated by an empirical expression (34). The membrane response to the dispersed plug input can in principle be obtained by convoluting this input function (eq 12) with the membrane impulse response function (eq 6). However, a more convenient procedure is to carry out the convolutions in a reverse order.

The membrane impulse response function is first convoluted with the Gaussian operator in a manner analogous to the convolution of a simple exponential with a Gaussian function, solved by Sternberg (33). The result is a new impulse response function which in turn is convoluted with the rectangular input function, eq 9, giving

$$J^{RG}(t) = J^{SG}(t-t_r) - J^{SG}(t-t_r-\Theta) \tag{13}$$

where

$$J^{SG}(t_1) = 2J_{ss} \sum_{n=1}^{\infty} \left\{(-1)^n \right.$$

$$\left. \phi(\frac{t_1}{\sigma}) - \exp[(\frac{n^2\pi^2\sigma}{\tau\sqrt{2}})^2 - \frac{t_1 n^2\pi^2}{\tau}] \; \phi(\frac{t_1}{\sigma} - \frac{n^2\pi^2\sigma}{\tau}) \right\} \tag{14}$$

The superscripts RG and SG indicates that the rectangular and step inputs are modified with a Gaussian operator.

Equation 13 describes the response of an enzyme electrode in a FIA system and it may thus be used to show some characteristics of a composite system.

A set of output response curves (Figure 4; thick lines) were generated from eq 13 for various injection volumes (expressed by the dimensionless quantity Θ/τ). The corresponding input concentration-time profiles, calculated from eq 12, are also shown (Figure 4; thin lines). The curves relate to a FIA system and an electrode, characterized by fixed values of the dispersion and the characteristic diffusion time. The peak height of the response increases with the injection volume for small Θ / τ, while the peak width is fairly constant. For large sample volumes the peak width increases with Θ / τ while the peak height approaches the steady-state value. Figure 4 also illustrates that larger injection volumes are required to obtain the steady-state membrane response than to obtain the steady-state concentration outside the membrane.

Design considerations. Equation 13 can be used to study the influence of the system parameters on the peak height and the sample through-put in order to find optimum working conditions.

The dimensionless curves in Figure 5 a show the peak height as a function of the injection volume for different ratios of Θ/τ. The variables are reduced with the characteristic diffusion time, and the set of curves thus illustrates the effect of varying the dispersion in the flow system for a constant, arbitrary value of τ . The figure shows that the response increases linearly with the injection volume until a response of about one third of the steady-state value is reached. It can further be seen that a high sensitivity can be obtained already with a small injection volume in a FIA system with a low dispersion. The effect of the dispersion is negligible when σ is small compared with the characteristic diffusion time (i.e. when $\sigma/\tau < 0.03$) and the response curve can then simply be described by eq 10. Obviously, there is nothing to be gained by reducing the

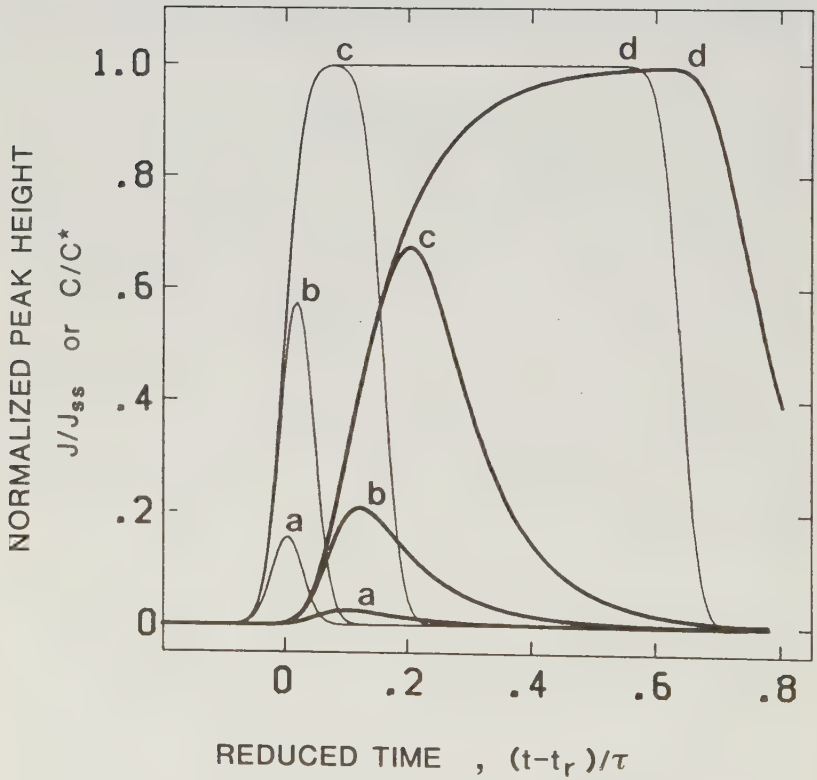

Figure 4 Calculated concentration time profiles (thin lines; eq 12) and the corresponding output response profiles (thick lines; eq 13) with σ / τ = 0.025 and with reduced injection times, Θ / τ of: (a) 0.01 ; (b) 0.04 ; (c) 0.16 ; (d) 0.64

dispersion below this limit.

The maximum sample frequency is limited by the width of the response peak, which depends on the same parameters as discussed above. The dimensionless curves in Figure 5 b shows the maximum sample frequencies which can be obtained with a carry-over of 1 %. Either of the parameters sample volume, dispersion or membrane characteristic diffusion time can be rate limiting in a real system and an increase of sample frequency can then be achieved only by making the appropriate changes which affect this parameter. Figure 5 b can be used to estimate the relative importance of such changes and the corresponding effect on sensitivity can then be evaluated from Figure 5 a.

Equation 13 can also be used to predict the effect of a changed membrane in a given FIA system. The performance, both in terms of sensitivity and sample throughput, improves with a decreasing characteristic diffusion time. The sample throughput will become independent of the membrane thickness when $\sigma / \tau > 1$, but the response peak height is erroneously predicted to increase indefinitely with decreasing characteristic diffusion time. The response will, of course, eventually be limited by the external mass-transfer or by other causes not included in the model.

It can be concluded that it should always be advantageous to use a membrane electrode with a small characteristic diffusion time provided that the enzyme activity is sufficiently high. The full exploitation of the merits of a thin membrane, however, demands a well designed FIA system. For a given membrane there is also a trade-off between the sensitivity and the sample throughput. A reasonable compromise seems to be obtained with a dispersion (σ) below 0.03 τ and with an injection time (Θ) of about 0.1 τ (compare Figure 5). The peak height will then be about half of the steady-state response and the through-put will be about 5000/ τ samples per hour, i.e. little has been traded off in speed compared to the maximum 6500/ τ.

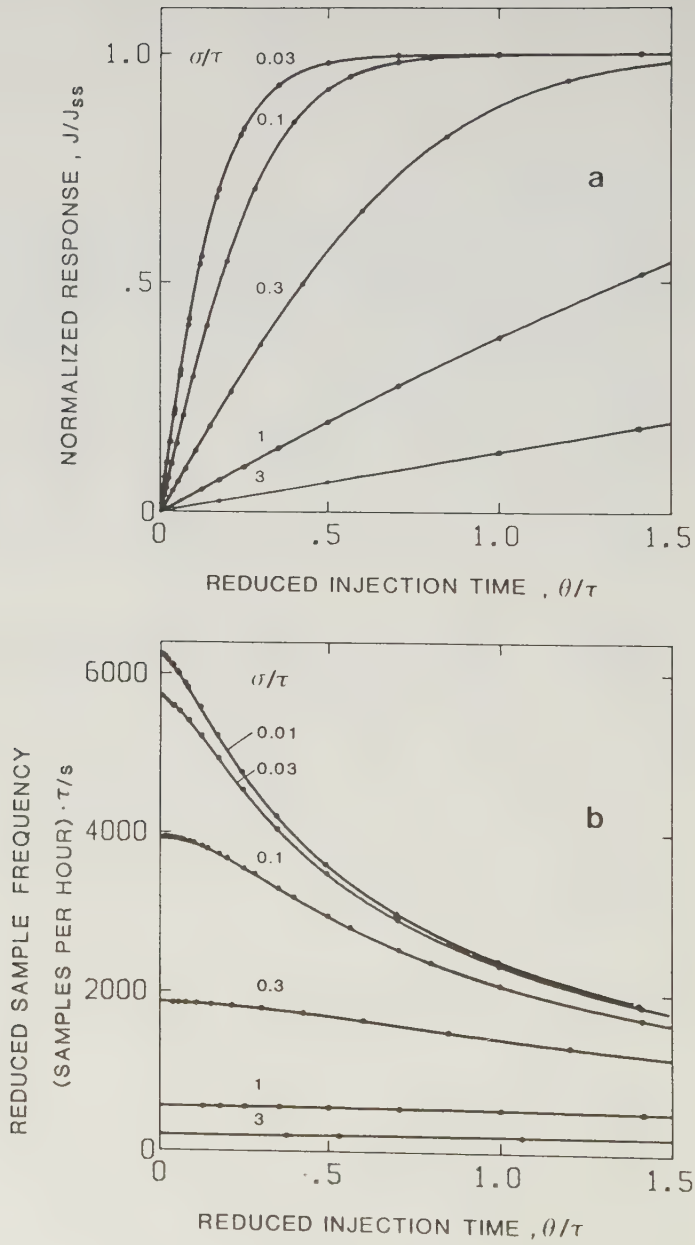

Figure 5

Theoretical peak parameters as a function of the reduced injection time, generated from peaks calculated from eq 13 for different ratios of σ / τ . Panel a shows the normalized peak height; b shows the reduced sample frequency, assuming a carry-over of 1%.

RESULTS AND DISCUSSION

Hydrogen peroxide was injected into the FIA system and the concentration peak profile in the electrode cell was determined by using an electrode without enzyme membrane. The responses for different injection volumes were normalized by division with the steady-state value and plotted in Figure 6 a, squares. The solid line fitted to the squares was obtained from peaks generated by eq 12 with a σ-value of 1.0 s and with Θ-values calculated from the injection volume and the flow rate.

The response of the membrane-covered electrode was next determined by injecting glucose samples. Figure 6 a, circles, shows the normalized peak heights obtained for different injection volumes. A characteristic diffusion time of $\tau = 24$ s resulted (through eq. 13) in the solid line fitted to the circles.

The results confirm that a membrane-covered electrode requires a larger injection volume than a naked electrode to reach a corresponding fraction of the steady state response. The response of the membrane electrode thus depends on both the concentration time profile in the cell compartment and on the characteristic diffusion time of the membrane.

The effect of the injection volume on the peak width at half maximum height ($w_{1/2}$) is shown in Figure 6 b. The peak width is almost linearly related to the sample volume at large injection volumes. For small sample volumes, the width of the concentration peak is determined by the dispersion alone. The response of the membrane electrode is in addition determined by the characteristic diffusion time of the membrane. The solid lines in Figure 6 b are derived from the same theoretical peak profiles as were used to construct the curves in Figure 6 a. The agreement between the theoretical curves and the experimental points is good, although the peaks obtained with the membrane electrode with large injection volumes are broader than predicted.

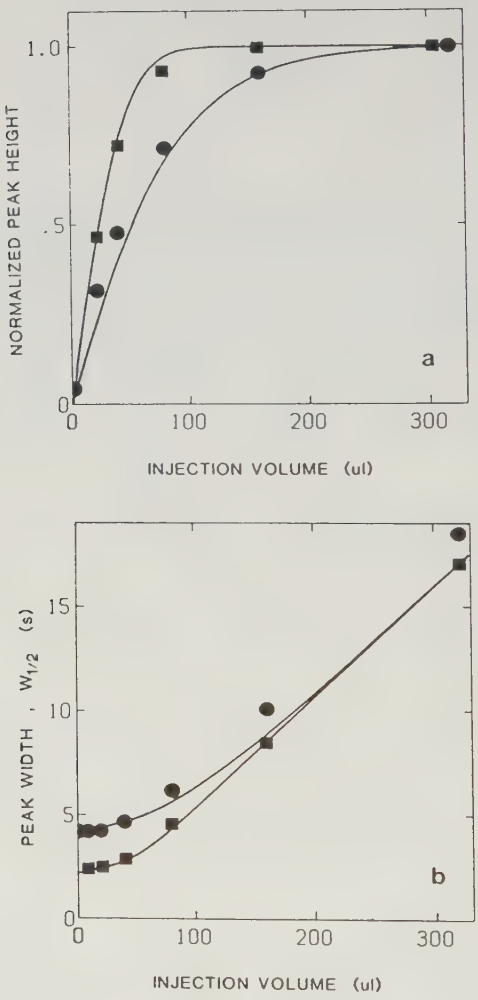

Figure 6

Effect of injection volume on FIA response peaks at a flow rate of 1.1 ml min^{-1}. Experimental results: (■) naked electrode; (●) membrane covered electrode. Solid lines are generated from theoretical peaks calculated from eq 12 (naked electrode) and eq 13 (membrane covered electrode) with τ = 24 s and σ = 1.0 s. Panel a shows the peak height normalized with respect to the steady-state response; b shows the peak width at half maximum height.

The steady-state current obtained with the enzyme membrane electrode was 40 μA M^{-1} β-D-glucose. The experimental current can be compared with the prediction of eq. 5 through the current-flux relation

$$i = nFAJ \qquad (15)$$

where the symbols have their usual significance. The apparent diffusivity of glucose and hydrogen peroxide in the membrane was estimated from eq 2 to $D_{eff} = 2 \times 10^{-6}$ $cm^2 s^{-1}$ by using a membrane thickness of 0.007 cm and the fitted value of the characteristic diffusion time, 24 s. A sensitivity of $130 \cdot \epsilon$ A M^{-1} is then predicted, which compares well with the experimental value for a partition and void factor, ϵ, of 0.3. The water content of a soaked enzyme membrane was determined to 46% by weight and an ϵ-value of this magnitude seems rational since glucose probably is transported only in the aqueous phase of the membrane (35). Strictly, eq 5 should not be used to predict the steady-state flux in the membrane since the diffusivity of hydrogen peroxide is 2.5 times that of glucose in hydrophilic membranes (18); the comparision made above is therefore rather crude. The enzyme loading factor of the enzyme-containing polyurethane layer of the membrane was estimated from D_{eff} and the enzyme content to be larger than 200, which validates the assumption of complete diffusional control.

The volumetric dispersion (σ_v) is quite independent of the flow rate in a single bead string reactor (22). The dispersion in time units (σ) with such a reactor will be related to the volumetric dispersion by

$$\sigma = \sigma_v / Q \qquad (16)$$

where Q is the volumetric flow rate. The device will thus produce a series of peaks with different σ-values if the flow rate is varied. Similarly the injection time (Θ) will increase in inverse proportion to the flow rate. The $w_{1/2}$ of hydrogen peroxide peaks detected with the naked electrode is given in Figure 7 b, squares. The experimental points conform to the inverse relation given by eq 16 for a fitted

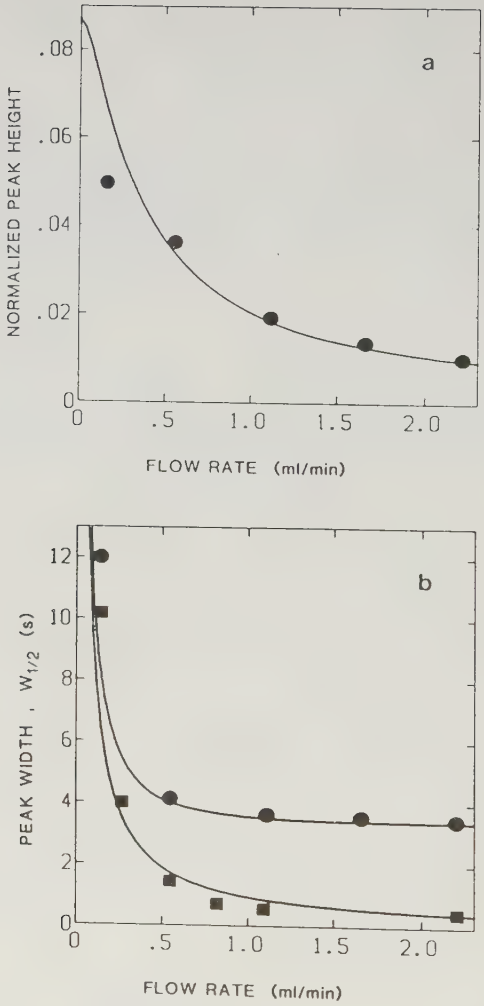

Figure 7

Effect of flow rate on FIA response peaks with 1.5 ul injection volume. Experimental results: (■) naked electrode; (●) membrane covered elecrode. Solid lines are generated from theoretical peaks calculated from eq 12 (naked electrode) and eq 13 (membrane covered electrode) with τ = 24 s and with σ computed from eq 16 with σ_v= 6.7 ul. Panel a shows the peak height normalized with respect to the steady-state response for a flow rate of 1.1 ml min^{-1}; b shows the peak width at half maximum height.

value of σ_v = 6.7 µl (lower solid line). The peak width measured with the membrane-covered electrode is also shown in the figure (circles) together with the theoretical curve, calculated with τ = 24 s and σ_v = 6.7 µl. It can be seen that the width of the response peak is almost independent of the flow rate when the width of the concentration-time profile is sufficiently small. This half width is determined by the characteristic diffusion time of the membrane.

The peak heights obtained with the membrane electrode were normalized with the previously obtained steady-state current and plotted versus the flow rate (Figure 7 a). The response increases with decreasing flow rate in accordance with the theoretical prediction of eq 13 (solid line). The good fit indicates that the assumtion of negligible mass transfer resistance in the external solution is valid except at the lowest flow rate where the peak height is lower than predicted.

The flow injection system with 1.5 µl injection volume was used at a flow rate of 1.1 ml min^{-1}. The system thus operated in the dispersion-independent region (see Figure 7 b) where the response curve is solely determined by the characteristic diffusion time of the membrane. The response curve should therefore be adequately described by the impulse response function, eq 6. Figure 8 a shows the experimental response curve (thick line) together with the theoretical impulse function (thin line) generated for τ =24 s. The low values of the reduced dispersion (σ/τ =0.015) and the reduced injection time (Θ/τ =0.003) validates the use of the pure impulse response function above (see Figure 5). The width of the experimental response peak at 1% of the maximum peak height was 12 s (Figure 8 a) and a throughput of 300 samples per hour was thus possible with a carry-over of 1% (Figure 8 b). This sample frequency is in close agreement with that predicted by the theory (Figure 5 b) and represents an ultimate limit for all systems containing this membrane.

The f.i.a. system was used to determine glucose at a sample throughput of 300 per hour. The response was linear from the detection limit of 10 µM up to 100 mM glucose with a sensitivity of 0.5 µA M^{-1}. The relative standard deviation for 25 successive injections of 1 mM glucose was 0.5 %.

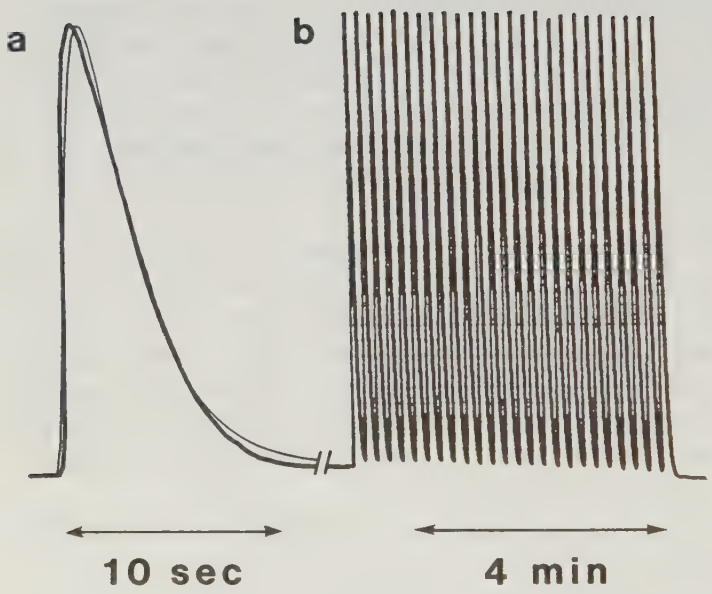

Figure 8 FIA response peaks obtained with an injection volume of 1.5 ul and a flow rate of 1.1 ml min^{-1}:
(a) Expanded view of an experimental response curve (thick line) and the theoretical membrane impulse response (thin line) calculated from eq 13 with a fitted value of τ = 24 s. The curves are normalized to equal height. (b) record of 25 injections of 1 mM glucose at a frequency of 300 samples h^{-1}.

The glucose determinations were made with a system optimized with respect to the sample frequency alone. It can be seen from Figures 5 and 6 that the sensitivity could have been increased substantially with only a minor reduction in sample frequency by increasing the injection volume.

The theory presented successfully predicts the transient behaviour and the operational characteristics of flow injection analysis with amperometric enzyme membrane electrode detection. Deviations from the predicted widths were, however, found for very large injection volumes. This is probably due to the simple single-parameter models for injection, dispersion and membrane diffusion used in the theory. More elaborated multi-parameter models for slug injection (20), non-Gaussian dispersion (22), and reaction-diffusion limited enzyme membranes (18) are available but each refinement will result in increasingly more complex expressions.

ACKNOWLEDGEMENTS

This work was made as a part of a cooperation supported by the Academy of Sciences of GDR and the Royal Swedish Academy of Sciences.

List of symbols

A	electrode area (cm^2)
C	instantaneous concentration (mol cm^{-3})
C^*	applied concentration (mol cm^{-3})
D_{eff}	effective diffusion coefficient ($cm^2 s^{-1}$)
F	Faradays constant (As mol^{-1})
J	flux at electrode surface (mol s^{-1} cm^{-2})
J_{ss}	steady-state flux at electrode surface for $t = \infty$, $C = C^*$ (mol s^{-1} cm^{-2})
K	pseudo-first order rate coefficient (s^{-1})
P	product
Q	volumetric flow rate ($\mu l\ s^{-1}$)
S	substrate
i	current (A)
l	membrane thickness (cm)
n	counter in summations, number of electrons in electrode reaction
t	time (s)
t_r	residence time (s)
t_1	dummy variable
x	distance (cm)
$w_{1/2}$	width of peak at half maximum height (s)
σ	standard deviation of axial dispersion (s)
σ_v	standard deviation of axial dispersion (μl)
τ	characteristic diffusion time, defined by eq 2 (s)
Θ	injection time (s)
ϵ	partition and void factor, dimensionless

REFERENCES

1. P.W. Carr and L.D. Bowers, 'Immobilized Enzymes in Analytical and Clinical Chemistry', John Whiley & Sons, New York, 1980
2. G.G. Guibault, 'Analytical Uses of Immobilized Enzymes', Marcel Dekker, New York, 1984
3. W.J. Blaedel, T.R. Kissel and R.C. Boguslaski, Anal. Chem., 44, 2030 (1972)
4. P. Racine and W. Mindt, Experentia Suppl., 18, 525 (1971)
5. D.A. Gough and J.K. Leypold, Appl. Biochem. Bioeng., 3, 175 (1981)
6. H.F. Hameka and G.A. Rechnitz, Anal. Chem., 53, 1586 (1981)
7. J.J. Kulys, Enzyme Microb. Technol., 3, 344 (1981)
8. J.K. Leypold and D.A. Gough, Anal. Chem., 56, 2896 (1984)
9. L.D. Mell and J.T. Maloy, Anal. Chem. 47, 299 (1975)
10. F.R. Shu and G.S. Wilson, Anal. Chem., 48, 1679 (1976)
11. P. Jochum and B.R. Kowalski, Anal. Chim. Acta, 144, 25 (1982)
12. C. Tran-Minh and G. Broun, Anal. Chem., 47, 1359 (1975)
13. A. Bergel and M. Comtat, Anal. Chem., 56, 2904 (1984)
14. P.W. Carr, Anal. Chem., 49, 799 (1977)
15. H.F. Hameka and G.A. Rechnitz, J. Phys. Chem., 87, 1235 (1983)
16. D.A. Gough and J.K. Leypold, J. Electrochem. Soc., 127, 1278 (1980)
17. K.H. Mancy, D.A. Okun and C.N. Reilly, J. Electroanal. Chem., 4, 65 (1962)
18. T. Schulmeister and F. Scheller, Anal. Chim. Acta, in press
19. J. Rucicka and E. Hansen, Anal. Chim. Acta, 99, 37 (1978)
20. J.M. Reijn, W.E. van der Linden and H. Poppe, Anal. Chim. Acta, 114, 105 (1980)
21. T.J. Vanderslice, K.K. Stewart, A.G. Rosenfeld and D.J. Higgs, Talanta, 28, 11 (1981)
22. J.M. Reijn, W.E. van der Linden and H. Poppe, Anal. Chim. Acta, 126, 1 (1981)
23. J. Rucicka and E. Hansen, 'Flow Injection Analysis', John Wiley & Sons, New York, 1981, Chapter 3
24. H. Poppe, Anal. Chim. Acta, 114, 59 (1980)

25. L. Macholan, P. Londyn and J. Fischer, Coll. Czech. Chem. Commun., 46, 2871 (1981)
26. V. Pacakova, K. Stulik, D. Brabcova and J. Barthova, Anal. Chim. Acta, 159, 71 (1984)
27. F. Scheller et. al in 'Methods in Enzymol.' 1985, in press.
28. F. Scheller, D. Pfeiffer, I. Seyer, D, Kirstein, T. Schulmeister and J. Nentwig, Bioelectrochem. Bioenerg., 11, 155 (1983)
29. J. Crank, 'The Mathematics of Diffusion', 2nd ed., Claredon Press, Oxford 1975, p. 49
30. O. Levenspiel, 'Chemical Reaction Engineering' 2nd ed., John Wiley & Sons, New York, 1972, p. 258
31 S.W. Feldberg in 'Electroanalytical Chemistry', Vol. 3, A.J. Bard, Ed., Marcel Dekker, New York, 1969, Chapter 4
32. R. Annino in 'Advances in Chromatography', vol. 15, J.C. Giddings, Grushka, Cazes and Brown, Eds., Marcel Dekker, New York, 1977, Chapter 2
33. J.C. Sternberg in 'Advances in Chromatography', vol. 2, J.C. Giddings and R.A. Keller, Eds., Marcel Dekker, New York, 1966, Chapter 6
34. M. Arbramowitz and I.D. Stegun, 'Handbook of Mathematical Functions (AMS 55)', National Bureau of Standards, Washington D.C., U.S. Government Printing Office, 1964
35. R.Z. Ginzburg and A. Katchalsky, J. Gen. Physiol. 47, 403 (1963)

Tryckericentralen
AVC Lund 1985